UNITED STATES DEPARTMENT OF THE INTERIOR

GEOLOGICAL SURVEY

THERMAL PROPERTIES OF ROCKS

by

Eugene C. Robertson [1]

Open-File Report 88-441

This report is preliminary and has not been reviewed for conformity with U.S. Geological Survey editorial standards and stratigraphic nomenclature.

[1] Reston, Virginia

1988

CONTENTS

FIGURES

TABLES

THERMAL PROPERTIES OF ROCKS

By Eugene C. Robertson

ABSTRACT

All the important thermal properties of rocks can be estimated from the graphs and tables in this report. Most of the useful published data are summarized herein to provide fairly accurate evaluations of thermal coefficients and parameters of rocks for many engineering and scientific purposes.

Graphs of the published data on common rocks and minerals were prepared to show the relationships of thermal conductivity with decimal solidity (one minus decimal porosity), water or air pore content, content of certain highly conducting minerals, and temperature. Tables are given of pressure effect on thermal conductivity of minerals and rocks, anisotropy of conductivity, thermal expansion, heat transfer, density, heat generation in rocks, and activation energies of conduction mechanisms in single crystals of minerals. A series of graphs show the specific heats of rock-forming minerals as a function of temperature; with these graphs the specific heat of a rock can be calculated from its mode as accurately as it can be measured. Calculations of conductivity, diffusivity, and thermal inertia of a rock from its mode are described. Discussions of radiative thermal conductivity, radioactive heat generation, and heat transfer in rocks are provided.

INTRODUCTION

Evaluation of the conduction and absorption of heat in the upper crust of the Earth for practical and for research purposes requires knowledge of the thermal properties of the rocks found there. Heat transmission in the earth occurs principally by conduction and secondarily by convection and radiation; all are summarized in the Appendix. By radiation, heat is transmitted optically through a transparent medium or space. Convective heat is transferred between a convecting fluid and a solid or other fluid. Conduction within a solid, liquid , or gas is the principal mode of heat transfer in the earth and is the principal thermal property considered herein. Summary discussions are provided of radiative conductivity and of convective heat transfer coefficients; a transfer coefficient is not a property of a substance but involves mass transport of heat by a fluid and conduction of heat in a solid and the fluid through their contact surface.

This compilation attempts primarily to summarize the best published observational data on thermal conductivity of rocks and minerals as affected by composition, porosity, water content, pressure, and temperature. Data are given for the common igneous and metamorphic rocks and for sedimentary sandstone, shale, and limestone and summary data are given for other less-common rocks. Specific heats for rocks can be obtained from data on rock-forming minerals. It is anticipated that values of these thermal properties of rocks and minerals will be useful for radioactive waste management, heat flow studies, and geothermal resource appraisals, and other thermal problems in the earth.

The approach taken is to provide graphs and simple formulas from which a thermal property of a rock can be closely estimated from a minimum knowledge of its compositional and textural characteristics. They are especially useful for friable, porous rocks and dense but inaccessible rocks. Tables are provided of data inappropriate for graphical presentation. In using these laboratory data, the rocks are assumed to be isotropic and homogeneous, although of course, rocks in place have large-scale inhomogeneities of bedding, foliation, fracturing, and other variations in composition and structure. However, one can usually assume large scale homogeneity due to randomness of mineral distribution and grain orientation.

An alternative approach is to take data from graphs and tables of measurements on rock-forming minerals to calculate from its mineral composition (mode) a combined value for a rock of its thermal conductivity, as described in the next section. Unfortunately, modes are seldom determined on rocks, so the above empirical approach using graphs is more feasible.

The best published compilation of thermal conductivities of rocks is in the tables of Clark (1966, section 21). The theory of conduction of heat is described for geologic purposes by Ingersoll and others (1954), and the classic treatise is by Carslaw and Jaeger (1959). The basis for the graphs of conductivity shown hereafter is the finding for vesicular basalt by Robertson and Peck (1974) that thermal conductivity varies as a function of the complement of porosity squared, air or water pore saturation, and content of highly-conducting phenocrysts.

Thermal conductivity is given emphasis in this compilation because it is needed in all calculations involving heat conduction in the earth. (An earlier compilation is in Robertson, 1979.) In figures 1-13 the effects of porosity, water content, and quartz, olivine, pyroxene, and clay content on conductivities of most felsic and mafic rocks are shown. Data for other less-common igneous rocks are listed in table 1. Anisotropy data for metamorphic rocks are given in table 2. The effect of temperature on conductivity is shown for the common rocks in figures 14-19 and for rock-forming minerals in figures 21-26. Conduction mechanisms and activation energies as a function of temperature in mineral crystals and aggregates are considered in the text associated with figures 28 and 29 and tables 3-5; however, the data on conduction mechanisms in rocks are still inaccurate. The available data on the effect of pressure and vacuum on conductivity of rocks and minerals are given in tables 7 and 8. The conductivities of most of the common minerals, both single crystal and polycrystalline, are given in an accompanying open-file report of Diment and others (1988), as well as in Horai (1971) and in Clark (1966, Sec. 21).

Thermal expansions (from Skinner, 1966), and densities (from Robie and others, 1967) are listed for single crystals of the common minerals in table 9. Expansions and densities of common rocks are given in tables 10 and 11.

The specific heats at constant pressure of many rock-forming minerals as a function of temperature are plotted in joules per kelvin per unit weight in figures 30-36 and in joules per kelvin per unit volume in figures 37-42. These plots are from tables of Robie and Waldbaum (1968). The specific heat of a rock is easily calculated from values of the minerals in its mode (fig. 43 and discussion); this approach is unique, as the usual calculation is from oxides from chemical analyses. Values of specific heat for a rock are useful for many other purposes than heat conduction, of course.

Measurements have been reported on the thermal diffusivities of rocks and minerals, but they are sparse, and so are not assembled separately here. Reasonably accurate values for the diffusivities and for thermal inertia, the parameter of periodic heat conduction in rocks, can be calculated from conductivities, specific heats, and densities of the mineral components, and data plotted or tabulated in this report can be used.

Convective heat transfer coefficients applicable to rocks are described and listed in table 14; characteristic thicknesses and conductivites of air, water, and steam are provided in tables 15 and 16 to estimate transfer coefficients for earth environments, although only roughly. Radioactive heat generation values in rocks are discussed and listed in table 17.

The author gratefully acknowledges the encouragement and help from William H. Diment, and from Richard A. Robie and Bruce S. Hemingway, who provided the specific heat data used in figures 30-42. The author is grateful also to Rudolph Raspet and R. W. Werre for apparatus construction and maintenance. The author acknowledges the helpful collaboration of Dallas L. Peck who established the effect of olivine phenocrysts on increasing conductivity. Helpful comments have been given by David D. Blackwell and John Sass, and other colleagues and are much appreciated.

Units

The SI units are shown on all drawings, but cgs units and English units are still common in thermal-property literature. The following conversion relations may be useful:

Thermal conductivity:	1 W/m•K	= 2.390 x10^{-3} cal/cm sec °C
		= 0.5797 Btu/ft hr °F
Thermal diffusivity:	1 m^2/sec	= 10^4 cm^2/sec
		= 10.764 ft^2/sec
Heat flow:	1 W/m^2	= 23.9 x 10^{-6} cal/cm^2 sec
		= 554 Btu/ft^2 hr
Heat transfer coefficient:	1 W/m^2K	= 23.9 x 10^{-6} cal/cm^2 sec °C
		= 308.0 Btu/ft^2 hr °F
Specific heat:	1 J/kg K	= 239 x 10^{-6} cal/gm °C
	1 J/m^3 K	= 0.239 x 10^6 cal/cm^3 °C
Thermal gradient:	1 K/km	= 1 °C/km
		= 0.5486 x 10^{-3} °F/ft
Energy:	1 J	= 6.2414 x10^{18} e V
		= 10^7 ergs
		= 0.239 cal
Pressure:	1 Pa	= 1 N/m^2
		= 10^{-5} bar
		= 7.7 x 10^{-3} torr or mm Hg

Symbols

Btu	British thermal unit
$\underline{C}$	Celsius
$\underline{C}_p$	specific heat at constant pressure
CU	conductivity unit, 10^{-3} cal/cm sec ^{o}C
$\underline{E}$	activation energy
F	Fahrenheit
I	thermal inertia
J	joule
$\underline{K}$	thermal conductivity [1]
K	Kelvin[1]
$\underline{P}$	pressure
$\underline{T}$	temperature
W	watt
cal	calorie
$\underline{d}$	density
ft	foot
g	gram
$\underline{h}$	heat transfer coefficient
hr	hour
$\underline{k}$	thermal diffusivity
kg	kilogram
km	kilometer
m	meter
$\underline{n}$	decimal fractional volumes of mineral phases 1, 2, ...
s	second
$\underline{x}$	decimal fraction of composition
α	thermal expansion
γ	solidity
ϕ	porosity

[1] A possible confusion may occur in distinguishing between the symbols, italic $\underline{K}$ for conductivity and Roman K for kelvins, the SI units of temperature. The usage and the italic underline should prevent ambiguity.

THERMAL CONDUCTIVITY

Introduction

In plotting the following graphs of thermal conductivity K of rocks and minerals from published data, the tacit assumptions were made that among the various investigators, the samples of each rock type were uniform and the experimental measurements were accurate, producing comparable grain-to-grain thermal conduction around pores and through pore fluids. As a distinct advantage over the tables of K, these graphs provide a full range of the porosity and water content effects on K, which can be interpolated quantitatively. The scatter of the data on the graphs attests to the presence of some nonuniformities and inaccuracies among the results and provides an estimate of uncertainty. Widely aberrant data were not plotted or listed, but many somewhat uncertain values were used due to the scarcity of conductivity measurements in general. Techniques of measurement of thermal conductivity have been described by Birch (1950), Beck (1965), and Sass and others (1971).

As described below, the K of a rock calculated from its mode generally is too high, and requires a correction factor, and since modal analyses are usually not available anyway, the following empirical graphs and tables for rocks and minerals are provided to make estimates of K. With some training in petrography, hand lens inspection of rock specimens should provide adequate approximations of phenocryst content of critical minerals, porosity, and water content; study of thin sections would provide closer estimates. A few less-common rocks, like dunite, amphibolite, pyroxenite, phyllite, and schist, are not plotted due to lack of data on K with respect to porosity and water content, and recourse to figures 15-19, to tables 1, 2, and 6, and to mode calculations to estimate K may be necessary.

Measurements of K based on the available data in the literature for common rocks, made at about 30 °C (303 K) and 50 bars (5 MPa), are plotted in figures 1 through 13. Separate figures are given for air and water filling the pores, and each shows the relation of K to solidity (described below) and phenocryst content, as in the conductivity study of vesicular basalt by Robertson and Peck (1974).

There is a large decrease in K with increasing temperature T for quartz-rich felsic, carbonate, and ultramafic rocks (figs. 15 through 19) and for most rock-forming minerals (figs. 21 through 26). Some feldspathic rocks and most basalts (fig. 15) and rock glasses (fig. 20) have a small positive change of K with T.

The acronym "CU" will be used for "conductivity unit", with the following equivalences,

$$1\ \text{CU} = 10^{-3}\ \text{cal/cm sec °C} = 0.4184\ \text{W/m} \cdot \text{K}.$$

Solidity

The parameter used here to account for the thermal coupling between grains and the insulating effect of pore spaces on conductivity is called solidity. Solidity, γ, is defined as the ratio of the volume of solid to the bulk volume, or the ratio of bulk density to solid grain density, d_B/d_G; it is the complement of porosity, ϕ, that is, $\gamma = 1 - \phi$. Robertson and Peck (1974) found that the thermal conductivity of basalt varies linearly as the square of the solidity, γ^2. All rocks in the earth's crust have some porosity which impedes heat conduction. Thermal conduction in a rock is controlled primarily by the relative effectiveness of grain-to-grain paths, and conduction through fluids in the pores is much less important. A theoretical model can be deduced by analogy with the model for electrical conductivity in rocks.

Thermal Impedance

The effect of the pore space on electrical resistivity of rock is given by Archie's Law, in which resistivity of the rock varies inversely as the square of porosity (see Greenberg and Brace, 1969); the electrical conduction is apparently controlled primarily by the electrolyte in the connected pores. A theoretical physical model for Archie's Law was investigated by Adler and others (1973) and Shankland and Waff (1974) by using electrical resistor simulations to show that the bulk electrical conductivity of a three-dimensional lattice is proportional to the square of the fraction of conducting nodes. As Shankland (1975) in his important review paper on rocks and minerals points out, the second-power exponent of Archie's Law holds in rocks in which much of the porosity does not

contribute to electrical conduction, as when the pores are dead-end cracks or almost-isolated voids. In rocks with connected pores, simulated by all branches of the resistor network, electrical conductivity varies as porosity to the first power. Shankland (1975) uses electrical conductivity rather than resistivity in analyzing data on minerals because the parallel conduction is additive in conductivity and not in its reciprocal.

Although the mechanisms for the transport of heat and electricity are different, the electrical model described by Shankland (1975) can be carried over to a thermal model; the solid grains of rock in thermal conduction are analogous to the pores of rock in electrical conduction, which are simulated by the nodes of the resistor network. Analogously also, the thermal conductivity was found to vary as solidity squared (Robertson and Peck, 1974) because like the isolated electrical nodes, the solid grains are apparently almost isolated by cracks and contact each other at only a few points.

The isolation of grains in rocks is implicit in explaining the difference between the theoretical intrinsic thermal conductivity of a completely solid rock, and the extrapolated conductivity observations at $\gamma = 1$, for 5 percent olivine, as described by Robertson and Peck (1974) for basalt. The same explanation applies to limestone and dolostone, as shown in this report. The extrapolated intercept of the isopleths at $\gamma^2 = 1$, at the fully solid condition, is less than the intrinsic value of a theoretically zero-porosity aggregate of crystals (see figs. 1, 2, 5, 6, 7, 8). The results on basalt show an intercept well below the calculated average of mineral $\underline{K}$'s and the measured average of the powdered sample. The effective $\underline{K}$ is 30 percent below the intrinsic $\underline{K}$ for water-saturated basalt in samples of $.995 < \gamma < 1$, due to the insulating effect of thin air-filled pores, minute vesicles, microfractures created by cooling stresses, and other inaccessible pores.

Interestingly, the effectiveness of pressure in closing cracks and increasing thermal conductivity is an order of magnitude smaller (10^{-2}kb $^{-1}$; see table 7) than the pressure effect of closing cracks and thereby decreasing electrical conductivity (10^{-1} kb $^{-1}$ see Shankland and Waff, 1974). In other words, thermal coupling between grains is not improved by a given pressure as much as electrical conduction is diminished by crack closing.

Calculation of Composite Models

If the mineral composition, or mode, of a rock is known, several theoretical models can be used to calculate its composite intrinsic thermal conductivity from tables of values for minerals. (See Robertson and Peck, 1974, for a comprehensive discussion of models and the accompanying open-file report of Diment and others (1988), or Horai (1971) or Clark (1966, Sec. 21) for mineral conductivities.) The parallel and series models in equations (1) and (2) below have been used fairly successfully to combine mineral values for relatively dense ($\gamma > 0.98$) felsic rocks by Birch and Clark (1940), Beck and Beck (1958), and Horai and Baldridge (1972). In a composite rock with grains arranged in a parallel orientation to the direction of heat flow, the conductivity is given by

$$\underline{K}_p = n_1 \underline{K}_1 + n_2 \underline{K}_2 + n_3 \underline{K}_3 + \ldots \qquad (1)$$

where $\underline{K}_p$ is the parallel bulk rock conductivity, n_1, n_2, n_3... are fractional volumes of mineral phases 1,2,3,..., and $\underline{K}_1$, $\underline{K}_2$,$\underline{K}_3$, ... are conductivities of minerals 1,2,3,... Note that the parallel format of equation 1 is often used also to calculate a composite value for density, thermal expansion, diffusivity, or specific heat of a rock from corresponding values of these parameters for the minerals of its mode.

In a rock with mineral grains arranged in a layered sequence perpendicular to the heat flow direction, the series conductivity is given by

$$\frac{1}{K_s} = \frac{n_1}{K_1} + \frac{n_2}{K_2} + \frac{n_3}{K_3} + \ldots$$

where $\underline{K}_s$ is the series conductivity. It has been found that the mean of $\underline{K}_p$ and $\underline{K}_s$ provides compromise values that fit observed values closely, especially for more porous rocks.

$$\underline{K}_{ps} = 1/2\,(\underline{K}_p + \underline{K}_s) \qquad (3)$$

The geometrical mean of conductivities $\underline{K}_g$ is empirical, but it also gives a useful average that fits observed values.

$$\log \underline{K}_g = n_1 \log \underline{K}_1 + n_2 \log \underline{K}_2 + \ldots \qquad (4)$$

The composite value of $\underline{K}$ calculated by equations 3 and 4 for the mode of a basalt with 5 percent olivine was accepted by Robertson and Peck (1974) to be the fully solid intrinsic $\underline{K} = 6.1$ CU. This value was corroborated by the direct measurements made by R. J. Munroe (written commun., 1972) on two powdered samples of the basalt in a conductivity wet cell (described by Sass, and others, 1971), which establishes the validity of using equations 3 or 4 to calculate the intrinsic $\underline{K}$ of fully solid rock.

Equations 1 to 4 and several others were used to compare observed and calculated $\underline{K}$'s for porous vesicular basalt by Robertson and Peck (1974). In order to compare calculated $\underline{K}$'s with observed $\underline{K}$'s, the porosity had to be accounted for; the pore constituent (air or water) and its fractional volume and conductivity were included with the mineral phases, and the calculated $\underline{K}_p$, $\underline{K}_s$, $\underline{K}_{ps}$, or $\underline{K}_g$ was multiplied by the appropriate γ^2. However, the final calculated $\underline{K}$'s were still about 30 percent higher than the observed $\underline{K}$'s (Robertson and Peck, 1974, figs. 4, 5, 9, and 10). Apparently, correction for thermal impedance has two parts, one accounted for by γ^2 and the other being a linear correction factor.

In the analogy between the relationship that thermal conductivity in a rock varies as the square of solidity and Archie's Law that electrical conductivity varies with the square of porosity, apparently the squared parameters in both are the primary factors. In addition, in Archie's Law, there is a subtracted correction term of porosity for a threshold electrical conduction, and analogously in thermal conduction, there is an additional correction factor for thermal impedance between grains to be multiplied times the intrinsic thermal conductivity calculated from the mode and the solidity-squared factor to obtain the observed value of $\underline{K}$.

$$\underline{K}_{ci} = \underline{C}_i (\gamma)^2 \underline{K}_c \qquad (5)$$

where $\underline{K}_c$ is calculated conductivity, $\underline{K}_{ci}$ is impedance-corrected (equal to observed) conductivity, γ is solidity, the fractional grain volume, and $\underline{C}_i \leq 1$ is a thermal impedance factor, due probably to inaccessible microcracks and pores between grains.

The thermal impedance correction factors, $\underline{C}_i$, have been fairly closely estimated for basalt (Robertson and Peck, 1974, figs. 4, 5) and for carbonate rocks (figs. 5 to 8), and their decimal values are as follows.

Rock	Correction factor $\underline{C}_i$	
	Air in pores	Water in pores
Basalt.....	0.62	0.77
Limestone.....	.78	.84
Dolostone.....	.80	.89

Impedance correction factors for felsic rocks are not well established. The $\underline{C}_i$ for dense granitic rocks, based on the calculations by Birch and Clark (1940), Beck and Beck (1958). and Horai and Baldridge (1972), is 0.8-0.95; it is nearly 1.0 for felsic rocks with very low porosity and with parallel arrangement of quartz grains. Modes and textures of sandstones and shales are quite variable, and factors vary widely; $\underline{C}_i$'s are 0.6-0.9. Note that the correction factor for water-saturated sandstone will be larger than the factor for air-saturated sandstone; with air in the pores the thermal impedance is greater, that is, $\underline{K}$ is reduced (figures 9, 10). Petrographic investigations of textures, porosities and modes of all rock types, but especially felsic rocks, are badly needed to determine their

correction factors to values of calculated conductivity. Until these $\underline{C}_i$ values are better determined, calculation from a rock mode of a corrected $\underline{K}_{ci}$ value will produce low correspondence to observed values. Thus the empirical plots based on observed $\underline{K}$'s in figures 1 through 13 are offered in this report for estimating $\underline{K}$ directly, obviating the need for knowing correction factors.

Pore Fluid

The influence of the fluid in the pores on the $\underline{K}$ of a rock is large. The enhancement of $\underline{K}$ by saturation with water rather than air is shown by comparison of the pairs of figures 1-4 and 9-10. (Some data are available for the effects on $\underline{K}$ by various gases and hydrocarbon fluids in pores, mostly in certain porous rocks; no attempt is made to show them here; see Woodside and Messmer, 1961; Sukharev and Sterlenko, 1970; Zierfuss and Vliet, 1956; Kunii and Smith, 1961; Assad, 1955.) The values of $\underline{K}$ for dry samples with air in the pores and those for saturated samples with water in the pores are shown by separate plots for each of the principal rock types (figs. 1-13).

In the earth, most rocks are saturated with water below the water table, which occurs generally at depths shallower than 100 m. For certain purposes, however, partial saturation must be considered. The increase in $\underline{K}$ with increasing water saturation is nonlinear, varying according to rock type, pore geometry, and fluid permeability.

The following rough linear approximation to determine $\underline{K}$ for a partially water-saturated rock can be used by interpolating between values from the air-saturated and the water-saturated plots: at a given γ, and given percent olivine, quartz, etc., about 80 percent of the increase in $\underline{K}$ due to addition of water in the pores is attained at about 50 percent saturation; linear interpolations can be made between the air-saturated and the water-saturated values of $\underline{K}$ from this point, constituting the locus from which to estimate $\underline{K}$ at any water-saturation percentage.

In figures 1 and 2 for basalt, the control by the data on the line position at low γ^2 is good, so the extrapolated intercept at $\gamma^2 = 0$ can be seen clearly to be higher than the values of $\underline{K}$ both for air and for water. The explanation for lack of correspondence may be that because the web of rock around the pores conducts heat better than the air or water in the pores therefore a relatively large increase in $\underline{K}$ occurs at very low γ^2.

In figures 3-13, for the other rocks, the intercepts are fixed at the air and water values of $\underline{K}$, due to lack of data at low γ.

Quartz, Olivine, Pyroxene, Amphibole, and Clay Content

In using figures 1-13 to estimate $\underline{K}$, the content of phenocrysts of olivine, pyroxene, and amphibole in mafic rocks and the content of all grain sizes of quartz and mica in felsic rocks should be known approximately. A hand lens estimate of these high-conductivity minerals should be adequate and is feasible for other than aphanitic rocks.

In the study of basalt by Robertson and Peck (1974), Peck observed that $\underline{K}$ increases systematically with increase in content of olivine phenocrysts in the samples, as shown by the isopleths in figures 1 and 2. On the other hand, the ground mass of the rocks is fine-grained (about 0.03 mm dia.), augite and labradorite mostly, and this matrix $\underline{K}$ apparently varies linearly with γ^2. The relation of $\underline{K}$ to γ^2 is taken as applicable to andesite, the other ubiquitous mafic rock on the earth; andesite has more feldspar and less pyroxene, amphibole, or olivine in the ground mass, and so $\underline{K}$'s may actually be slightly lower than indicated by the plots.

An even more important mineral affecting rock conductivity is quartz. At 35 °C and 50 bars, the average $\underline{K}$ of quartz is about 18 CU; the $\underline{K}$ of felsic rocks increases rapidly with quartz content. The effect of quartz content was ascertained in large part from measurements of mineral compositions, solidities, and conductivities of a suite of sandstones made by Hutt and Berg (1968), which are shown in figures 9 and 10; supporting data were also taken from modal and conductivity observations of Woodside and Messmer (1961), Zierfuss and Vliet (1956), and Clark (1941).

In figures 3 and 4 for felsic igneous and metamorphic rocks, plots of $\underline{K}$ variation with γ^2 are shown with air or water in the pores. The increase of $\underline{K}$ with quartz content is clear. These plots are adapted from those for sandstone (figs. 9 and 10) using data of Gordon Greene (written commun., 1966) and Birch and Clark (1940). Feldspars of all compositions ($\underline{K}$ about 4 CU) and the usually minor mafic minerals ($\underline{K}$ about 10 CU) in felsic rocks have about the same values of $\underline{K}$, and accounting for quartz with its high $\underline{K}$, figures 3 and 4 can be applied to granite,

rhyolite, syenite, and other felsic igneous rocks.

The graphs for sandstone (figs. 9, 10) provided the bases for making sense of the available data for $\underline{K}$ of shale and soils. For the same reasons as for felsic igneous rocks, only two studies of shales included mineral compositions, but several studies of soils did include compositional chemical and mineral information, and could be used. Fortunately the water-saturated data for soils fits reasonably well with the sandstone and usable shale data. Air saturated soils are very different, as described for figure 13 below.

Clay minerals, like montmorillonite, illite, and kaolin, are found with flakes parallel to bedding in shaly rocks, and their presence lowers the conductivity normal to bedding. This lowering is due to the low conductivity normal to clay flakes, about 1 CU, compared to 8 CU parallel to the flake layers, a very large anisotropy ratio. The normal $\underline{K}$ may be reduced also by the presence of air-filled pore space between flakes. The decrease in $\underline{K}$ by the presence of clay minerals is opposite to the increase due to quartz content; correction schemes accounting for quartz and clay in estimating $\underline{K}$ are discussed under figures 11, 12, and 13, for shales and soils.

ROCK CONDUCTIVITY AT 300 K

Introduction

Figures 1-13 show the conductivity measurements of rocks near room temperature (300K), with either air or water in the pores. Each figure is described individually below, giving references to sources of data, and explaining use of symbols, numbers on the plots, intercepts, and other matters to be emphasized. In the figures, $\underline{K}$ is plotted against γ^2, and isopleths show variation with olivine or quartz content. As can be seen, the values alongside the plotted points do not define the locations of the isopleths exactly; such secondary effects on $\underline{K}$ as anisotropy and variation in composition and texture affect the grain-to-grain thermal coupling of the matrix of the rock samples and account for the lack of correspondence. Reference can be made to tables 1 and 2 and to figures 14-19 for $\underline{K}$ values for rocks not shown in figures 1-13.

Intercepts are given with each figure for easy calculation of interpolated values, and the following formula can be used:

$$\underline{K} = \underline{K}_F + \gamma^2 [(\underline{K}_S + p\underline{S}) - K_F] \qquad (6)$$

where $\underline{K}_F$ is pore fluid intercept at $\gamma^2 = 0$, $\underline{K}_S$ is the solid rock intercept at $\gamma^2 = 1$ for zero percent quartz or other mineral, p is percent quartz or other mineral, and $\underline{S}$ is a slope constant equal to the change of $\underline{K}$ with quartz, olivine, or other mineral per unit percent contained, obtained from intercept values at $\gamma^2 = 1$ on the figures.

The values of solidity γ can be obtained from the relation with porosity ϕ, $\gamma = 1 - \phi$, and from the ratio $\gamma = \underline{d}_B / \underline{d}_G$, where $\underline{d}_B$ is bulk density, and $\underline{d}_G$ is grain density. By laboratory measurements, γ can be obtained from the weight of a dry sample $\underline{W}_D$ and the sample weights saturated with water in air $\underline{W}_{WA}$, and immersed in water, $\underline{W}_{WW}$, as follows:

$$\gamma = (\underline{W}_D - \underline{W}_{WW})/(\underline{W}_{WA} - \underline{W}_{WW}) \qquad (7)$$

Another procedure is to prepare the rock sample into a simple shape, measure its volume and weigh it to get $\underline{d}_B$, and then estimate $\underline{d}_G$ from the mode, using Equation 1, substituting densities for conductivities.

The pairs of graphs for rocks with air and with water in the pores will be needed to estimate $\underline{K}$ for rocks partially saturated with water. As described under the section on Pore Fluid, a simple double-line interpolation can be used. As an example, referring to figures 1 and 2, we can use the sample marked 35 percent olivine on the 30 percent olivine line, at solidity, $\gamma^2 = 0.70$, (that is, $\gamma = 0.837$); the end values are $\underline{K}_A = 3.42$ CU and $\underline{K}_W = 4.79$ CU. We will estimate the $\underline{K}$'s for partial water contents of 25 and 85 percent. The 80 percent increase in $\underline{K}$ due to 50 percent water saturation would be 3.42+0.8 (4.79-3.42) = 4.52. The $\underline{K}$ at 25 percent saturation would be 3.42+(25/50) (4.52-3.42) = 3.97 CU; and $\underline{K}$ at 85 percent water saturation would be 4.52+(35/50) (4.79-4.52) = 4.71 CU.

The scatter of point values in the graphs can be taken as a measure of the uncertainty in estimating values of $\underline{K}$. Both SI and cgs units are shown in the figures, and the conversion factor for thermal conductivity is: 1W/m· K = 2.390×10^{-3} cal/cm sec °C. The acronym CU will be used for conductivity unit = 10^{-3} cal/cm sec °C.

Mafic Igneous Rocks, Air in Pores

The points plotted in figure 1 are data from Robertson and Peck (1974) on tholeiitic basalt samples, dry, with air in the pores. The olivine content of the samples is shown adjacent to each point, and the moderate scatter of values with respect to the isopleth lines is clear. The fine-grained feldspar and pyroxene matrix can be assumed to have an essentially constant $\underline{K}$, varying uniformly with solidity. The following intercepts apply for purposes of calculation in Equation 6.

(Solidity)	Olivine (Volume percent)	Conductivity intercept (CU)		Factor $\underline{S}$ CU/percent
0	0	$\underline{K}_F$	0.45	
1	0	$\underline{K}_S$	3.60	
1	30	$\underline{K}_S$	4.68	0.036

The control of points is good enough to place the intercept (0.45 CU), at $\gamma^2 = 0$, higher than the actual air value (0.063 CU), and the intercept (3.78 CU), at $\gamma^2 = 1$ for 5 percent olivine, lower than the calculated and observed value (6.10 CU). The isopleth lines have been drawn radially to the single point (0.45 CU), at $\gamma^2 = 0$, as a better fit than a set of parallel lines, which would give the next easiest arrangement for calculation purposes.

The interpolated lines in figure 1 can reasonably be used to estimate $\underline{K}$'s of other mafic rocks, especially andesite, as the modes are quite similar. Andesite has more feldspar, somewhat less calcic then basalt, but the $\underline{K}$ of plagioclase is nearly constant, about 4 CU, from andesine through anorthite (fig. 23). Some andesite has phenocrysts of pyroxene, commonly augite, and since the $\underline{K}$'s of olivine, pyroxene, and amphibole are nearly the same (about 10 CU, see fig. 24 and Diment and others, 1988), the isopleths of figures 1 and 2 are applicable. Figures 3 and 4 can be used for quartz-bearing andesite.

Data for norite and gabbro from Birch and Clark (1940) are given in table 1. Values for dense ultramafic rocks can be obtained from figure 19.

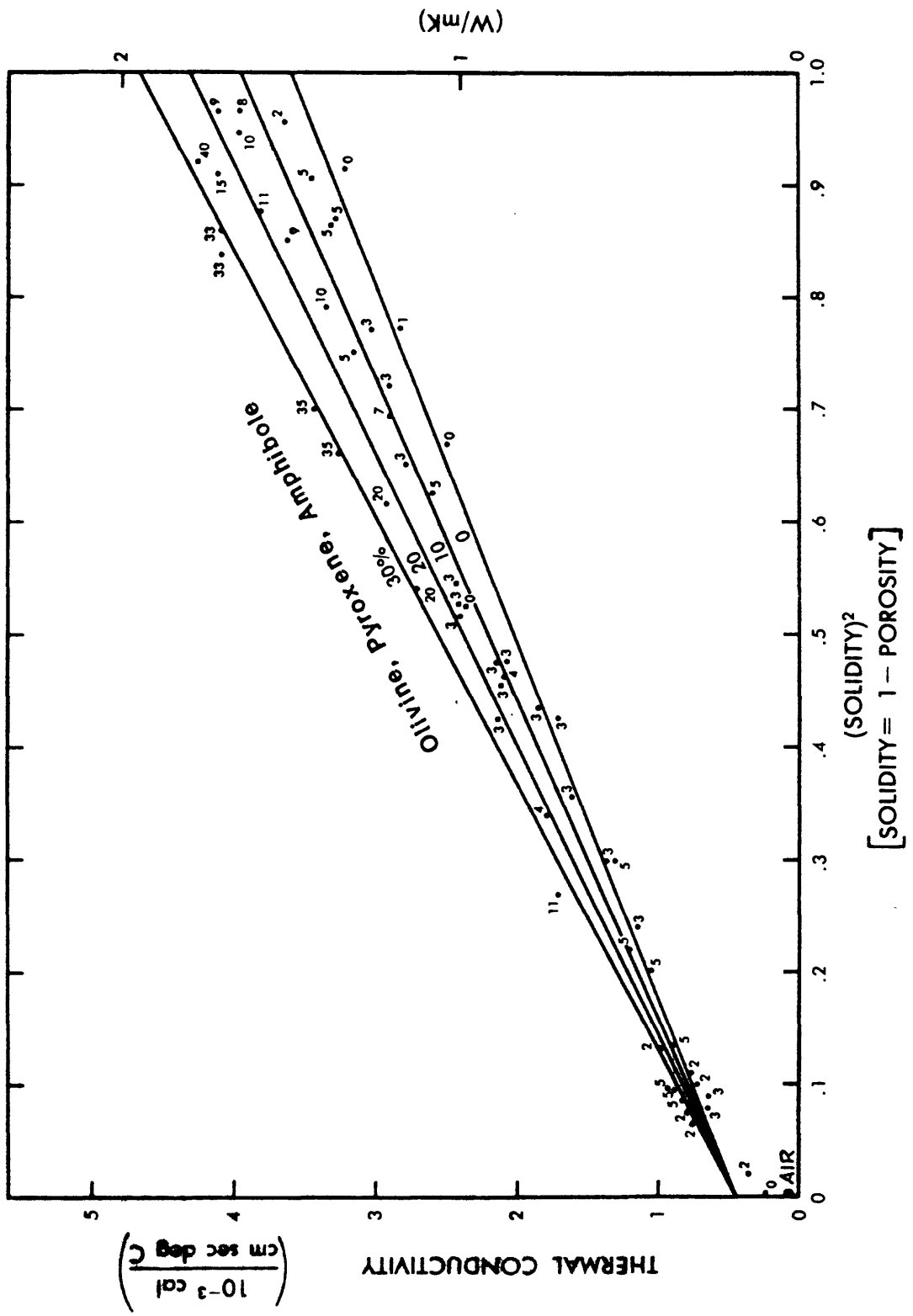

FIGURE 1. Thermal conductivity of mafic rocks with air in the pores, showing variation with solidity and percent phenocrysts of olivine, pyroxene, or amphibole, at 300 K, 5MPa.

Mafic Igneous Rocks, Water in Pores

The points in figure 2 are from observations of Robertson and Peck (1974) on conductivity of water-saturated basalt. As with figure 1, the lines in figure 2 can be used to estimate $\underline{K}$ for andesite as well. The isopleth lines are shifted upward from figure 1 by an improved thermal conduction through the water compared to air in pores in the rocks. The following intercepts can be used in calculating $\underline{K}$, equation 6.

$(\text{Solidity})^2$	Olivine (Volume percent)	Conductivity intercept (CU)		Factor $\underline{S}$ CU/percent
0	0	$\underline{K}_F$	1.80	
1	0	$\underline{K}_S$	4.40	
1	30	$\underline{K}_S$	6.20	0.060

The intercept at $\gamma^2 = 0$, is 1.80 CU, which is higher than the value for water, $\underline{K} = 1.48$. At $\gamma^2 = 1$, the intercept from observed data on basalt with 5 percent olivine is 4.70 CU, whereas the zero porosity $\underline{K}$ calculated from the mineral composition without the impedance correction is 6.10 CU.

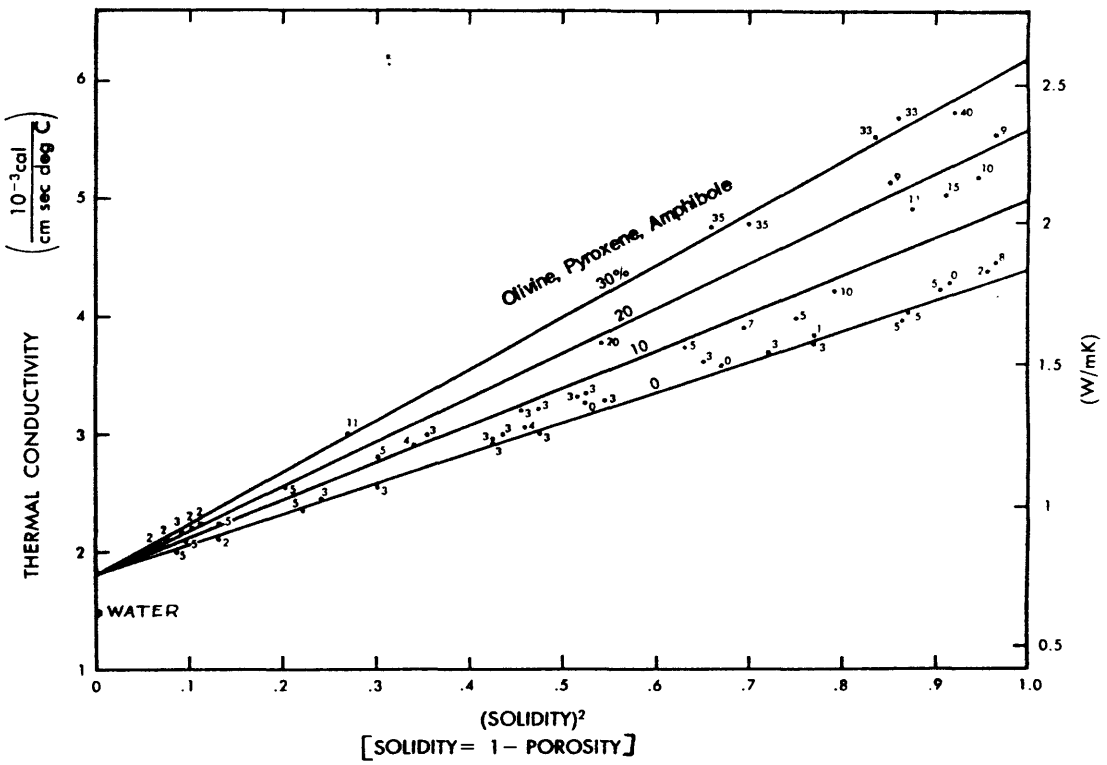

FIGURE 2. Thermal conductivity of mafic rocks with water in the pores, showing variation with solidity, and olivine, pyroxene, or amphibole phenocryst content, at 300 K, 5MPa.

Felsic Igneous Rocks, Air or Water in Pores

The data on a number of felsic igneous rocks, air saturated, shown in figure 3, are merely representative of hundreds of measurements made on felsic rocks, and are taken from Birch and Clark (1940) and Beck and Beck (1958) (numbered x's and circles, respectively). The unnumbered points for $\gamma^2 < 0.9$ are from Gordon Greene (written commun., 1966). Most all points are averages of 2 to 10 measurements. These data fit the quartz isopleths of figure 9 from which this graph was drawn; all quartz is used, not just phenocryst content. The $\underline{K}$'s for all feldspars are nearly the same, about 4-5 CU, and the mafic material content is usually low, about 5 percent or less, so the use of the same isopleths is acceptable for most of the common felsic igneous and metamorphic rocks. The intercepts of figures 3 and 4 are given below.

There are no data on $\underline{K}$ for porous, water-saturated, felsic igneous rocks; figure 4 is adapted primarily from figure 10 and repeats some data on dense rocks in figure 3.

$(\text{Solidity})^2$	Quartz (Volume percent)	Conductivity intercept (CU)		Factor $\underline{S}$ (CU/percent)
		Air in pores		
0	0	$\underline{K}_F$	.063	
1	0	$\underline{K}_S$	3.50	
1	100	$\underline{K}_S$	12.50	0.090
		Water in pores		
0	0	$\underline{K}_F$	1.48	
1	0	$\underline{K}_S$	3.63	
1	70	$\underline{K}_S$	14.63	0.157

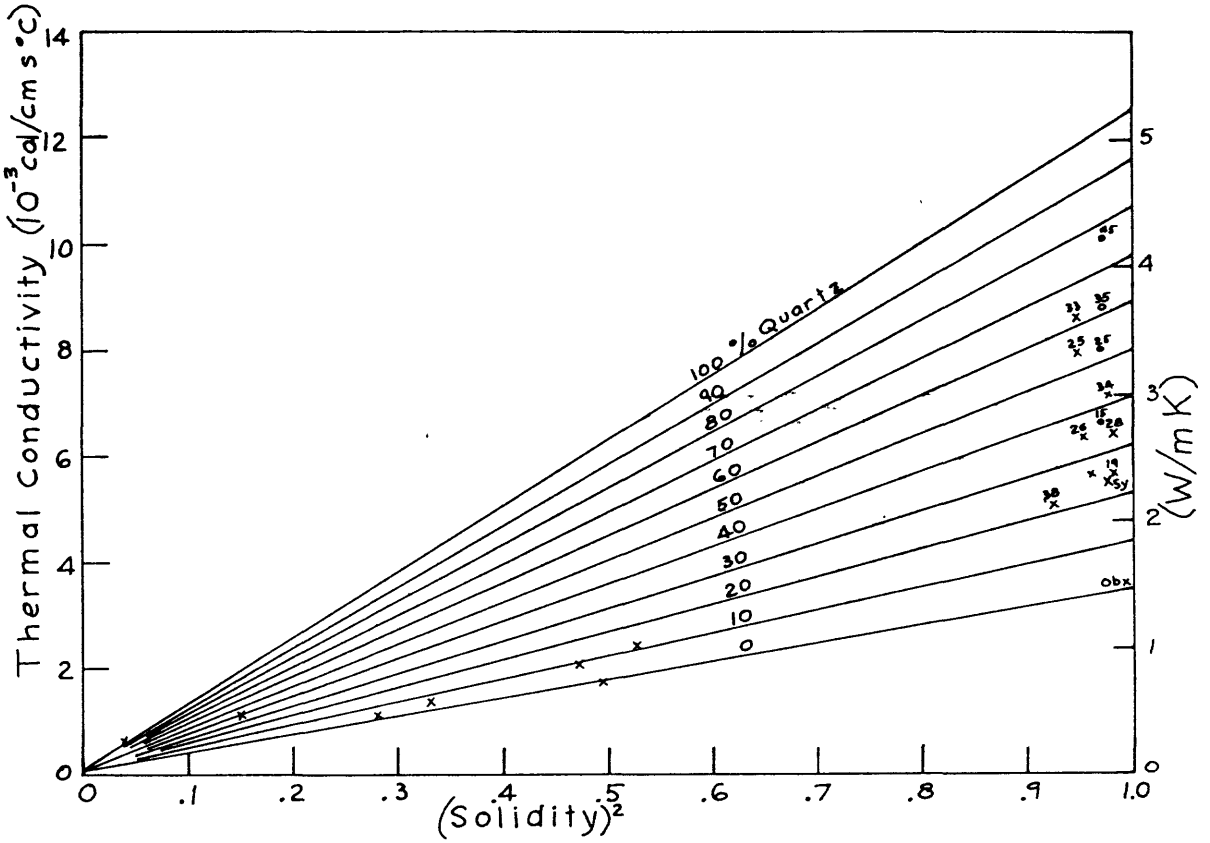

FIGURE 3. Thermal Conductivity of felsic rocks with air in the pores, showing variation with solidity and quartz content, at 300 K, 5MPa.

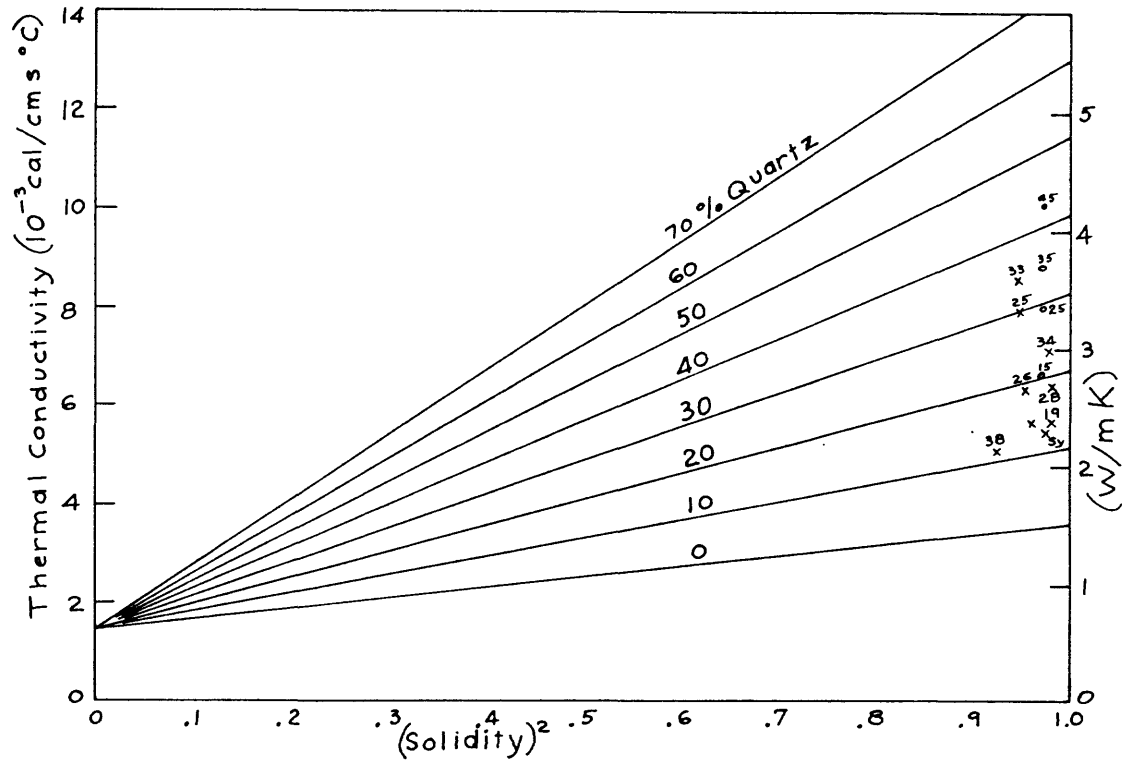

FIGURE 4. Thermal conductivity of felsic rocks with water in the pores, showing variation with solidity and quartz content, at 300 K, 5MPa.

Limestone, Air or Water in Pores

The samples of limestone, on which measurements were made to provide the points plotted in figure 5, were relatively pure polycrystalline calcite. The $\underline{K}$ intercept at the value at $\gamma^2 = 0$ for air (.063 CU) seems acceptable, but the $\underline{K}$ intercept at $\gamma^2 = 1$ is well below the average for calcite crystal, 8.2 CU. The calcite samples were measured by Horai (1971) and by Birch and Clark (1940). The limestone measurements were made by Clark (1941), Zierfuss and Vliet (1956), Zierfuss (1969), and Beck and others (1971), and at γ^2 of 0.99 an average of 41 samples, measured by Robertson (1959).

Relatively pure calcitic limestone samples were used for the measurements in figure 6 also. Although there is some scatter, the linear variation of $\underline{K}$ with γ^2 seems fairly well established by the data. The intercept $\underline{K} = 1.48$ CU, the value for water, fits the trend reasonably well at $\gamma^2 = 0$. As with limestone in figure 5, the intercept at $\gamma^2 = 1$ is less than the single crystal average, 8.2 CU (Horai, 1971; Birch and Clark, 1940). The data are plotted here are from Clark (1941), Bullard and Niblett (1951), Misener and others (1951), Zierfuss and Vliet (1956), and Beck and others (1971); the point at $\gamma^2 = .99$, $\underline{K} = 6.75$ CU, is an average of 41 samples, measured by Robertson (1959).

The intercepts for the figures are listed below:

Pore Fluid	Figure number	$(\text{Solidity})^2$	Conductivity intercept (CU)	
Air	5	0	$\underline{K}_F$	0.063
		1	$\underline{K}_S$	6.40
Water	6	0	$\underline{K}_F$	1.48
		1	$\underline{K}_S$	7.10

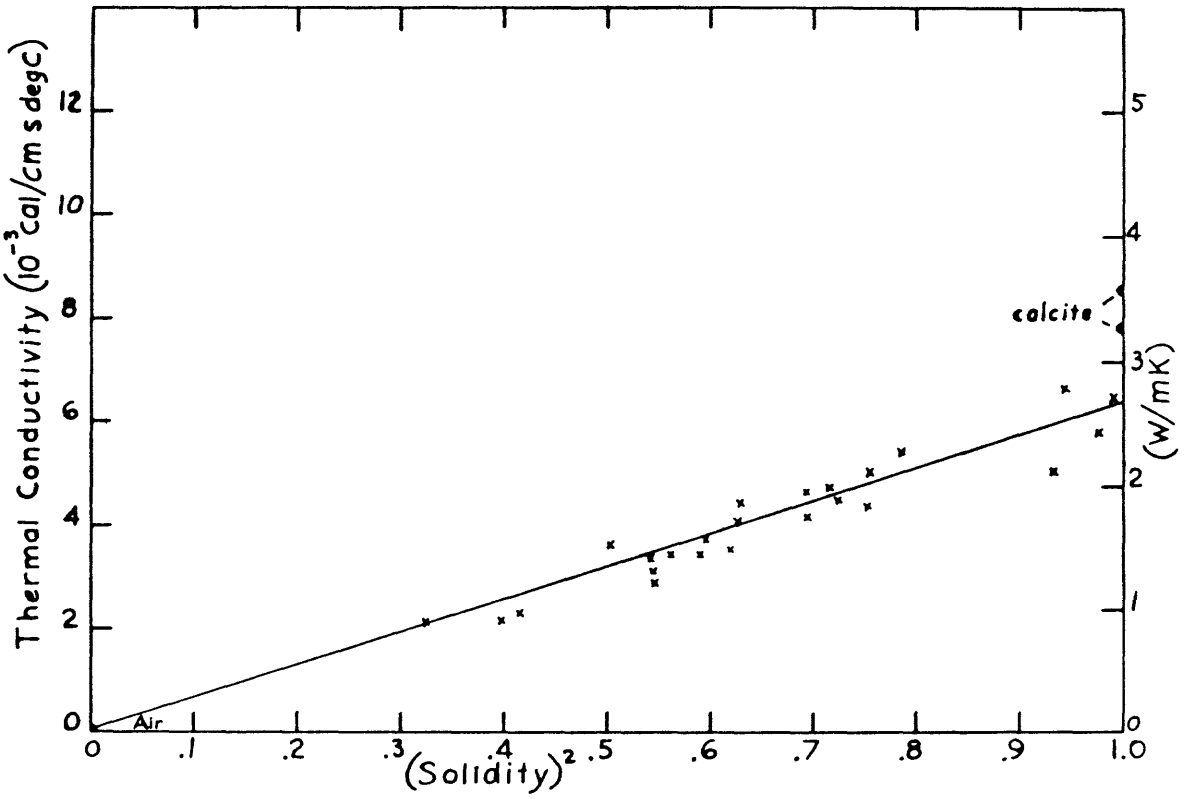

FIGURE 5. Thermal conductivity of limestone with air in the pores, showing variation with solidity, at 300 K, 5MPa.

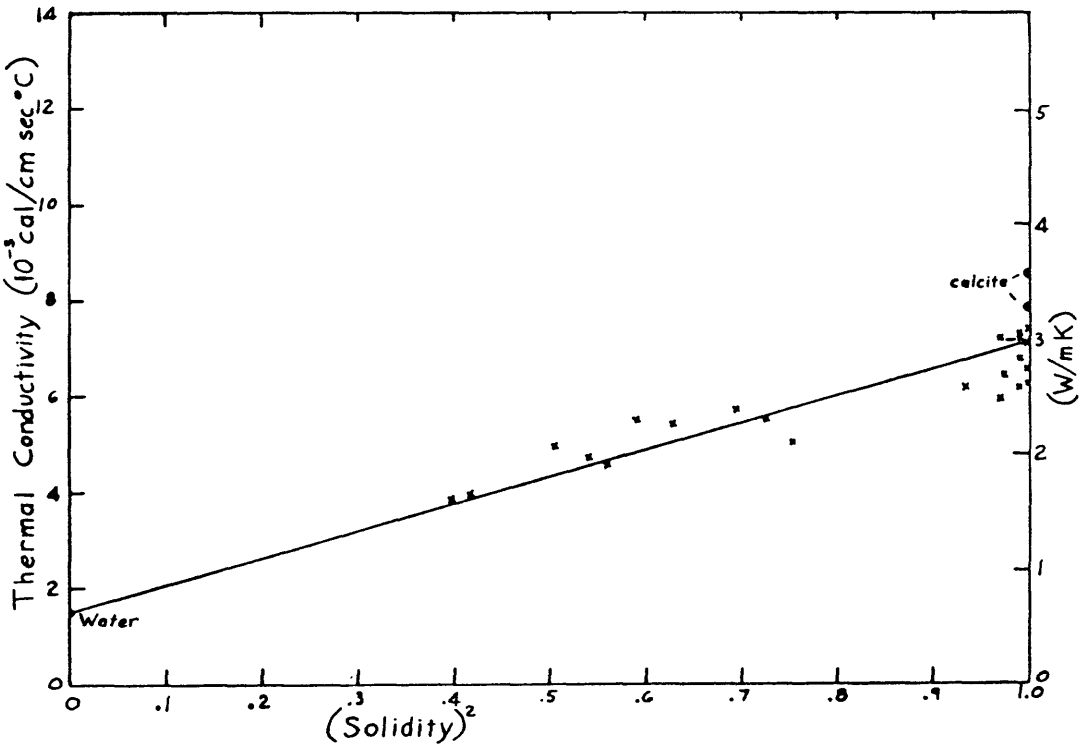

FIGURE 6. Thermal conductivity of limestone with water in the pores, showing variation with solidity, at 300 K, 5MPa.

Dolostone, Air or Water in Pores

The data for dolomite rock with air in the pores define a line in figure 7 through $\underline{K}$ for air (0.63 CU) at $\gamma^2 = 0$, and an intercept of $\underline{K}$ at $\gamma^2 = 1$ considerably less than the single crystal average. The dolomite crystal measurements were made by Horai (1971) and by W.H. Diment (written commun., 1968). The central data points are from Zierfuss (1969); the higher point, at $\gamma^2 = 0.985$, is from Bullard (1939), and the lower one at $\gamma^2 = 0.995$, is an average of 52 samples from Robertson (1959).

Aside from the single crystal measurements on dolomite by Horai (1971) and Diment (1968), there is only one point for water-saturated dolostone in figure 8. This value is an average of measurements made on 52 samples of fairly pure dolomite rock by Robertson (1959).

The intercepts for the figures are listed below:

Pore Fluid	Figure number	(Solidity)^2	Conductivity intercept (CU)	
Air	7	0	$\underline{K}_F$	0.063
		1	$\underline{K}_S$	10.20
Water	8	0	$\underline{K}_F$	1.48
		1	$\underline{K}_S$	11.04

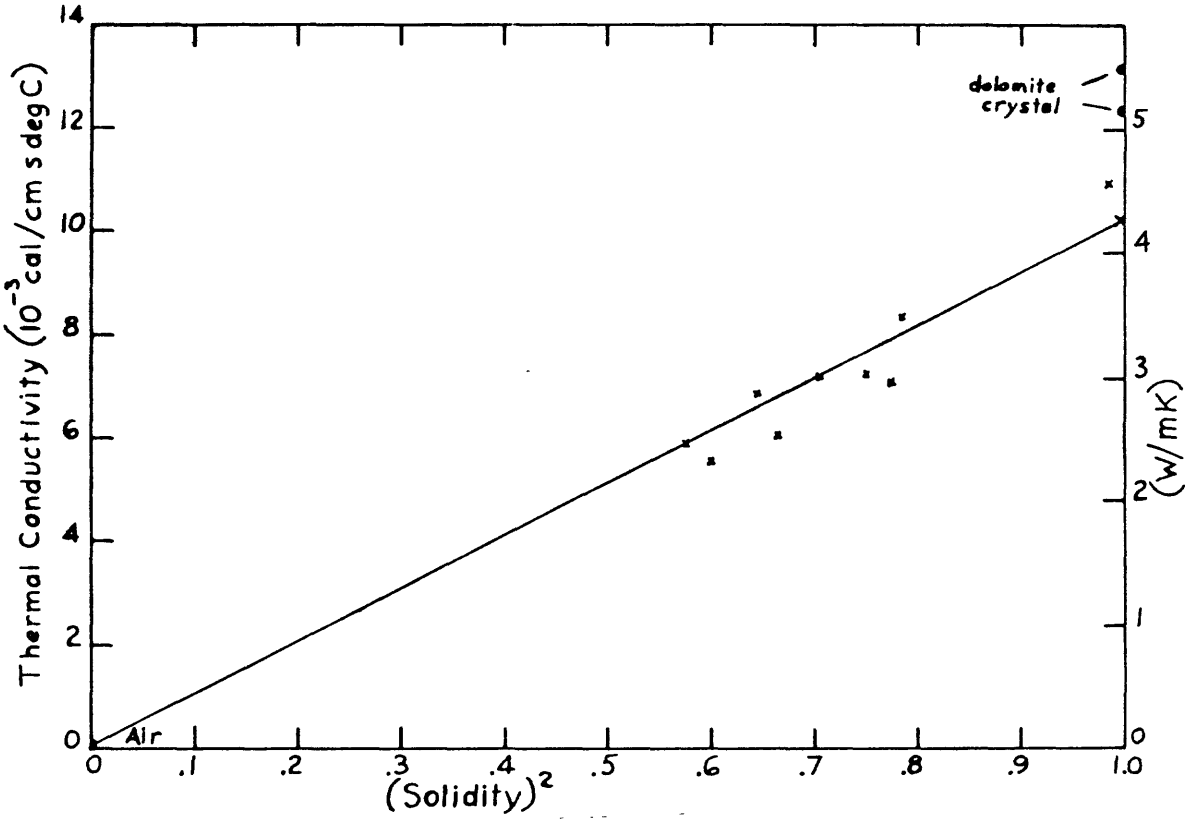

FIGURE 7. Thermal conductivity of dolostone with air in the pores, showing variation with solidity, at 300 K, 5MPa.

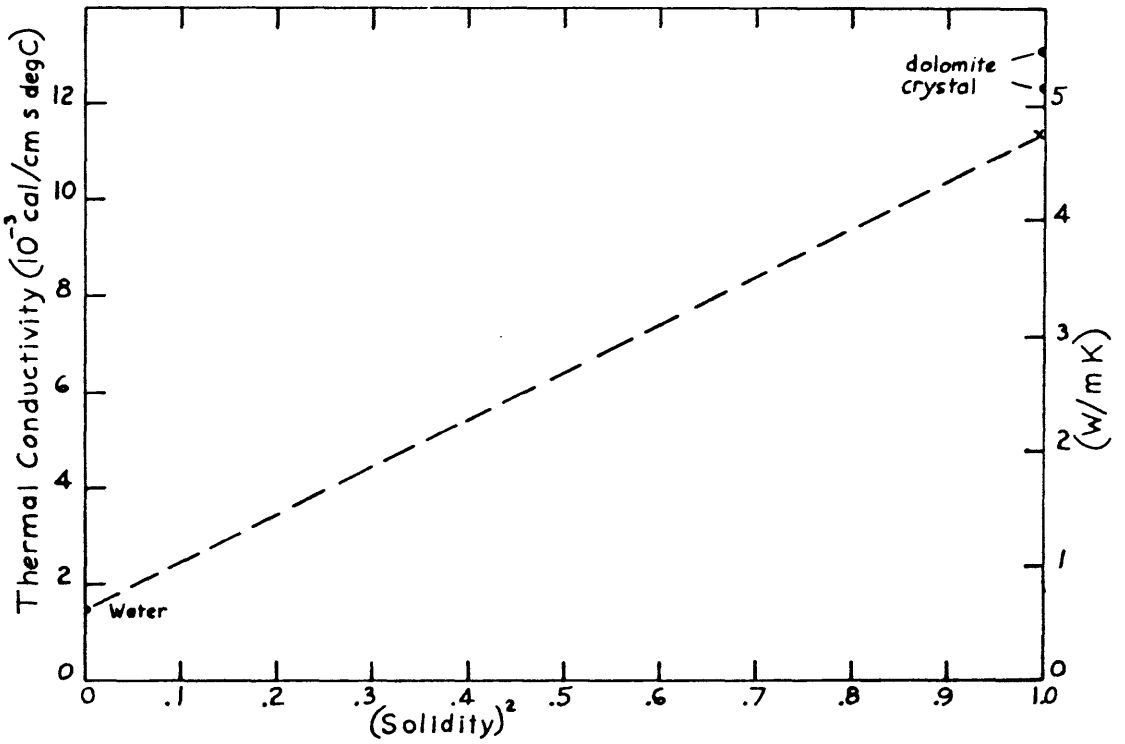

FIGURE 8. Thermal conductivity of dolostone with water in the pores, showing variation with solidity, at 300 K, 5MPa.

Sandstone, Air in Pores

The significant raising of $\underline{K}$ by increasing the quartz content in sandstone is clear in figure 9; the volume percentages of quartz are marked adjacent to the points. Unfortunately, only a few investigators did petrographic work on these air-saturated samples, but by adding to those data the requirement of internal-consistency of pairs of measurements made on the same samples with air (fig. 9) and then with water (fig. 10) in the pores, this graph was filled in satisfactorily. As clay content is usually low in sandstones, the lowering of $\underline{K}$ by clay is estimated to be small in these sandstones. As with basalt (figs. 1 and 2), the matrix of nonquartz minerals, mostly feldspars, are assumed to vary uniformly with solidity, so that only the quartz content need be known. Note that because of its very high $\underline{K}$, the content of all quartz, from small- to large-sized grains, is used in the felsic rock graphs, in contrast with the use of just phenocryst content of olivine, etc., in the mafic rock graphs.

The measurements of single crystal quartz of Birch and Clark (1940) were used to calculate the average K = 17.90 CU for quartz shown in figure 9 at $\gamma^2 = 1$; the range is from 14.62 CU to 24.36 CU perpendicular and parallel to the C-axis respectively. The high values in figure 9, above the 100 percent quartz line, are probably for well-cemented sandstones, possibly with preferred grain orientations of their C axes in the high heat-flow direction.

The measurements of $\underline{K}$ on sandstones used in preparing this graph were made by Bullard (1939), Clark (1941), Zierfuss and Vliet (1956), P.E. Byerly (written commun., 1958), Woodside and Messmer (1961) Sugawara and Yoshizawa (1961, 1962), Sucharev and Sterlanko (1970), Anand and others (1973), and Birch and Clark (1940).

The locations of the isopleths are forced slightly in order to intercept the $\underline{K}$ value for air, 0.063 CU, at $\gamma^2 = 0$, and to be evenly spaced. The intercepts for figure 9 are as follows.

$(\text{Solidity})^2$	Quartz (Volume percent)	Conductivity intercept (CU)		Factor S (CU/percent)
0	0	$\underline{K}_F$	0.063	
1	0	$\underline{K}_S$	3.50	
1	100	$\underline{K}_S$	12.50	0.090

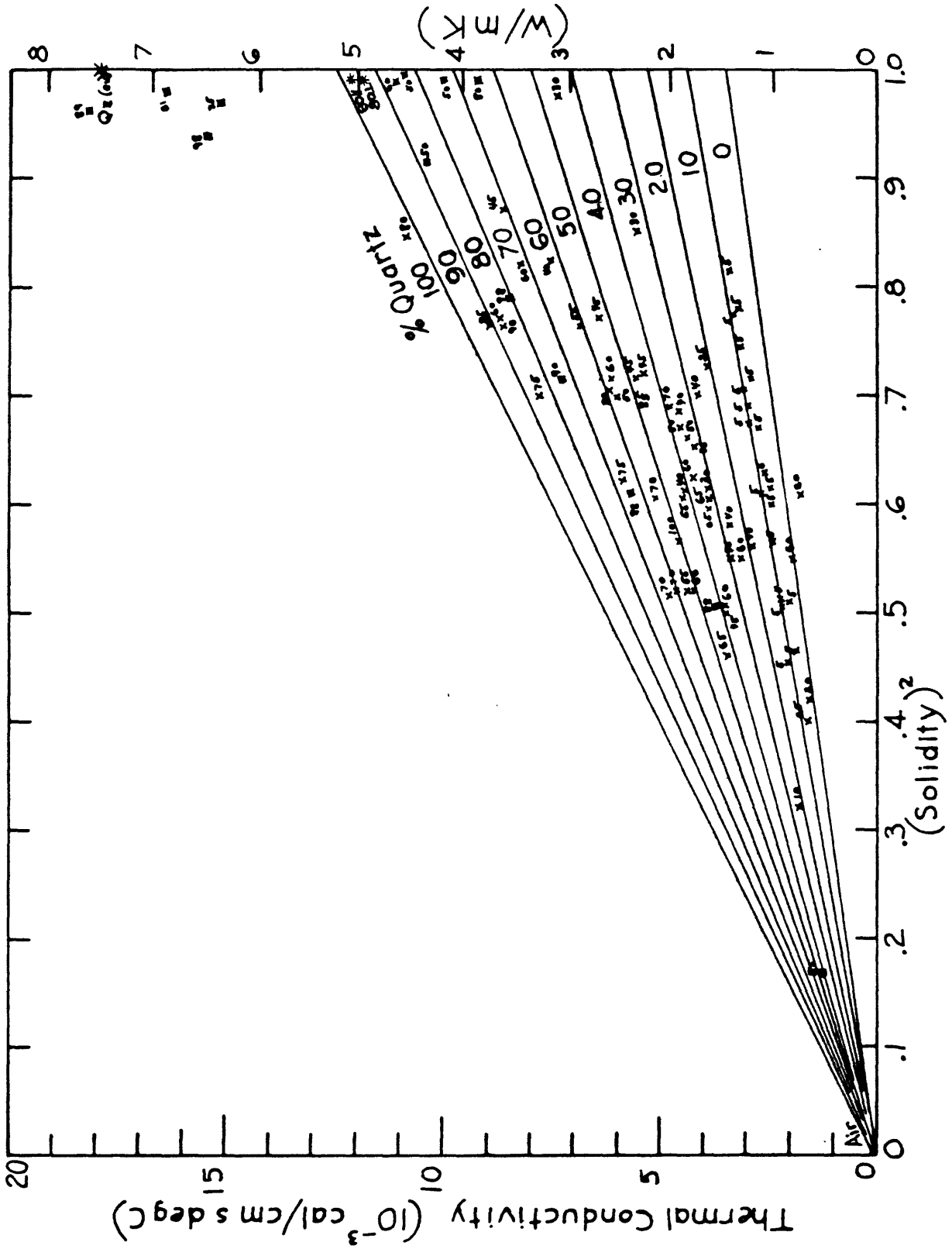

FIGURE 9. Thermal conductivity of sandstone with air in the pores, showing variation with solidity and quartz content, at 300 K, 5MPa.

Sandstone, Water in Pores

With water saturating the pores of sandstone, the effect shown in figure 10 of raising the $\underline{K}$ with increasing quartz content is much enhanced over air-saturated pores (fig. 9). Quartz percentages are placed adjacent to the points. The self-consistency in quartz contents of pairs of measurements in figures 9 and 10 is useful, but there are many more sample modes available for figure 10. Clay content is usually low and is not important in lowering $\underline{K}$ of water-filled sandstones.

The average value for quartz crystal, $\underline{K}$ = 17.90 CU, falls near the 100 percent quartz intercept at $\gamma^2 = 1$. The single crystal measurements were made by Birch and Clark (1941).

The isopleths of figures 9 and 10 are quite well-substantiated by measurements, and as they proved to fit the more sparse data for felsic igneous rocks and for shale, they were used as the base for each of those two quartz-bearing rocks. At $\gamma^2 = 1$, with no porosity, the isopleths properly should coincide. However, because of an enhanced thermal impedance due to inaccessible pores, the isopleths for the air-saturated samples are lower than those for water, at $\gamma^2 > 0.9$. Partial saturation values are obtained by the rule of 80 percent increase in $\underline{K}$ for 50 percent saturation described in the Introduction.

The data used to make this chart are from Clark (1941), Bullard and Niblett (1951), Asaad (1955), Zierfuss and Vliet (1956), Kunnii and Smith (1961), Woodside and Messmer (1961), Sugawara and Yoshizawa (1961, 1962), Hutt and Berg (1968), and Anand and others (1973).

The intercepts from Figure 10 are listed below.

$(\text{Solidity})^2$	Quartz (Volume percent)	Conductivity intercept (CU)		Factor S (CU/percent)
0	0	$\underline{K}_F$	1.48	
1	0	$\underline{K}_S$	3.63	
1	100	$\underline{K}_S$	19.35	0.157

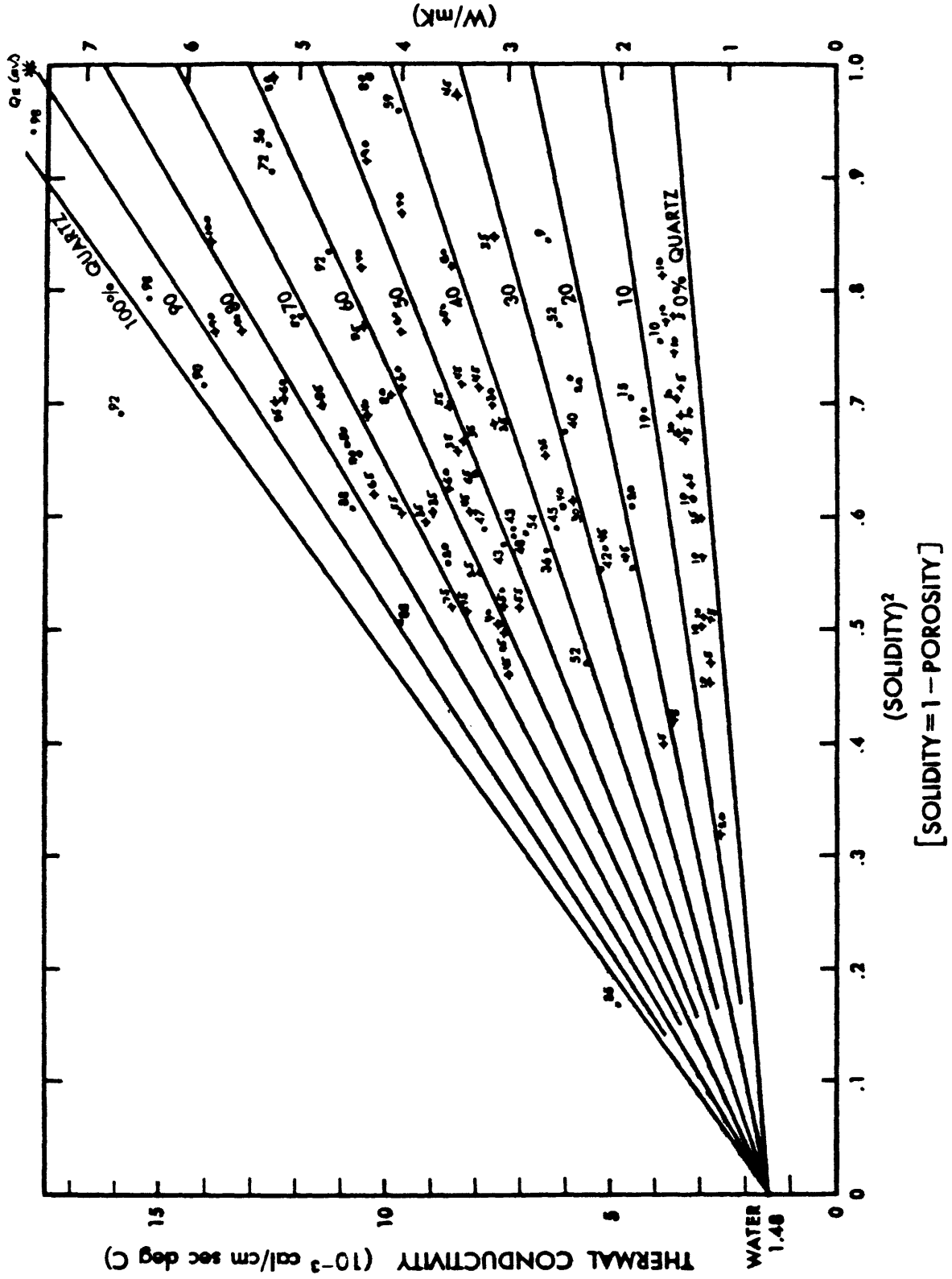

FIGURE 10 Thermal conductivity of sandstone with water in the pores, showing variation with solidity and quartz content, at 300 K, 5MPa.

Shale, Water In Pores

In figure 11 for water-saturated shale and soil, the display of isopleths of quartz content is taken from the sandstone plot of figure 10. By using the sandstone relations of $\underline{K}$ to quartz content, it is possible to estimate the effect of clay mineral content, illite, montomorillonite, and kaolin, in decreasing the $\underline{K}$ of shale. The feldspar content in both sandstone and shale is assumed to be constant in affecting $\underline{K}$. The lowering of $\underline{K}$ is due to the low conductivity of clay and mica minerals perpendicular to the layering of the flakes, ($\underline{K}_{perp}$ = 1 CU, $\underline{K}_{para}$ = 8 CU, W. H. Diment, written communication, 1968) and to the presence of many air-filled pores between flakes.

This graph is derived from measurements of shaley rock, comprised of the points of $0.5 < \gamma^2 < 1$, and of shaley soil, for which $0.12 < \gamma^2 < 0.5$. The "X" points for the soils and shales are marked with quartz content above and clay content below. The triangle points at $0 < \gamma^2 < 0.17$ are for oceanic muds from Radcliff (1960, and in Clark, 1966) and Butler (in Clark, 1966); no petrographic data are available on them.

The soils data are from Kersten (1949), Higashi (1952), and Penner (1963). A number of samples were measured by Penner (1963) both vertically across the bedding (and clay flake layering) and horizontally, parallel to it; the points are marked "v" and "h" respectively, at the same γ^2 value, separated by a difference of about $\underline{K}_h - \underline{K}_v = 0.5$ CU; this shows the anisotropy in $\underline{K}$ in these soils, due to the clay primarily.

The shale points (fig. 11) marked by a star between quartz content lines of 0-10 percent, are from Benfield (1947). The quartz values above the points of Benfield are the isopleth values from figure 12 for the same shale samples saturated with air; this internal-consistency method of finding quartz values was used for certain sandstone points also (figs. 9 and 10). The dot points lined up at about $\gamma^2 = 0.72$ are from a suite of shales measured by King and Simmons (1972); no modes are given. The nearly vertical line at $\gamma^2 = 0.97$ is from Sukharev and others (1972), and shows the spread of values for six samples of aleurite, containing 55-70 percent quartz. Other data on shales are from Bullard and Niblett (1951), Beck and Beck (1958), and Zierfuss (1969). The square point at $\gamma^2 = 0.72$, $\underline{K}$ = 2.41 CU, is from James Combs and C.A. Swanberg (written commun., 1975); it is their "best clay" calibration value for shales, and is for a layer containing 95 percent clay minerals.

The generalized scheme in the next paragraphs can be used to account for the quartz and clay effects on $\underline{K}$ for shales or soils with known solidity. The method involves correcting the quartz content for the clay content to a fictive value for quartz and then using the sandstone isopleths of quartz to find the value of the $\underline{K}$ at the given γ^2. The effect of anisotropy is neglected; only values of $\underline{K}$ normal to bedding are considered. For soil broken up from its natural state and reconstituted, there seems to be only a slight reduction in $\underline{K}$ by the clay minerals, and no anisotropy.

For shales and soils with quartz content more than 35 percent, the clay content is usually less than 30 percent, and for such shales the modal content of quartz would be reduced one-for-one by the modal clay content to attain a fictive value of quartz to use on the graph (fig.11). For example, with quartz = 50 percent, clay = 15 percent, the fictive quartz = 35 percent, the number to use on figure 11 to obtain the $\underline{K}$.

For shales and soils with quartz content less than 35 percent, the clay may range from low to high in proportion, but the clay apparently is not so effective in reducing $\underline{K}$. The following scheme may be used (albeit with some uncertainty). Subtract 20 percent from the clay content, and then subtract any remainder percentage of clay from the quartz percentage to obtain the fictive value of quartz to use on the graph (fig.11). For example, with quartz = 30 percent, clay = 60 percent, the fictive value would be quartz = 30 - (60 - 20) = - 10 percent, and thus the value of $\underline{K}$ would be below the zero quartz isopleth by 10 percent at the given γ^2. This scheme badly needs supportive or amending data. The intercept data for figure 11 for use in equation 6 are listed below.

$(\text{Solidity})^2$	Quartz (Volume percent)	Conductivity intercept (CU)		Factor S (CU/percent)
0	0	$\underline{K}_F$	1.48	
1	0	$\underline{K}_S$	3.63	
1	100	$\underline{K}_S$	19.35	0.157

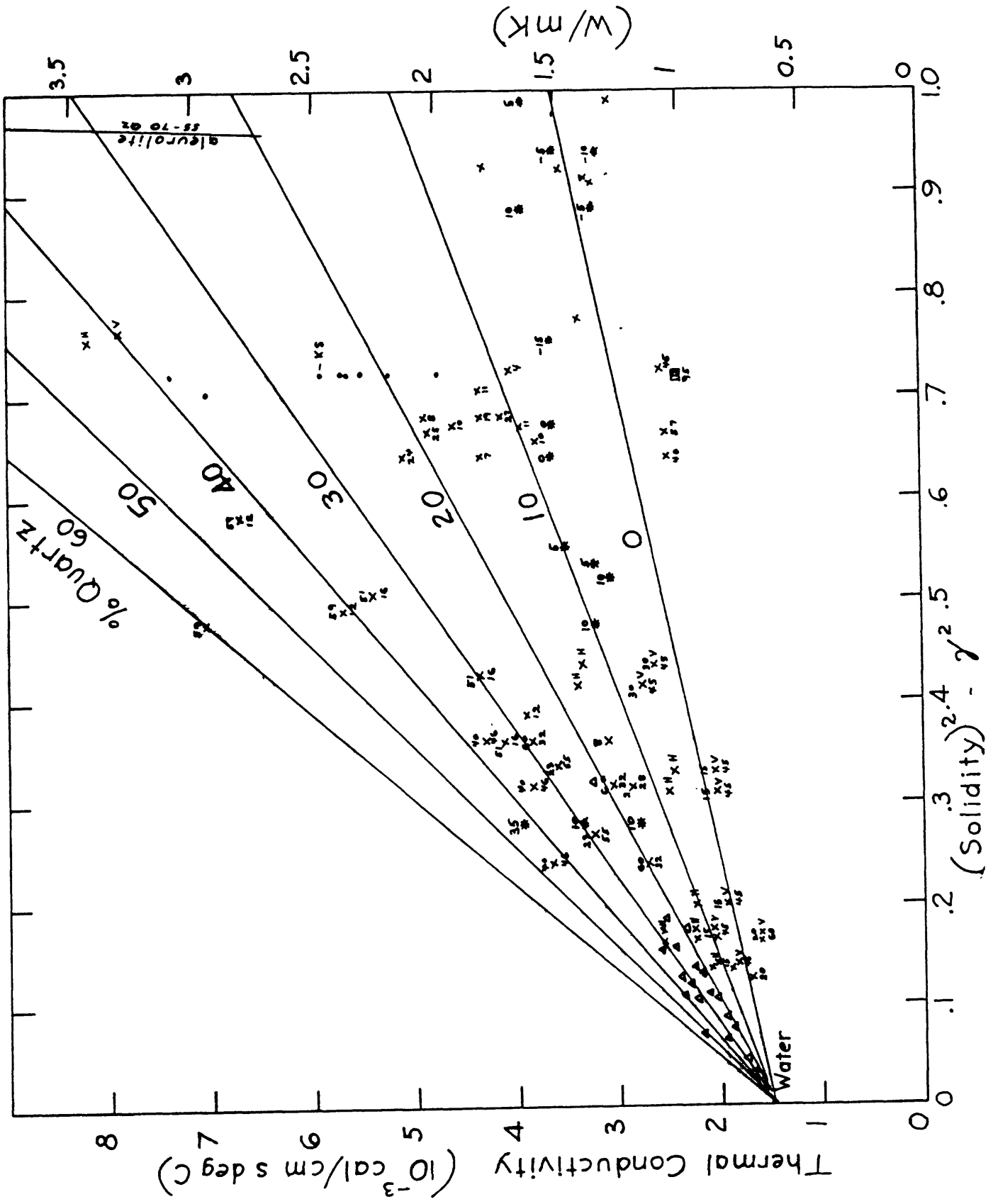

FIGURE 11. Thermal conductivity of shale with water in the pores, showing variation with solidity and quartz content, at 300 K, 5MPa.

Shale, Air in Pores

The quartz isopleths in figure 12 for shale are the same as those of air-saturated (that is, dry) sandstones in figure 9. There is no petrographic information at hand for the shale samples measured. The values of $\underline{K}$ for points marked with percent quartz are from Benfield (1947); the quartz contents are derived from figure 11 and are the internal-consistency values. The other, unmarked (quartz percent) observations for shale samples with air in the pores are from Bullard (1939), Benfield (1947), and Mossop and Gafner (1951). The points marked "h" and "v" are measurements, parallel and perpendicular (horizontal and vertical) to bedding, made by Beck and Beck (1958), which show that anisotropy of their sample is much greater with air in the pores than with water there (see fig. 11).

Without observations of quartz and clay content, the data plotted in figure 12 for dry shale cannot be analyzed for the effect of quartz and clay on $\underline{K}$. The values at the data points from Benfield (1947) in figures 11 and 12 are only relative and are not absolute quartz percentages; the unknown amount of clay in the shales would certainly decrease $\underline{K}$ below the amount that would be predicted using only the actual quartz content and the sandstone isopleths in figure 12. Similarly, the other points plotted are positioned at $\underline{K}$ values determined by the amount of clay as well as quartz in each sample. Lacking a clear relationship for air-saturated shale, the same procedure evolved for water-saturated shale to account for the effect of clay and to find a fictive quartz-value may be used, as described for figure 11. The intercept data for figure 12 foruse in Equation 6 are listed below.

$(\text{Solidity})^2$	Quartz (Volume percent)	Conductivity intercept (CU)		Factor S (CU/percent)
0	0	$\underline{K}_F$	0.063	
1	0	$\underline{K}_S$	3.50	
1	100	$\underline{K}_S$	12.50	0.090

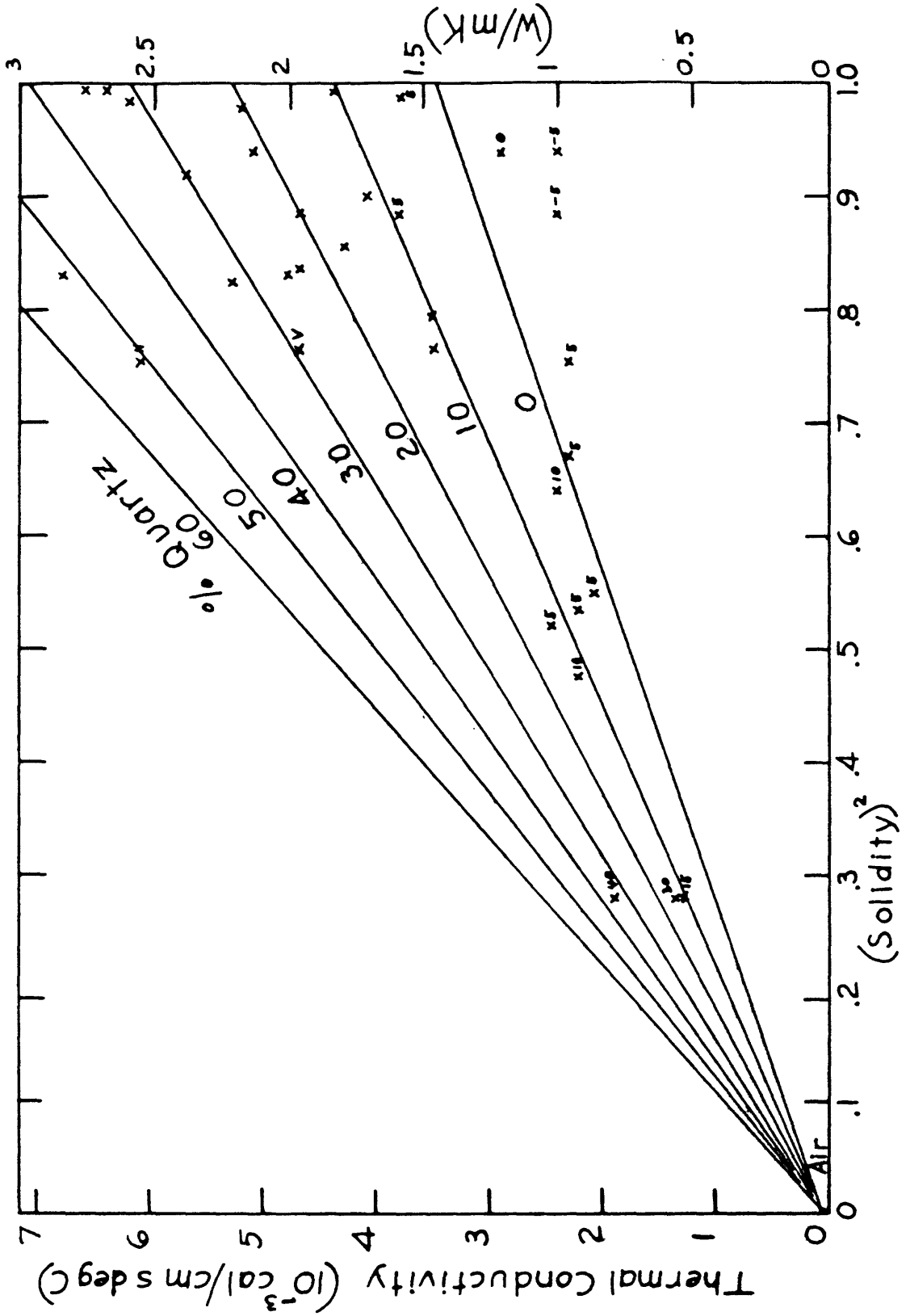

FIGURE 12 Thermal conductivity of shale with air in the pores, showing variation with solidity and quartz content, at 300 K, 5MPa.

Soils, Air in Pores

The values of $\underline{K}$ for dry soils, with air in the pores, most of which can be considered as unconsolidated shales, are very much lower than those for dry shales. In figure 13 a set of isopleths has been drawn (full lines) to fit the quartz content only of the dry soils; the lower three isopleths for shale from figure 12 are shown (dashed lines) for comparison of degree of consolidation. Similar to usage in figure 11, fictive quartz values can be obtained to estimate $\underline{K}$ in figure 12 by subtracting the clay percentage (numbers below the points) from the quartz (numbers above the points). Thus for quartz = 40 percent and clay = 15 percent, the fictive quartz = 25 percent, at the given γ^2.

Data used in plotting are from Smith and Byers (1938), Kersten (1949), and Higashi (1952). The quartz and clay contents for points from Smith and Byers were calculated for probable mineral compositions from chemical analyses of the soils.

The isopleths in figure 13 are forced through the $\underline{K}$ for air, and the pertinent intercepts are as follows.

$(\text{Solidity})^2$	Quartz (Volume percent)	Conductivity intercept (CU)		Factor S (CU/percent)
0	0	$\underline{K}_F$	0.063	
1	0	$\underline{K}_S$	0.84	
1	100	$\underline{K}_S$	2.49	0.0165

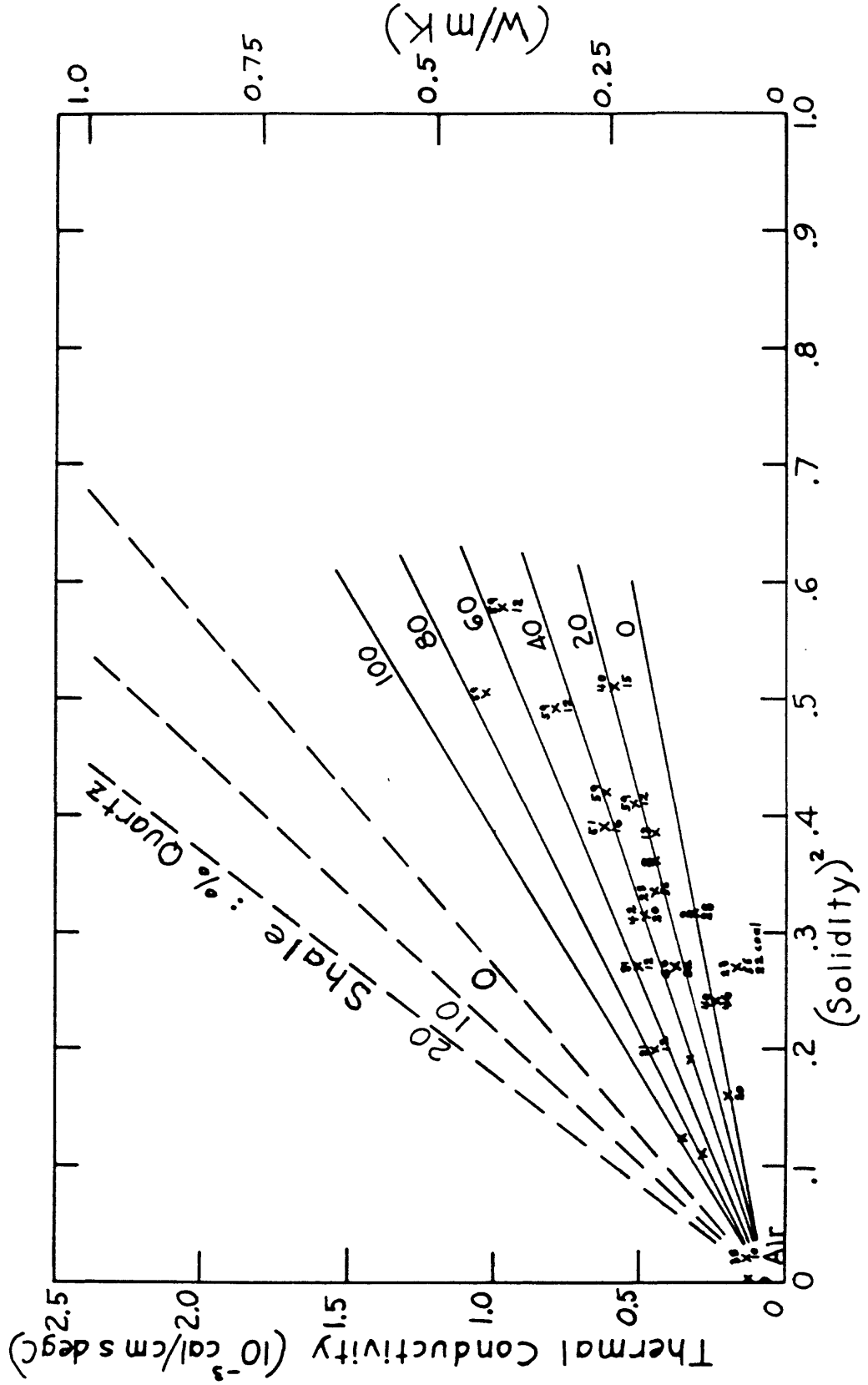

FIGURE 13 Thermal conductivity of inorganic soil with air in the pores, showing variation with solidity and quartz content, at 300 K, 5MPa.

Anhydrite and Gypsum, Air in Pores

Figure 14 was prepared to aid in assessing the possible use of anhydrite or gypsum beds as repository sites for radioactive waste or other purposes. The points plotted for $\underline{K}$ versus γ^2 are for monomineralic aggregate samples of anhydrite and gypsum. The point for gypsum is from Horai (1971), and the points for anhydrite are from Eucken (1911), Coster (1947), Bullard and Niblett (1951), and Herrin and Clark (1956). Many measurements were made by Zierfuss (1969) on impure anhydrite rock samples, but the values are much lower, averaging about $\underline{K} = 8$ CU at $\gamma = 0.95$, and are not plotted; the anhydrite probably contains considerable gypsum.

The lines of variation in figure 14 with γ^2 are forced through the value of $\underline{K}$ for air, and the intercepts are as follows:

Mineral	(Solidity)^2	Conductivity intercept (CU)	
Gypsum	0	$\underline{K}_F$	0.063
	1	$\underline{K}_S$	3.15
Anhydrite	0	$\underline{K}_F$	0.063
	1	$\underline{K}_S$	14.12

The inset drawing shows the effect of temperature on $\underline{K}$ of anhydrite and of some reference minerals and rocks, quartz, halite, granite, and basalt. The purpose of adding this inset is also to aid in radioactive waste assessments. The measurements on anhydrite were made by Weber (1895) from 0° to 110 °C, with a slope of -2.95 CU/100 °C. The other curves are taken from figures 15, 16, 21, and 27; the basalt has 11 percent porosity, but the other materials are quite dense.

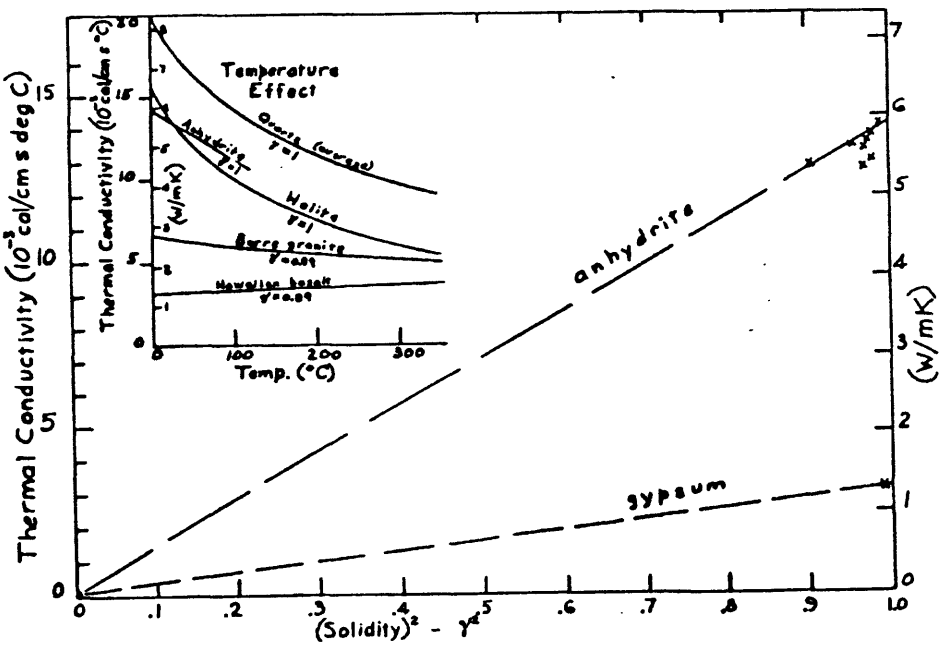

FIGURE 14. Thermal conductivities of anhydrite and gypsum with air in the pores, at 300 K, 5 MPa.

Selected Rocks

Some fairly common rocks have not been studied fully enough to allow graphs to be prepared of their $\underline{K}$, γ, and pore fluid values, but these supplemental values of $\underline{K}$ for dense ($\gamma > 0.95$) igneous and metamorphic rocks are listed in table 1. These rocks were tested at 300 K and 5M Pa with air in the pores. Most of the data are from Clark (1966 , Section 21), but the original references are shown.

TABLE 1.--Thermal conductivity at 300 K and 5 MPa of selected alkalic and ultramafic rocks

Rock type	Conductivity (10^{-3} cal/cm sec °C)		Number of samples	Reference
	Mean	Range		
Amphibolite.....	6.92	6.1-9.1	6	Birch (in Clark, 1966).
Gabbro.....	4.93	4.60-5.45	3	Birch and Clark, 1940.
Norite.....	6.42	5.5-7.3	5	Misener and others, 1951.
Syenite, syenite porphyry.	7.66	6.3-9.5	37	Misener and others, 1961.
Syenite.....	5.21		1	Birch and Clark, 1940.
Pyroxenite.....	10.3	10.1-10.5	2	Do.

Conductivity Anisotropy of Metamorphic Rocks

The layering in dense ($\gamma > 0.95$) metamorphic rocks may be a foliation or an inherited bedding, and its presence usually results in a difference in thermal conductivity between directions parallel and perpendicular to the layering. The anisotropy in $\underline{K}$ is represented in table 2 by the ratio of $\underline{K}$ parallel to foliation to $\underline{K}$ perpendicular to foliation, which ranges from 1.02 to 1.69. Data collections on anisotropy have been made by Clark (1966, Section 21) and by Hurtig (1986). The ultimate cause of anisotropy, the mineral layering, primarily of mica, is difficult to assess quantitatively (see Diment and others, USGS, Open-file Report, 1988).

TABLE 2.--Anisotropy of thermal conductivity at 300 K and 5 MPa in dense metamorphic rocks

[Perp, perpendicular to foliation; Para, parallel to foliation]

Rock type	Orientation	Conductivity (CU)			Number of samples	Reference
		Mean	Ratio (Para/Perp)	Range		
Gneiss	Perp.....	6.34		4.6-7.7	22	Clark and Niblett, 1956.
(Simplon	Para.....	8.90	1.40	6.0-11.4	8	
tunnel).						
Gneiss, mica-	Perp.....	6.27			12	Clark and Niblett, 1966.
(Loetschberg	Para.....	9.32	1.49		6	
tunnel).						
Gneiss	Perp.....	5.08			1	Birch and Clark, 1940.
(Pelham).	Para.....	7.19	1.42		1	
Gneiss, schist	Perp.....	6.95			15	Birch, 1950.
(Adams	Para.....	8.55	1.23		17	
tunnel).						
Gneiss	Perp.....	6.24			9	Clark, 1966.
(Vermont).	Para.....	8.33	1.33	6.1-10.4	9	
Gneiss, schist	Perp.....	7.23			8	Clark, 1961.
(Arlberg	Para.....	10.74	1.49		7	
tunnel).Granite gneiss	Perp.....	6.85			9	Clark, 1961
(Tauern	Para.....	8.87	1.29		13	
tunnel).						

Rock Type	Orientation	Conductivity (CU)			Number of samples	Reference
		Mean	Ratio (Para/Perp)	Range		
Gneiss, schist	Perp.....	5.51			10	Diment and others, 1965.
(Aiken, SC).	Para.....	7.01	1.27		10	
Limestone.....	Perp.....	5.9			1	Birch and Clark, 1940.
	Para.....	7.9	1.34		1	
Dolomite	Perp.....	9.35			58	Meincke and others, 1967.
(Thuringen).	Para.....	9.50	1.02		61	
Anhydrite	Perp.....	8.54			13	Do.
(Thuringen).	Para.....	8.71	1.02		12	
Marble.....	Perp.....	6.7			1	Birch and Clark, 1940.
	Para.....	6.9	1.03		1	
Phyllite.....	Perp.....	7.89		6.5-9.0	7	Do.
	Para.....	11.83	1.50	9.5-14.0	9	
Quartzitic	Perp.....	12.2			1	Do.
sandstone.	Para.....	12.6	1.03		1	
Quartzite,	Perp.....	7.0			4	Sass and Le Marne, 1963.
gneiss	Para.....	11.8	1.69		4	
(Broken Hill, Australia).						
Sandstone	Perp.....	4.59			28	Meincke and others, 1967.
(Thuringen).	Para.....	5.46	1.19		19	
Sandstone	Perp.....	7.14			17	Hurtig, 1956.
quartzite.	Para.....	7.74	1.08		17	
Schist	Perp.....	5.74		4.1-6.8	8	Clark and Niblett, 1956.
(Simplon	Para.....	7.50	1.31	6.8-8.9	7	
tunnel).						
Schist, gneiss	Perp.....	6.62			35	Diment and Werre, 1964.
(Washington.	Para.....	8.61	1.30		34	
D.C.)						
Slate, schist	Perp.....	3.62			2	Meincke and others, 1967.
(Thuringen).	Para.....	6.03	1.67		2	

ROCK CONDUCTIVITY CHANGE WITH TEMPERATURE

Introduction

The thermal conductivity K of most rocks decreases with increase in temperature T, about -30 percent from 0° to 100° for rocks rich in quartz, calcite, and olivine (figs. 14-19). Basalt, rock glass, and some porous sandstone conductivities increase slightly with temperature. No reliable data are available on shales and sandstones above 200 °C. The pressure applied to the rock samples in figures 14-19 was about 5 MPa.

In the following explanations of the figures, the measurements, and their sources are described. In general, these plots of T versus K for the principal rock types can be used as follows: first ascertain the value of K at some T, say 300 K, by actual measurement or by estimation from the previous γ^2 versus K charts, figures 1-13; then, using figures 14-19, follow the curve passing nearest the estimated K value at 300 K to the T of interest.

The effect of porosity above 5 percent on reducing K is important and a rough estimate of K for porous rocks can by made by constructing a line of K versus γ^2 between a value of K at the T of interest and the K for air, 0.063 CU, and interpolating at the γ^2 of the rock.

The data in these figures are from laboratory observations, and heat transfer occurs by all mechanisms, including solid conduction, radiation, and convection of fluids in the pores. Differentiating among these mechanisms was not attempted by the original investigators and is of course not possible here.

Basalt and Other Mafic Rocks

The upper curves in figure 15 are from Birch and Clark (1940) from data on intrusive dense diabase and gabbro samples (marked BC-D and BC-G) whereas the other curves and points are from extrusive basalt data. The other references for the data given on figure 14 include Poole (1914), "P", Bridgman (1924), "B", Stephens (1963), "S" (triangles, without fitted lines), Kawada (1966), "K", Kanamori and others (1969), "KMF", Petrunin and others (1971), "P", Robertson and Peck (1974), "RP", and Peck and others (1977), "PHS". The numbers in parentheses on figure 15 are decimal solidities. The slope of the line from Peck and others (1977), 0.19 CU/100 ° may be taken as an average for vesicular basalt. It is subparallel with Kawada's line, and falls on the trend of Stephen's points (triangles).

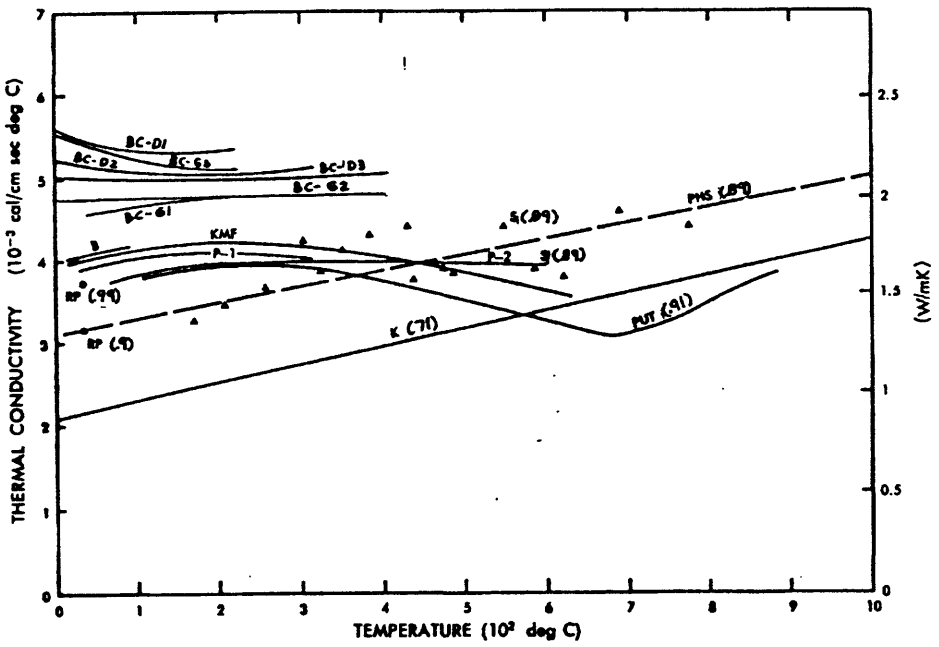

FIGURE 15. Temperature effect on thermal conductivity of basalt and other mafic rocks at 5 MPa; number in parentheses is decimal solidity.

Felsic Igneous Rocks

The curves in figure 16 are derived from the data on selected, felsic igneous rocks, named on appropriate curves, measured by Birch and Clark (1940). Birch and Clark used thermal resistivity (reciprocal of $\underline{K}$) for extrapolation and interpolation, but the conductivities plotted here emphasize the family character (quartz dependence primarily) of felsic rock curves. The interpolated curves were drawn to pass through values of $\underline{K}$ at 0.1 CU spacing at 35 °C. With an estimated $\underline{K}$ of a particular rock at a given $\underline{T}$, the nearest curve to that point can be followed to estimate the $\underline{K}$ at some other $\underline{T}$. The inset figure shows the relation of these curves to that of mean $\underline{K}$ for quartz. The anisotropy effect is shown by the two Pelham gneiss curves, parallel and perpendicular to the foliation of the mica minerals. Rockport-2 granite has a somewhat higher quartz content (33 percent) than Rockport-1 (25 percent). This granite has a closely interlocking grain texture and large subparallel quartz grains.

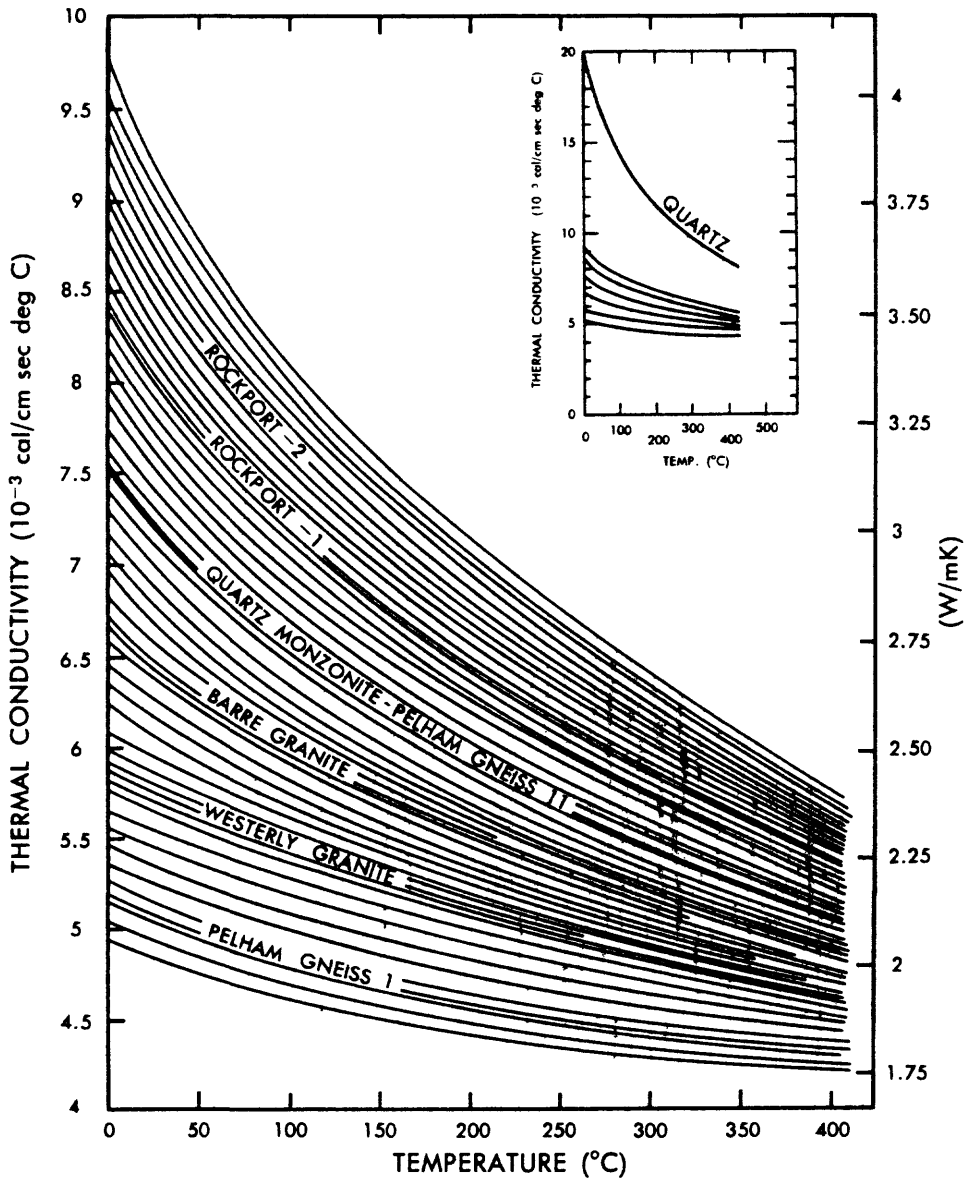

FIGURE 16. Variation of thermal conductivity with temperature for a series of dense felsic igneous rocks, at 5 MPa; smooth change in conductivity with quartz content is shown by inset figure.

Carbonate Rocks

The temperature effect on the $\underline{K}$ of limestone and dolostone is negative, as shown in figure 17. The curves marked "BC" are from Birch and Clark (1940); the letters following, "l", and "m", and "d" mean limestone, marble, and dolostone; the symbols "$\parallel$ " and "$\perp$" mean parallel and perpendicular to bedding; the number in parentheses represents decimal solidity γ. The curves marked "M" are from Mirkovitch (1968); the letters "l" and "d" and the numbers in parentheses have the same meaning.

For single crystals at 30 °C and 50 bars, average calcite $\underline{K}$ = 8.58 CU, and dolomite $\underline{K}$ = 13.16 CU (Horai, 1971), and as seen in figure 17, the rocks, limestone and dolostone, have lower $\underline{K}$'s than those of the mineral crystals (also described for figs. 5 and 7). The effect of decreasing solidity in reducing $\underline{K}$ is shown and the anisotropy due to bedding in carbonate rocks are also shown (fig. 17).

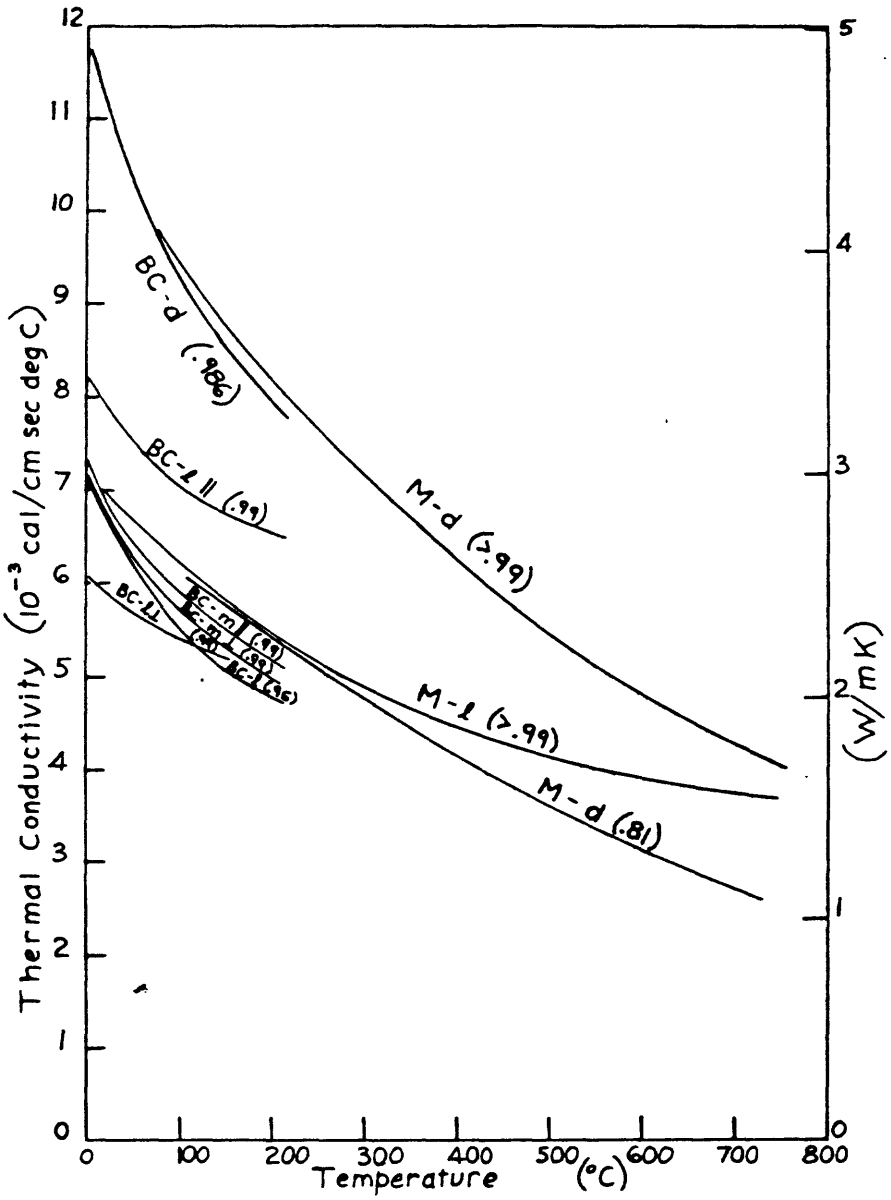

FIGURE 17. Temperature effect on thermal conductivity of dense limestone, marble, and dolostone, in directions parallel and perpendicular to bedding, with decimal solidity in parentheses, at 5 MPa.

Quartz-bearing Rocks

The upper curves in figure 18 are for dense quartzites and single crystal quartz, and they show a marked negative temperature effect on $\underline{K}$. The curves marked "BC - qz" are from single crystal measurements, parallel ($\parallel$) and perpendicular ($\perp$) to the C-axis, from Birch and Clark (1940); the average curve is obtained by weighting the perpendicular data by a factor of 2. The anisotropy of the rather dense quartzite measured by Birch and Clark $\parallel$ and $\perp$ to bedding is not large. The data for the curves marked "M - t" and "M - qt" are from Mirkovitch (1968) for dense taconite and quartzite.

The symbols on the curves in figure 18 at $\underline{T} < 200$ °C represent references, rock types, pore fluid type, and solidities, as follows. The letters "A", "BC", and "SY" are for Anand and others (1973), Birch and Clark (1940), and Sugawara and Yoshizawa (1961; 1962). The rock symbols are "ss" for sandstone, "sh" for shale, "sl" for slate; all "sy" curves are for sandstone. The pore fluids symbols are "a" for air and "w" for water saturated. The decimal values of γ are given in parentheses. At values of $\underline{K} < 5$ CU, the temperature effect is low and either slightly positive or negative, depending on the rock type and the method of measurement. The same value for γ signifies that the same rock specimen was used for both air-and water-saturated measurements. Extrapolation of these curves to higher temperature would be uncertain, although the $\underline{T}$ effect seems to be small for these porous rocks.

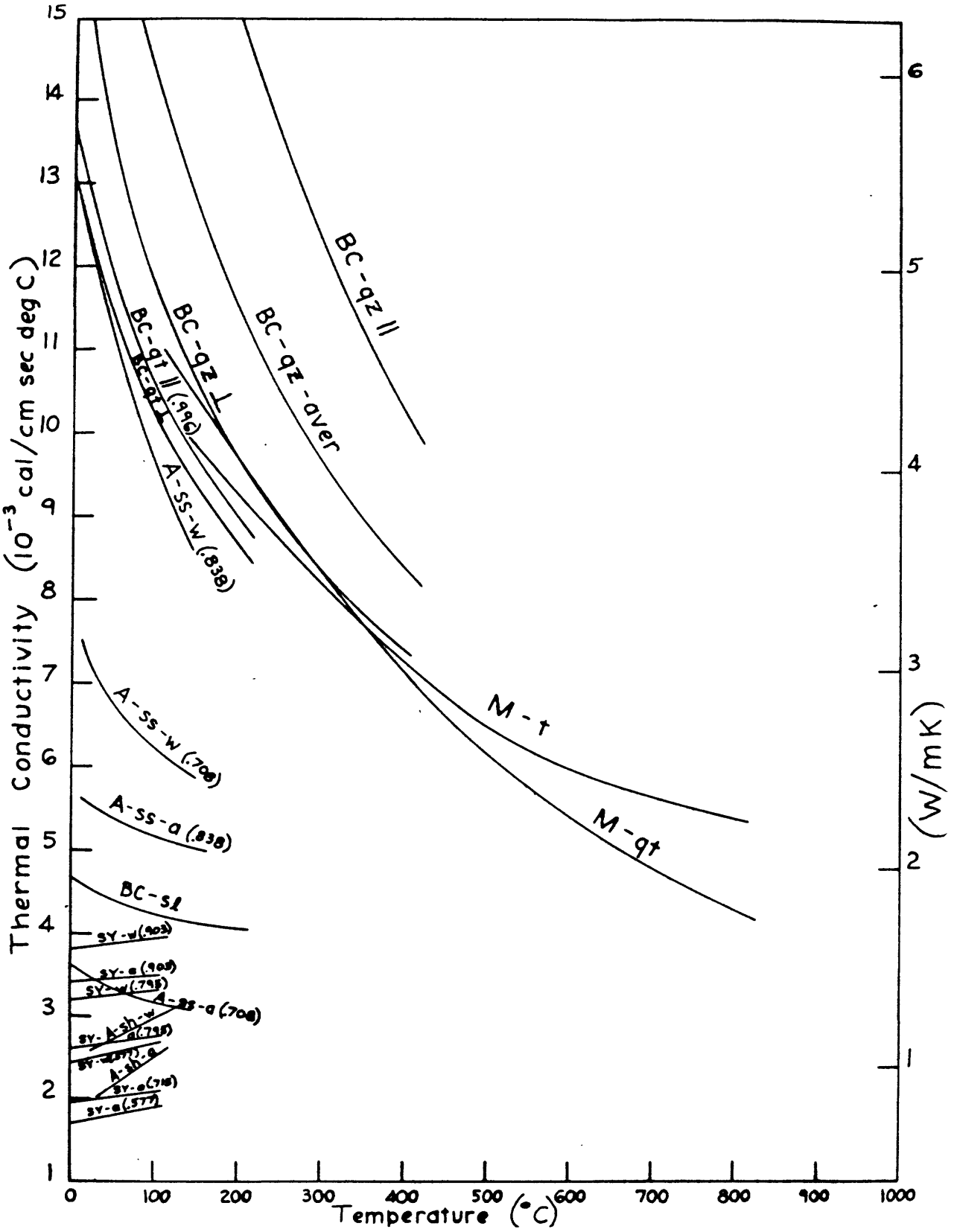

FIGURE 18. Temperature effect on thermal conductivity at 5MPa of sandstones, quartzites, and shales, with quartz shown for comparison; decimal solidity in parentheses.

Ultramafic Rocks

The ultramafic rocks shown in figure 19 have negative temperature coefficients of K. The curves are from the data of Birch and Clark (1940), marked "BC", and Kawada (1964, 1966), marked "K". The rock symbols are "hz" for harzburgite, "lh" for lherzolite, "du" for dunite, "hy", for hypersthenite, or "br" for bronzitite, "sp" for serpentinized peridotite, "p" for peridotite, and "ec" for eclogite. The numbers refer to different specimens taken from the same large block of rock.

The absolute values of K of Kawada's harzburgite and dunite (du-1) curves in figure 19 may be somewhat uncertain, as they remain high at the higher temperatures. A number of effects are not accounted for in these studies, such as, anisotropy of olivine grains due to preferred grain orientations, phenocryst versus fine grain differences, and conduction across fractures, pore, and grain-to-grain.

There is enough variety of rock type in figure 19 that the curves may be used to estimate K roughly at some T for most, dense ultramafic rocks, starting with a known K and T. To obtain a value of K for a porous ultramafic rock, a line of K versus γ^2 can be constructed between a value taken from figure 19 and K for air (0.063 CU), and an interpolation made.

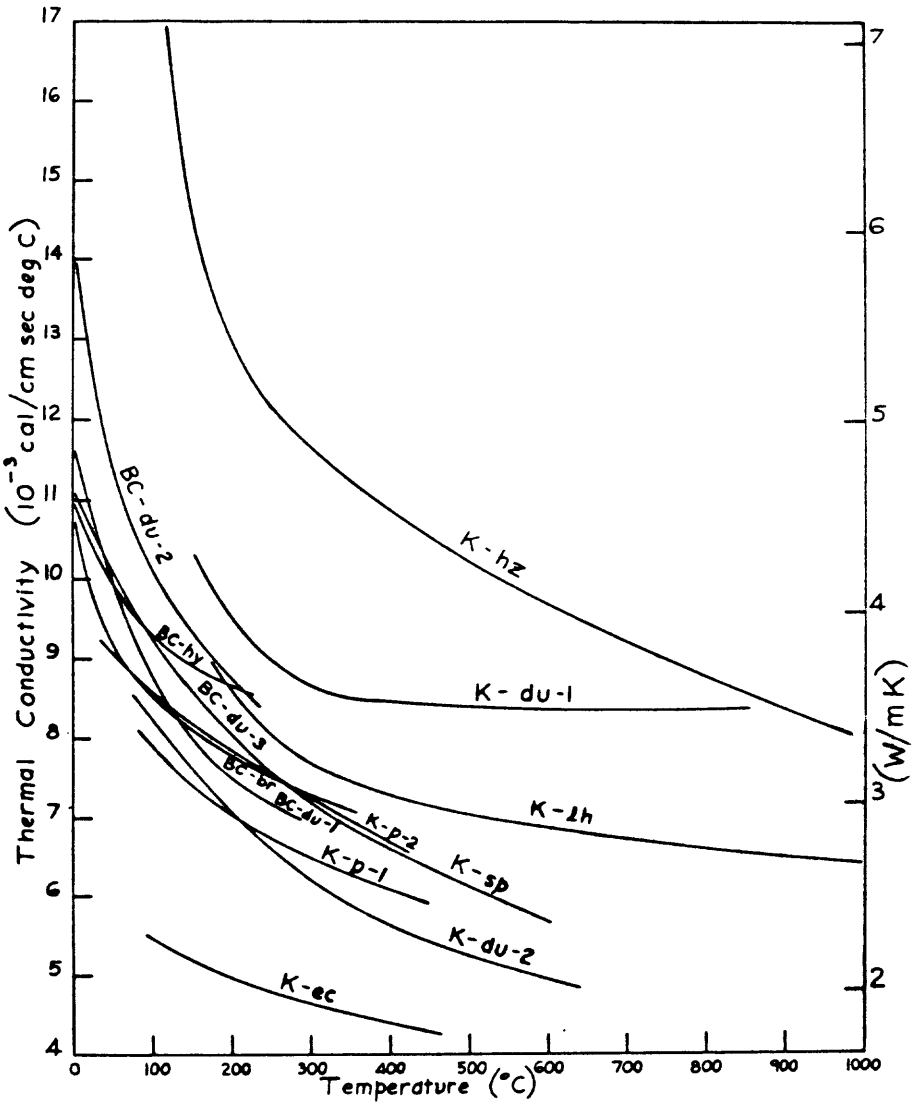

FIGURE 19. Temperature effect on thermal conductivity of several dense ultramafic rocks at 5MPa.

Rock Glasses

The curves in figure 20, marked BC and K, are from Birch and Clark (1940) and Kanamori (1968) respectively; the glasses are marked si, for silica, ob, for obsidian, and di, for diabase. The positive temperature coefficient of $\underline{K}$ for commercial glasses is well-established, and so the slopes shown in figure 20 are not surprising. (The anomalous temperature and pressure coefficients of the elastic moduli are well-known). The values of $\underline{K}$ for most commercial glasses are about the same as for the rock glasses shown for $\underline{T} < 500$ °C, and glasses for other rock compositions may be expected to have $\underline{K}$ values near the curves in this figure.

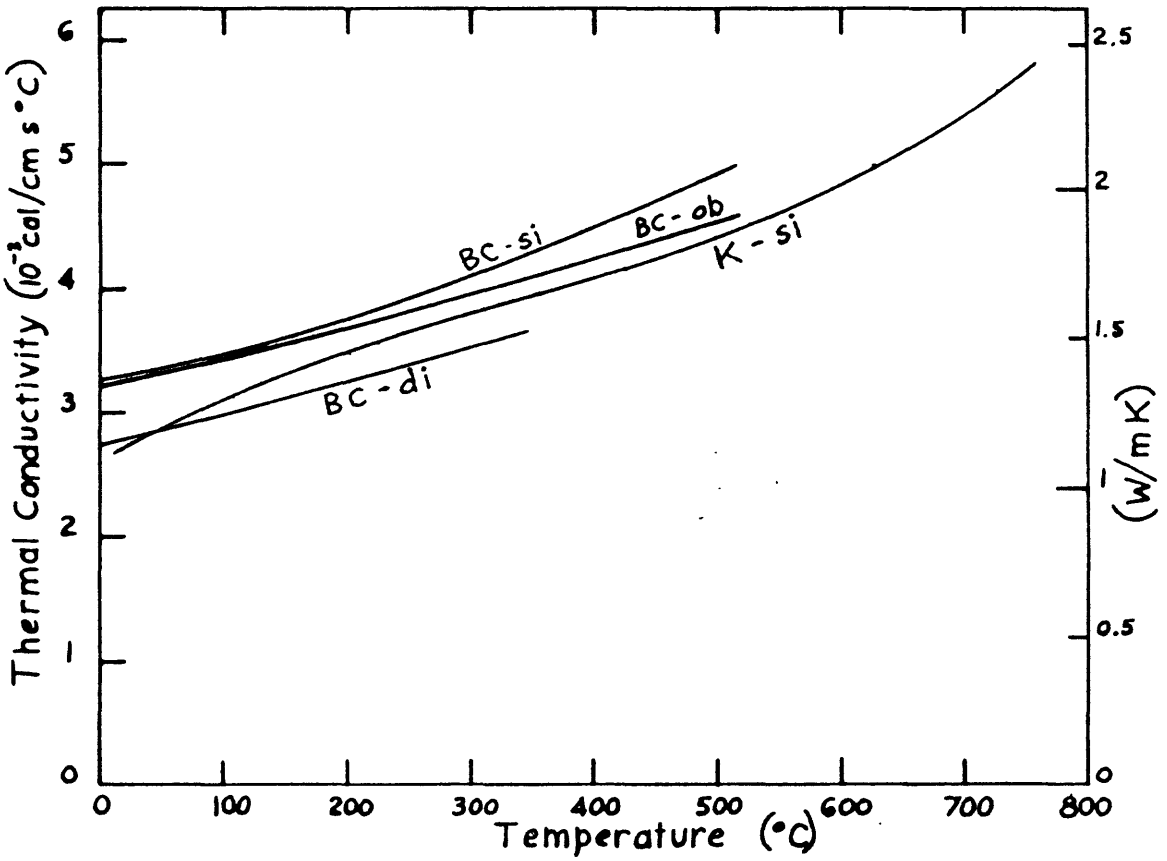

FIGURE 20. Temperature effect on thermal conductivity of diabase and silica glasses and obsidian at 5MPa.

MINERAL CONDUCTIVITY CHANGE WITH TEMPERATURE

Introduction

The thermal conductivity K of rock-forming minerals except feldspar decreases rather sharply between 0° amd 100°C, from -10 to -30 percent (figs. 21-27), and continues to decrease, more slowly, to about 600 °C, where it begins to increase for some minerals. The K of plagioclase and microcline is roughly constant with T. Separate plots (figs. 23 and 25) show the temperature variation of K for the two solid solution series of plagioclase, albite-anorthite, and of olivine, forsterite-fayalite. Only a few measurements of mica minerals are available at 30° C, and none for the T effect on K.

A comprehensive listing of K at 30° C and 5 bar for most of the common minerals is to be found in an accompanying open-file report by Diment and others (1988).

These data can be used not only to calculate K of a rock from its mode but also to adjust an initial estimate of the value of K for a rock to account for a significantly larger (or smaller) content of some mineral than is typical in such a type of rock; supposedly, figures 1-18 are for "typical" rocks. Another important use, of course, is to obtain values for the modal minerals from which to calculate the K of a rock at some T above 30° C.

Quartz

Quartz occurs as phenocrysts in felsic igneous and metamorphic rocks and as large to small grains in sedimentary rocks, and the combination of prevalence, large grain size, and very high thermal conductivity of quartz makes it the most important mineral to evaluate in estimating the thermal conductivities of rocks containing it. As shown by and described for figures 3, 4, 9 through 13, 16, and 18, the estimates of K from γ^2 and as a function of T of quartz-bearing rocks depend critically on the content of quartz. The effect of T on K of single crystal quartz is particularly large at T < 200 °C, as shown in figure 21.

The data for the curves "BC" in figure 20 are from Birch and Clark (1940), and curves marked "K" are from Kanamori and others (1968, 1969); the K's for Kanamori and others (1969) were calculated from diffisivities, using specific heats from figure 37. The triangular point at room temperature, marked "R", is from Ratcliff (1959). The symbols "||" and "⊥" mean parallel and perpendicular to the C-axis of quartz crystal. The curve marked "average" was determined from the Birch and Clark (1940) data to 700 K, and from Kanamori and others (1968) at higher temperature; this is the Voigt average, which is calculated by weighting the ⊥ value by a factor of 2.

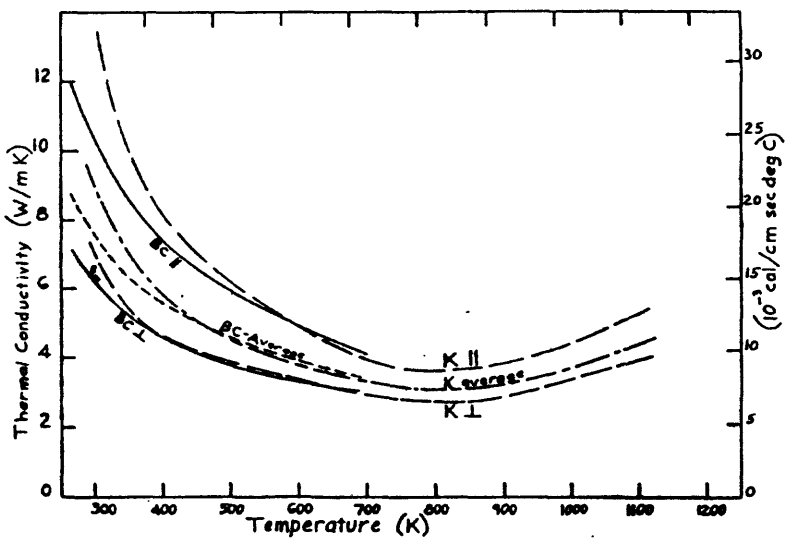

FIGURE 21. Temperature effect on thermal conductivity of single crystal quartz at 5MPa.

Feldspar

Feldspar minerals are even more prevalent than quartz in common rocks, and so are also very important in affecting the thermal conductivity K of rocks. Their K values are relatively low, as shown in figure 22. Experimental measurements made by different authors on K with increasing temperature T of feldspars are somewhat ambiguous; although some measurements indicate a rising K with increasing T, others shown a falling K. The curve from data of Kanamori and others (1968), marked "K, mic" for alkali feldspar is opposite (and uncertain) in trend to the curves from data of Birch and Clark (1940), marked "BC", and Magnitski and others (1971), marked "M". (The K values for feldspars from Kanamori and others (1968), and from Magnitski and others (1971) were calculated from diffusivities using $d = 2.60$ g/ cm^3 and figure 31, and using $\gamma = 1$ and figure 38, respectively.)

Measurements of Sass (1965), marked "S", were made only at 30 °C (303 K); his values of K for single crystals of the potash feldspars, microline and orthoclase, are averages of values of K taken in three crystallographic directions; the range in K is from 5.2 to 6.9 CU. Plagioclase measurements were made parallel to (001) on crystals and otherwise were made on aggregates. The data of Horai (1971) on slurry samples are low and are not shown in figure 22. The experimental results of Petrunin and Yurchak (1973) on polycrystalline albitite show an aberrant threefold decrease in K at about 330 °C (603 K), and are not plotted in figure 22 either.

The symbols used in figure 22 are explained as follows: mic, Or 61 (61 percent orthoclase, 39 percent albite); An 15 (15 percent anorthite, 85 percent albite); av, average of three crystallographic directions; ⊥, perpendicular and ||, parallel to [010] or [001], as shown.

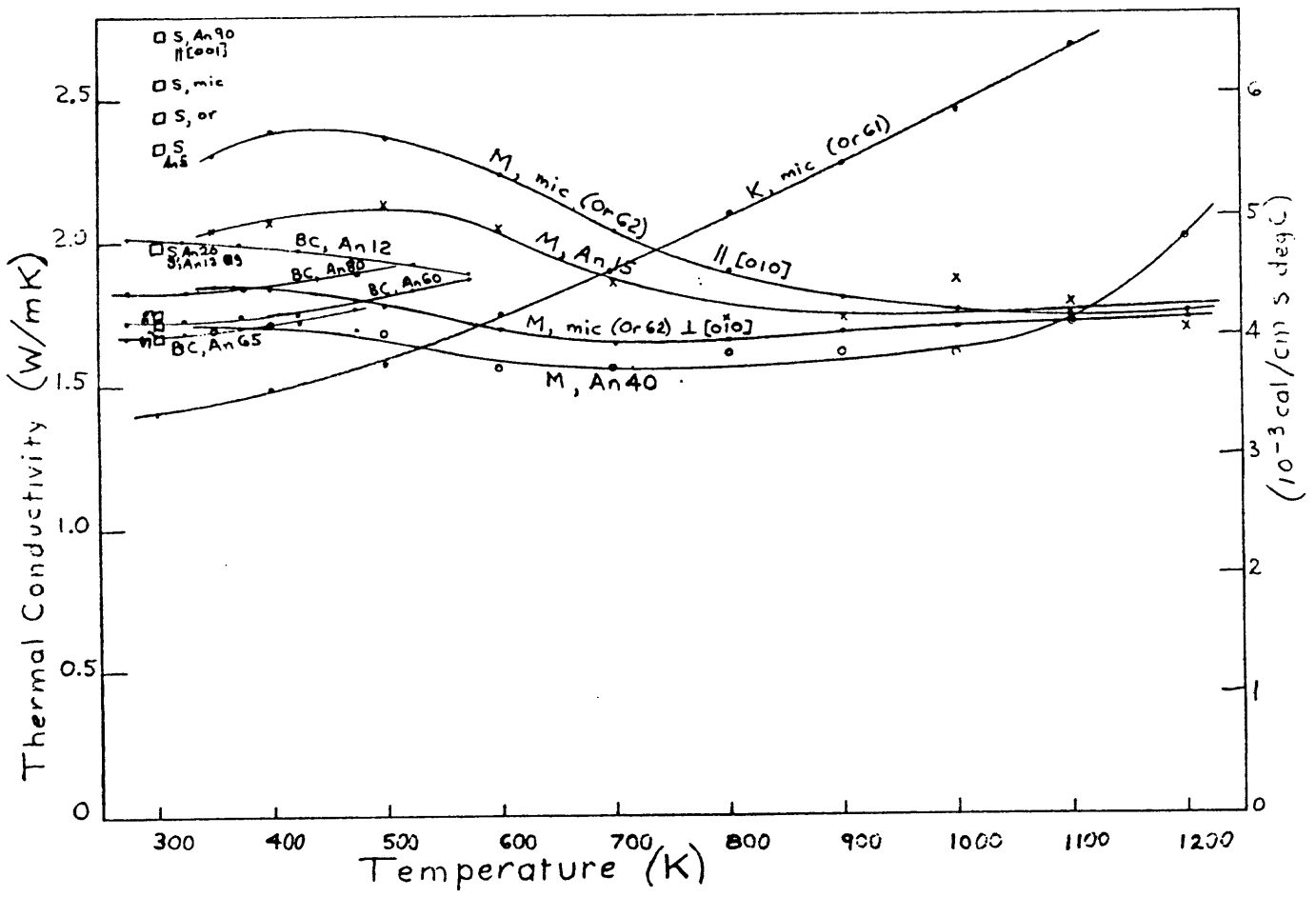

FIGURE 22. Temperature effect on thermal conductivity of various feldspar minerals at 5MPa.

Plagioclase

The variation in thermal conductivity K in the solid solution plagioclase series, albite-anorthite, is shown in figure 23 as a function of anorthite (An) content. There seems to be a minimum in K in the midrange of composition, near andesine, as pointed out by Horai (1971). In a gross way, albite and oligoclase have slightly higher K than the calcic members, labradorite, bytownite, and anorthite. Taking some liberties with the data, tentative curves of equal T have been drawn in figure 23; in general, the calcic members seem to have a positive temperature coefficient and the sodic members a negative coefficient.

The symbols used are H, Horai (1971) for data at 300K; S, Sass (1965) for data at 300 K; C, Clark (1966) for data at 300 K; BC, Birch and Clark (1940) for T<800 K; and M, Magnitski and others (1971) for T<1200 K. Two square points, marked S [001], are for K measured ‖ [001].

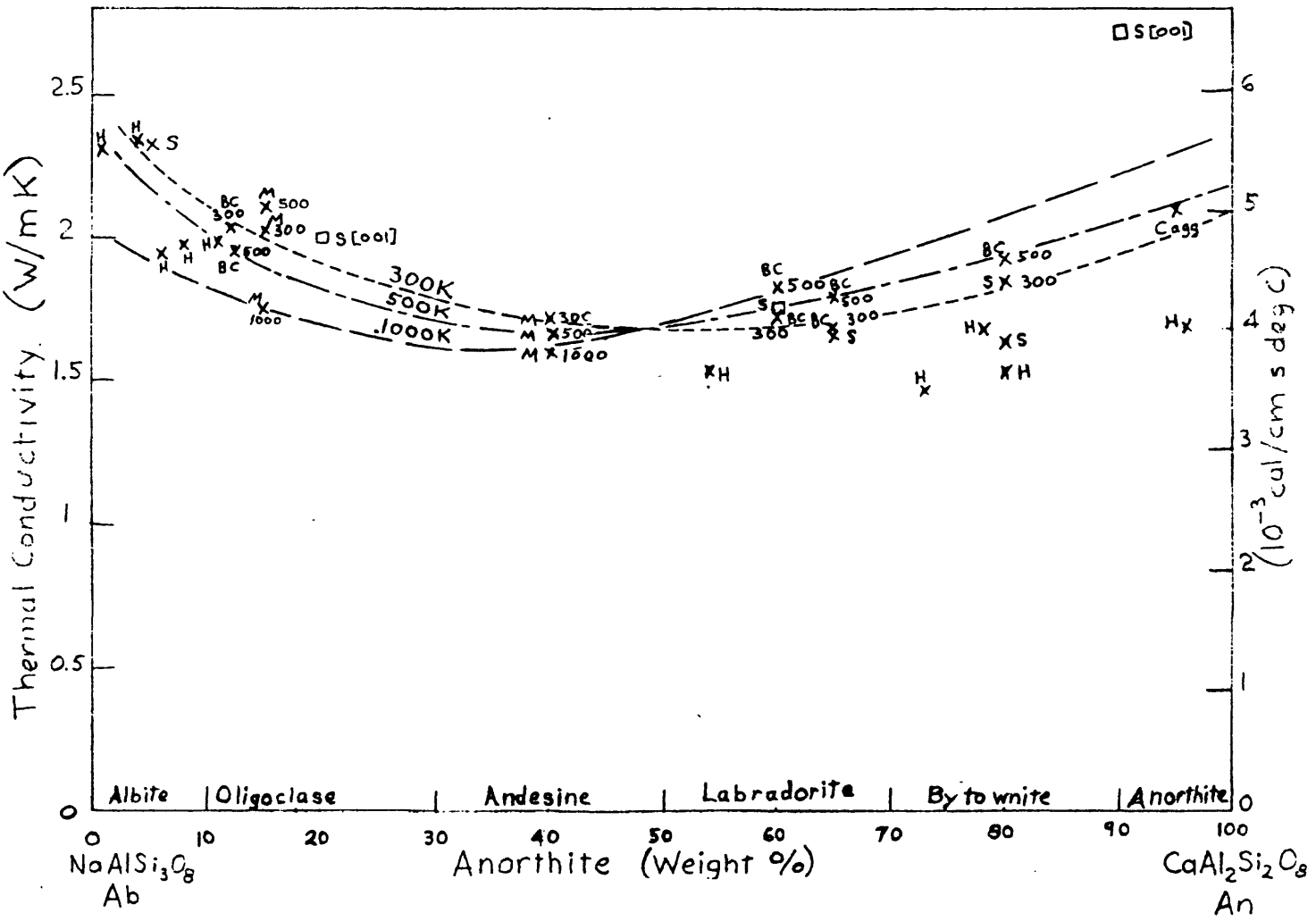

FIGURE 23. Variation in thermal conductivity with albite-anorthite solid solution in the plagioclase at 5MPa; temperature effects at 300 K, 500 K, and 1000 K are plotted at several compositions with tentative isothermal lines.

Mafic Silicate Minerals

The ferromagnesian minerals, like olivine, pyroxene, and amphibole, are important constitutents of basalt and other volcanic rocks and of rocks derived from or residing now in the Earth's upper mantle. The thermal conductivity $\underline{K}$ of mafic minerals at high temperature $\underline{T}$ is of interest in studies of heat transfer in the mantle, particularly by radiation (Clark, 1957a; Shankland and others, 1979). Data on $\underline{K}$ of several single crystal and polycrystalline mafic minerals at $\underline{T}$ from 0° to 1600 °C are plotted in figure 24.

At $\underline{T}$ below 300 °C, the $\underline{K}$ of these minerals decreases very rapidly with increasing $\underline{T}$. At $\underline{T}$ above 300 °C, the results of the various measurements are ambiguous; some results indicate a continued slow decrease in $\underline{K}$ with $\underline{T}$, with a small or no reversal, and others show a sharp reversal to increasing $\underline{K}$ with $\underline{T}$, presumably due to radiative heat transmission.

Measurements of $\underline{K}$ by Birch and Clark (1940) to 200 °C on nearly monomineralic rocks were corrected for impurities, and their corrected data are plotted in figure 24 as follows: "BC, Fo 92" is forsterite 92 percent, fayalite 8 percent; "BC, Hy" is hypersthene; "BC, Br" is bronzite. The thermal diffusivity measurements of Kanamori and others (1968) have been converted to $\underline{K}$ values and plotted as function of $\underline{T}$ in figure 24 also; symbols and conversions are as follows: "K, Fo 82" [001], single crystal olivine, parallel to [001], forsterite 82 percent; "K, Jad", polycrystalline jadeite (converted by using $\underline{d} = 3.40$ g/cm^3 and figure 32); "K, Gar" pyrope-almandine crystal (converted using $\underline{d} = 3.86$ g/cm^3 and specific heats from R.A. Robie and others, 1978).

Schatz and Simmons (1972) obtained $\underline{K}$ values to high temperatures $\underline{T} \leq 1600$°C on five minerals, as follows: "SS, Fo 92", forsterite, 92 percent, fayalite, 8 percent, parallel to [010]; "SS, Fo 86", forsterite 86 percent, parallel to [010]; "SS, Fo-sin," sintered forsterite 100 percent, "SS, Fo 94, dun", Twin Sisters dunite, forsterite, 94 percent; "SS, En 82", enstatite 82 percent, ferrosilite 18 percent. Rather wide uncertainties in $\underline{K}$ are given for measurements at $\underline{T} > 700$ °C by Schatz and Simmons (1972), but values from interpolated curves in their drawings are used here. Radiative heat transmission was identified by Kanamori and others (1968), and Schatz and Simmons (1972) as becoming effective at about 600 °C, but the former authors show a much greater increase in conductivity by radiation than the latter do (fig. 24).

The effect of pressure to 56 kb, in the range 30 °C < $\underline{T}$ < 130 °C, on single crystal enstatite, in the three crystallographic directions [100], [010], and [001], was measured by Schloessin and Dvorak (1972), and averages of the three directions at four pressures are plotted in figure 24. Curves are marked "SD, En-av, 56 kb", etc. The change with temperature is negative and quite large, whereas the pressure effect is small in comparison. However, a considerably larger pressure effect was found by Fujisawa and others (1968) for sintered forsterite and fayalite (fig. 23); "F, Fo-sin, 30 kb", is for sintered forsterite at 30 kb, and "F, Fo-sin, 50 kb", is the same at 50 kb; "F, Fa-sin, oliv," is for sintered fayalite, of olivine crystal structure at 48.5 kb; and "F, Fa-sin spin" is sintered fayalite of spinel structure at 48.5 kb. Neither set of authors carried measurements to temperatures high enough to obtain radiative transfer.

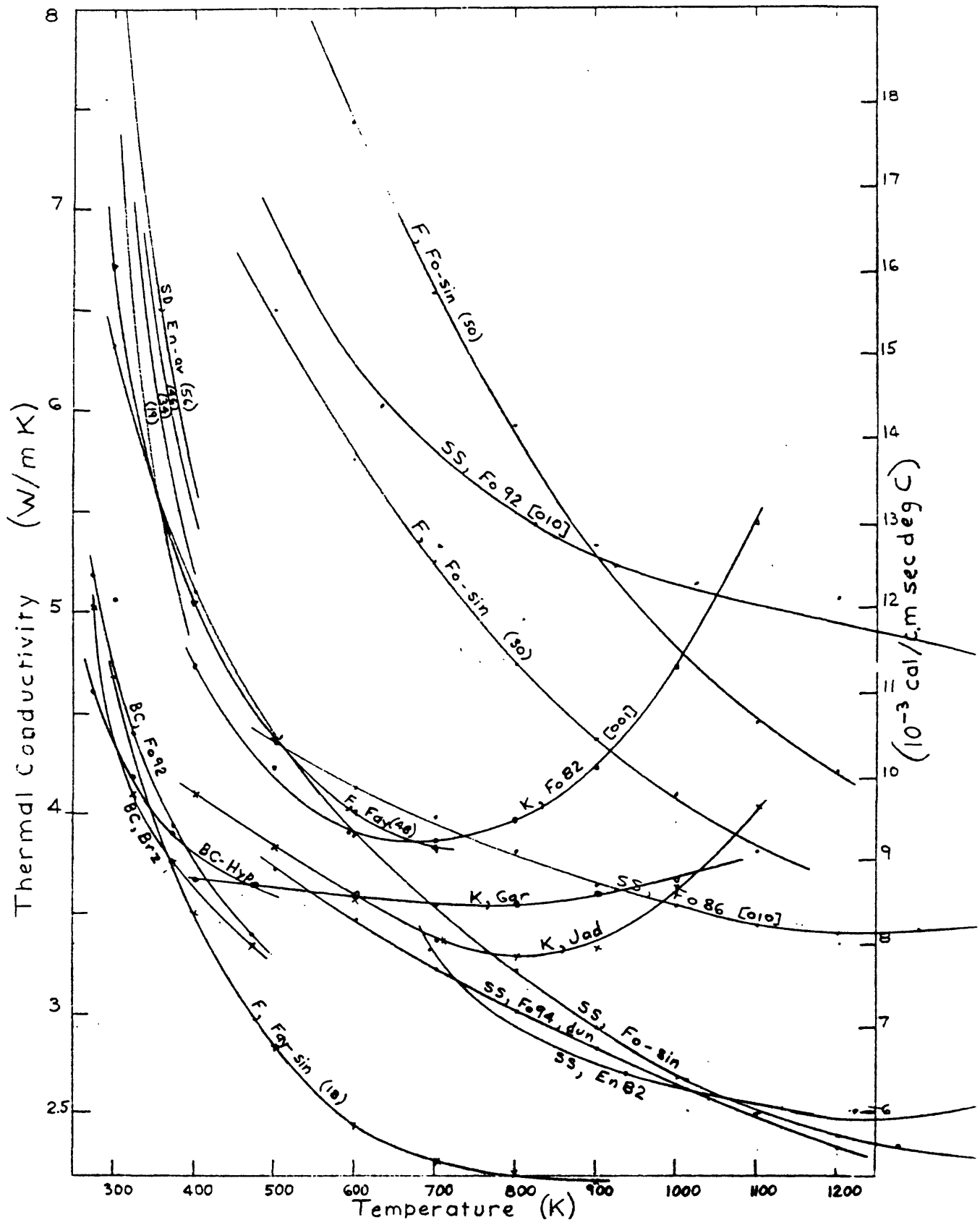

FIGURE 24. Temperature effect on thermal conductivity of various mafic silicate minerals at 5 MPa.

Olivine

A series of olivine solid solution samples, from near forsterite to near fayalite, were measured at 30 °C by Horai (1971), and his thermal conductivites K of powdered specimen suspensions in water are shown in figure 25; the data points are marked "H". Data on olivine from measurements of others, shown in figure 24, are also plotted in figure 25. A review of most of the available data on K of olivine is given by Scharmeli (1977).

A wide range in values of K is apparent in the forsterite-rich samples of this solid solution series in figure 24, and only sparse measurements are at hand toward the fayalite end, so the variation of K with composition is not distinct. With regard to the temperature effect, Horai (1971) suggested the probable shape, as shown by the roughly-drawn curve for data at T = 300 K, showning a minimum near fayalite, (fig. 25). By analogy with the curve at 300 K, two other tentative curves have been sketched in figure 25 for T = 500 K and 1000 K. The differences in measurements due to sample type, whether single crystal, polycrystalline, or sintered grains, need to be accounted for, as well as the pressure effects, so the variation of K with composition in this series is not very closely fixed.

The symbols used are as follows: H, "Horai (1971), powdered olivine crystals in suspension at 300 K, 1 atmosphere; "BC", at "300 K" and "500 K," Birch and Clark (1940) corrected values for olivine, Fo 92; "SS, sin", "dun", "[010]" at "500 K" and "1000K", Schatz and Simmons (1972) on sintered and dunite samples and single crystals parallel to [010]; "HS", at "373 K" and "573 K" sintered olivine, Hughes and Sawin (1967); "K", olivine crystal, Kanamori and others 1968, parallel to [001] at "300 K," "500 K," and "1000 K"; "F", sintered samples, Fujisawa and others (1968), forsterite, "Fo" at "30 kb" and "50 kb" and at "500 K" and "1000 K" and fayalite, "Fa" at 48.5 kb and at "300 K," "500 K," and "1000 K"; sintered samples, Fujisawa and others (1968), forsterite, "Fa" at 48.5 kb and at "300 K," amd "1000K", of the olivine crystal structure.

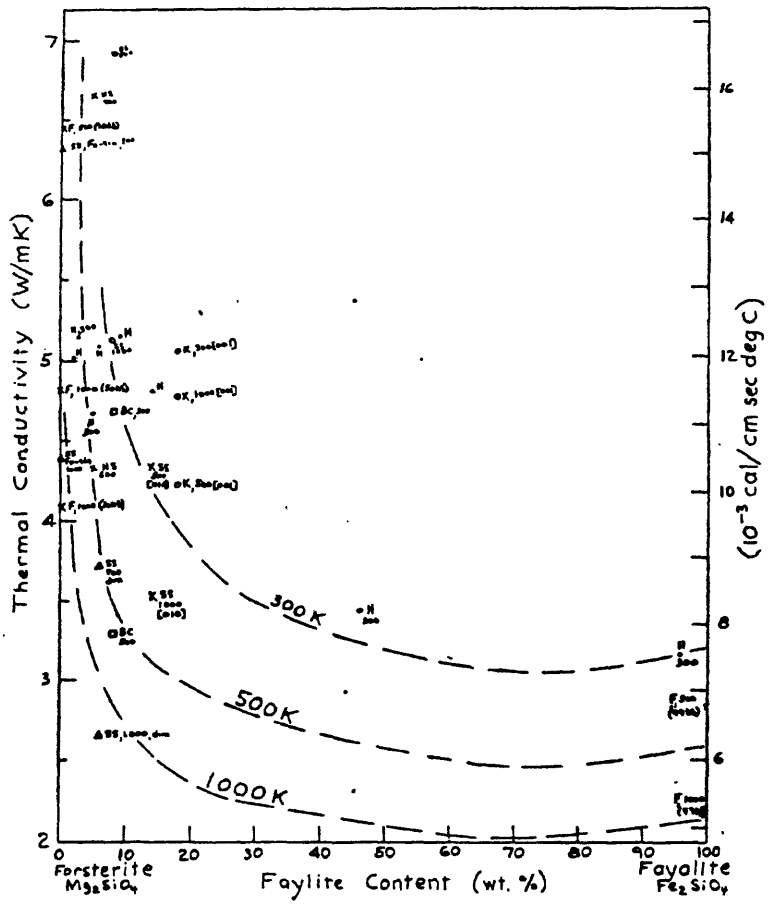

FIGURE 25. Variation in thermal conductivity in the forsterite-fayalite solid solution in olivine at 5MPa; tentative curves show the temperature effect at 300 K, 500 K, and 1000 K.

Calcite and Aragonite

The best measurements of the effect of $\underline{T}$ on $\underline{K}$ to 400 °C (673 K) of single crystal calcite were made by Birch and Clark (1940), and they are plotted in figure 26. As with most minerals, there is a sharp decrease in $\underline{K}$ for 20 °C (293K) < $\underline{T}$ < 200 °C (473 K). Data at higher temperatures are given by the curve marked "M" for data from Mirkovich (1968) on limestone of 93 percent calcite with impurities of dolomite (4 percent), clay (2 percent), and quartz (1 percent); the curve shows a marked flattening at $\underline{T}$ > 500 °C (773 K).

The curve for aragonite is from Petrunin and Yurchak (1973) on a polycrystalline sample. (The $\underline{K}$ values were calculated from diffusivities, using $\underline{d}$ = 2.77 g/cm^3 and ϕ = 2.52 percent).

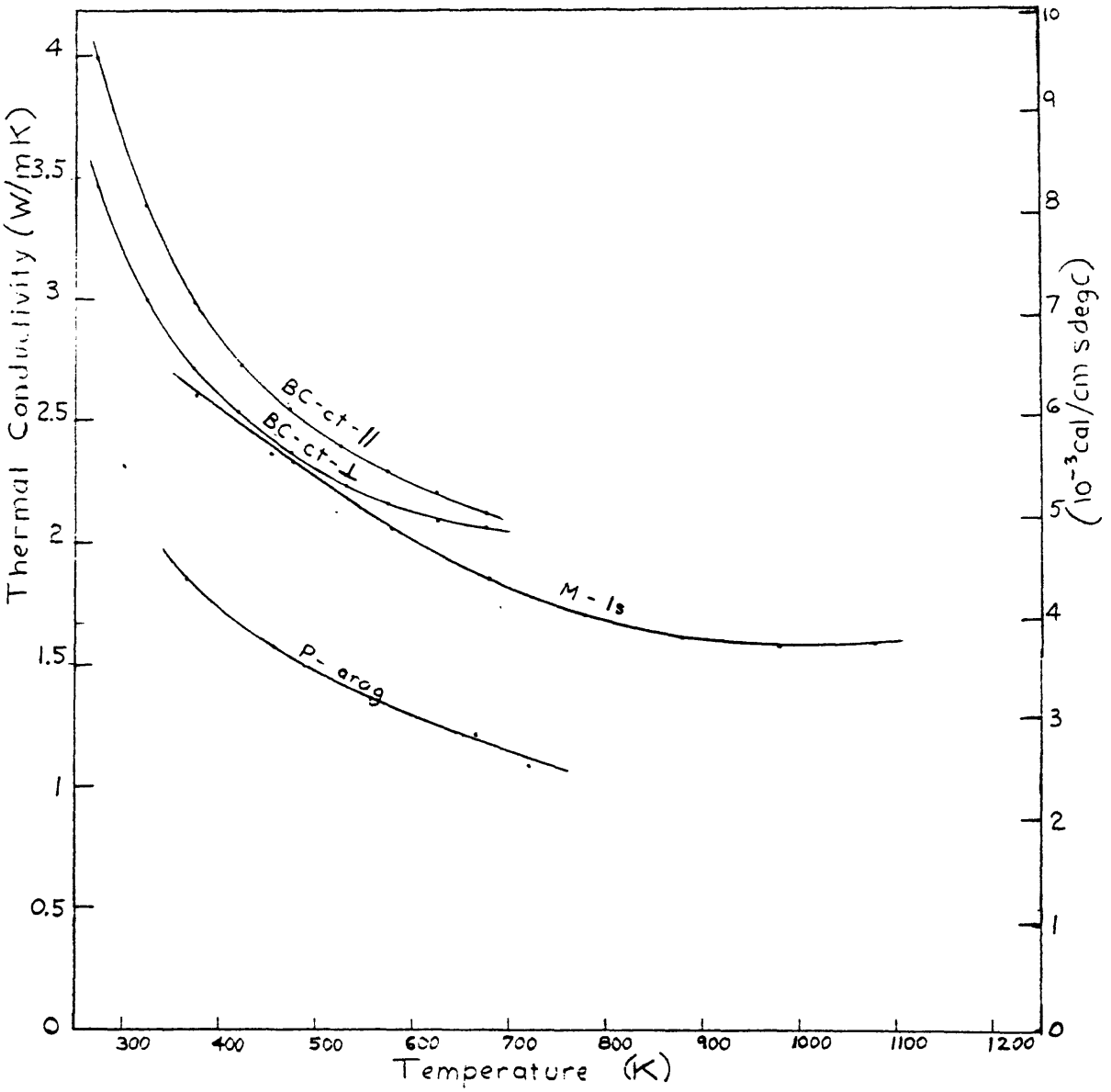

FIGURE 26. Temperature effect on thermal conductivity of calcite parallel (||) and perpendicular (⊥) to C-axis and aragonite at 5MPa.

Halite

In assessing rock salt beds and domes as repositories for radioactive waste, the temperature coefficient and the pressure coefficient of $\underline{K}$ for halite are important to know. In figure 27, the curves shown the $\underline{T}$ effect on $\underline{K}$ for single crystal halite at atmospheric pressure and are from sources as follows: "BC", Birch and Clark (1940), "E", Eucken (1911) and "MB", Mc Carthy and Ballard (1960). The curve marked "S" is from the data of Schneider (1961), taken on sintered rock salt at 1 bar. Two sets of preliminary results on rock salt to about 300 °C were, determined for the Office of Waste Isolation program by D.D. Smith (written commun., 1976) and by J.G. Moore (written commun., 1977), and lie quite near and parallel to the atmospheric pressure curves for halite.

The pressure effect on $\underline{K}$ of single crystal halite between -28 °C and +113 °C was measured by Alm and Backstrom (1975); curves from their data in figure 27 are marked "AB", with the pressure in kb in parentheses. The average pressure coefficent is $+3.04 \times 10^{-5}$ bar^{-1}, and it applies in the range, 1 bar to 30 kb and from -28 °C to 113 °C. These data translate to +3 percent/kb, which is a minor effect on $\underline{K}$ compared to the $\underline{T}$ effect in the near-surface crust of the Earth.

The curves marked "F" were calculated from measurements of diffusivity of Fujisawa and others (1968) at 29 kb on sintered halite, which seem to be considerably in error. (K's were calculated from $\underline{d} = 2.16$ g/cm^3 and figure 30). The curve for halite sinter at 29 kb lies higher than the curve (greatly extrapolated) at 30 kb of Alm and Backstrom (1975).

The tentative designs of excavations for disposal of radioactive waste in salt include placing a backfill of crushed rock salt in the canister chambers. The thermal conductivity of such a porous salt aggregation can be estimated by drawing a line of $\underline{K}$ versus γ^2like that in figure 6 for limestone; draw between $\underline{K}$ for $\gamma^2 = 1$ at the $\underline{T}$ of interest from figure 27 and the value for air, $\underline{K} = 0.063$ CU, at $\gamma^2 = 0$. An estimate of the backfill can be made, and a value for $\underline{K}$ of the porous salt can be estimated at the appropriate γ^2. Admittedly, such a figure would be only an approximation, but it should be usable in this application.

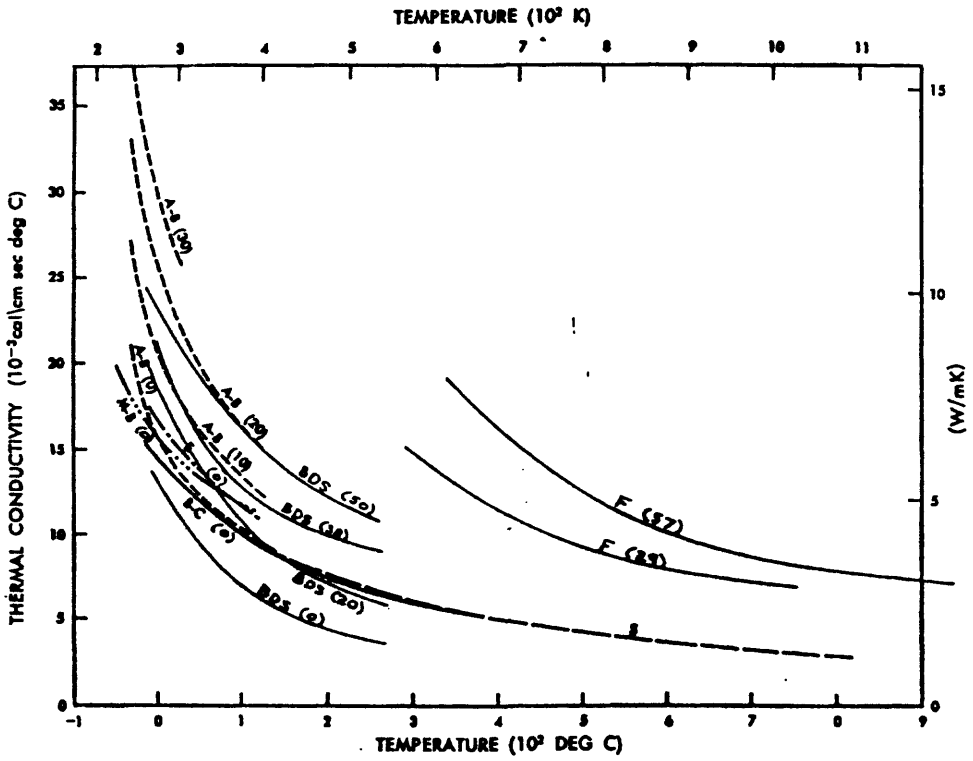

FIGURE 27. Temperature and pressure effects on thermal conductivity of halite.

MINERAL CONDUCTION MECHANISMS

The atomic scale explanations of thermal conductivity are usually based on lattice vibrations, harmonic and anharmonic, on scattering at defects, and on radiative processes (for example, see Klemens, 1958, and Goldsmid, 1965). In 1911 Eucken showed that K of an electrically insulating crystal is inversely proportional to absolute temperature, but this relation is only approximately valid, and only at relatively low temperatures for minerals (see for example, Schloessin and Dvorak, 1972). Birch and Clark (1940) showed that plots of thermal resistivity (1/K) of minerals against absolute temperature yield straight lines, in accordance with the concept that thermal resistivitities are additive. A comprehensive review of the physical theory of thermal conductivity is given by Parrott and Stuckes (1975).

Phonon and Imperfection Conductivity

Phonon conduction is a concept of lattice vibrational heat transfer based on an analogy with molecules of a gas. The vibrational motion of an enormous number of atoms is more easily visualized as being replaced by a gas of phonons, and appropriately, the Boltzmann equation can be used to determine the phonon distribution function and scattering processes. Imperfections, such as, grain boundaries and other discontinuities, cause the scattering of lattice waves. (See Parrott and Stuckes, Chap. 4, 1975).

By the 3-phonon processes, K is found to vary inversely with absolute temperature in the range 300 - 600 kelvins (K). Most solids deviate from strict T^{-1} behavior, suggesting that in addition to 3-phonon interactions a scattering process at imperfections contributes to the thermal resistance. (See Schneider, 1961; MacPherson and Schloessin, p. 59-61, 1982). In the analysis of data in Figures 21-27 by the Boltzmann relation that follows, temperature regimes of both phonon and imperfection conduction are identified if they differ sufficiently from each other.

Radiative Conductivity

The experiments of Clark (1956, 1957a, 1957b) on high temperature heat conduction in several minerals showed that radiative heat transfer is as important as phonon conduction in the earth's mantle. Optical measurements of the absorption coefficient of probable mantle minerals (Fukao, 1969; Aronson and others, 1970; Shankland and others, 1979) can be used in the following equation to estimate radiative conductivity.

$$K_{rad} = 16 n^2 \sigma T^3/3e \qquad (8)$$

where n is the refractive index, σ the Stefan-Boltzmann constant, T the absolute temperature, and e the extinction coefficient; e consists of an absorption term and a small, usually neglected scattering term.

Experimental results indicate that the absorption coefficient increases with increasing temperature and that absorption bands due to ferrous and ferric iron contribute to increase in absorption (Shankland and others, 1979; Fukao, 1969). Pressure effects on absorption are positive but much smaller than the temperature effects (Shankland, 1970). A review of work on radiative conductivity is given by MacPherson and Schloessin (1982).

Aronson and others (1970) measured the absorption coefficient of olivine and diopside to 1450° C and found an increase with temperature both with and without iron in the minerals. A value for single crystal olivine at 1723 K was K_{rad} = 2.5 W/m•K, somewhat lower than measurements of Fukao and others (1968); and a value for diopside at 1443 K was K rad = 2.4 W/m•K close to the values obtained by Clark (1957b). As shown in Figure 24, phonon K for olivine at 700 K is between 2 and 4 W/m•K, which is about equal in value to its radiative conductivity above 700K.

Following the method of Kanamori and others (1968), MacPherson and Schloessin (1982) obtained values for K_{rad} by extrapolating the linear phonon conductivity to higher temperatures and subtracting the phonon contribution from the observed conductivity. They found a linear relation between K_{rad} and T^3, (equation 8). Their values of K_{rad} for single crystal calcite range from 0.4 W/m•K at 550 K to 1.8 W/m•K at 1000 K under 7 kb pressure; values for single crystal halite were very nearly the same in the same temperature range under 30 kb. Phonon K for

calcite at 700 K in Figure 26 is about 2.2 W/m•K, about equal to the $\underline{K}_{rad}$. Schatz and Simmons (1972) conclude that $\underline{K}_{rad}$ does not exceed phonon $\underline{K}$, and in general the two may be assumed to be nearly equal above 700 K.

Radiative conductivity is presumed to occur at temperatures above about 700 K in the data in figures 21-27 and replotted in figures 28-29 below.

Analysis of Mechanisms

By analogy with electrical semiconductor analysis, the mechanisms of lattice heat conduction can be inspected by use of the Boltzmann equation (Parrott and Stuckes, p. 56, 1975), which can be assumed to be additive in thermal conductivity,

$$\underline{K} = \underline{K}_o \exp(-\underline{E} / \underline{k}\,\underline{T}) \qquad (9)$$

where $\underline{K}_o$ is the intercept conductivity constant, $\underline{E}$ is activation energy, and $\underline{k}$ is the Boltzmann constant. As described by Shankland (1975), electrical conduction mechanisms are thermally activated processes and additive in conductivity, as shown by this exponential relation between $\underline{K}$ and $1/\underline{T}$ for a number of minerals, and a similar analysis is followed here for thermal conduction mechanisms.

The sum of the conduction mechanisms is given by the Boltzman equation. Utilizing this relation, mineral data used in Figures 21 through 27 are replotted in Figures 28 and 29. The linear segments of log $\underline{K}$ vs $1/\underline{T}$ (Figs. 28, 29) designate the temperature intervals of and help identify possible conduction mechanisms in each mineral; $\underline{K}_o$ and $\underline{E}$ for the line segments are listed in Table 3. The symbols used in Figures 28 and 29 are explained in the text for Figures 21 - 27 and for Table 3.

With exponential dependence of $\underline{K}$ on $\underline{T}$, a single mechanism presumably dominates in the range of $\underline{T}$ of each line segment. Data are plotted for single crystals and aggregates of the minerals, quartz, plagioclase, microline, calcite, halite, olivine, enstatite, garnet, aragonite, and corundum.

The following conduction mechanisms and their applicable ranges of $\underline{T}$ have been rather arbitrarily selected from Figures 28 and 29, and are listed in table 3; the effect of pressure is shown for some minerals. The linear segment from about 0° to about 200° C may be taken for most minerals to represent phonon-phonon and umklapp conduction, a mechanism of elastic wave scattering and anharmonic lattice vibrations. In this range, except for the feldspars, $\underline{K}$ decreases markedly with increasing $\underline{T}$. In the middle range from about 200° to about 600° C, the line segments are taken as representing a scattering at crystal imperfections and defects, like impurity atoms, dislocations, domain boundaries, and grain boundaries. The $\underline{T}$ effect on $\underline{K}$ of most minerals in this range is to decrease its value.

In the range from about 600° to about 900° C, the lines are taken to represent radiative heat transfer, and for almost all minerals the effective $\underline{K}$ increases with increasing $\underline{T}$. The negative slope of $\underline{K}$ with $\underline{T}$ of some lines may be due to the use of sintered samples, with their poorer thermal coupling between grains compared to conduction in single crystals or dense polycrystalline aggregates, for example, forsterite and fayalite (Fujisawa et al, 1968) and halite (Schneider, 1961; Fujisawa et al, 1968). Measurements in the range $\underline{T} > 1100$° C made by Schatz and Simmons (1972) show an increase in $\underline{K}$ with $\underline{T}$ for enstatite and forsterite; in this high temperature range, charge carriers, like ions, ion vacanies, or electron-hole pairs, can be presumed to operate as the conduction mechanisms.

The values of activation energy $\underline{E}$ and intercept constant $\underline{K}_o$ in equation (7) listed in table 3 were rounded and combined in the four temperature ranges described above and are listed in tables 4 and 5. Calculations of variation of conductivity with temperature of rocks from their modes are not accurate from these data; eventually it should be possible to obtain better values from more carefully determined values of $\underline{E}$ and $\underline{K}_o$.

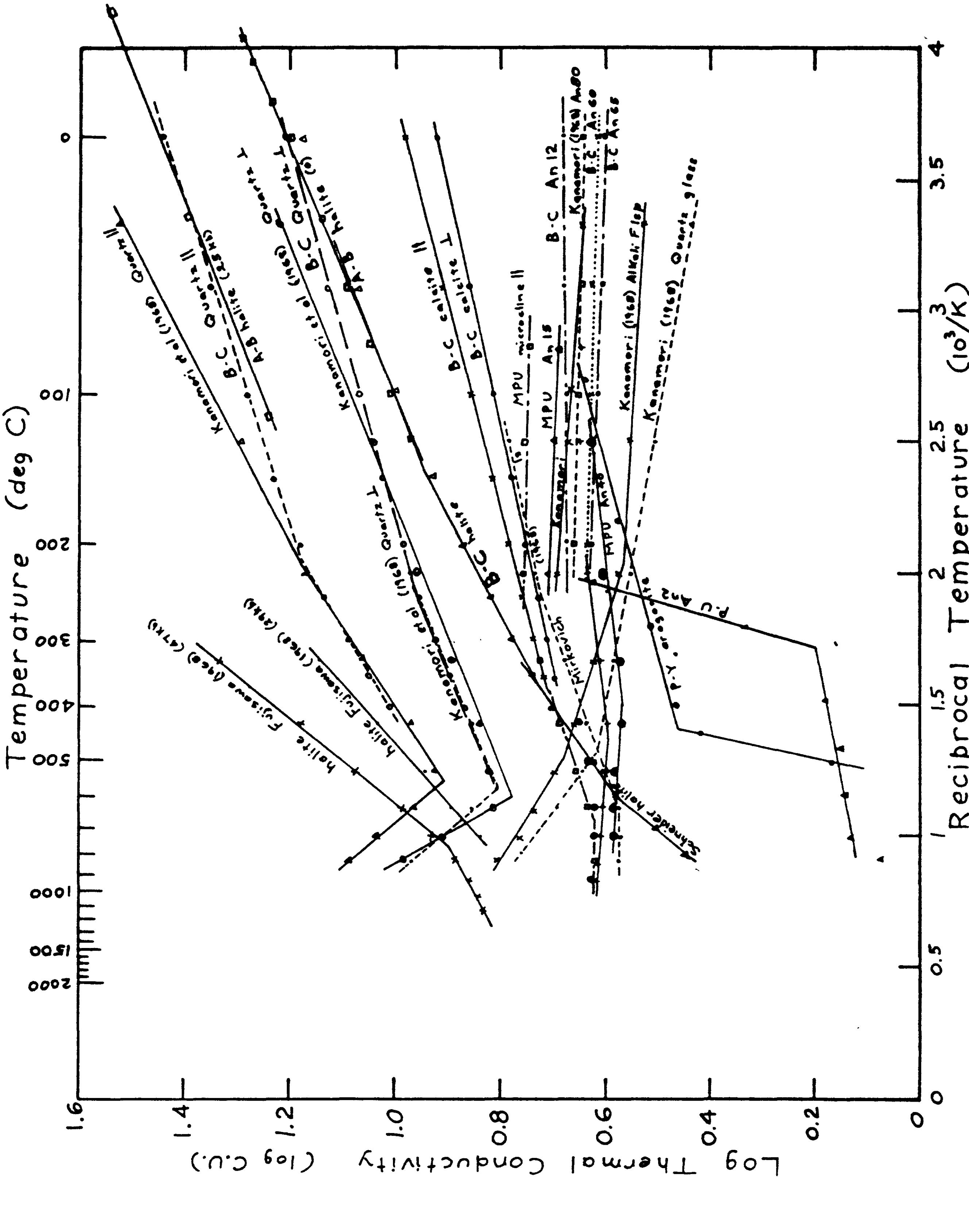

FIGURE 28. Semilogarithmic plot of thermal conductivity versus reciprocal temperature for felsic minerals.

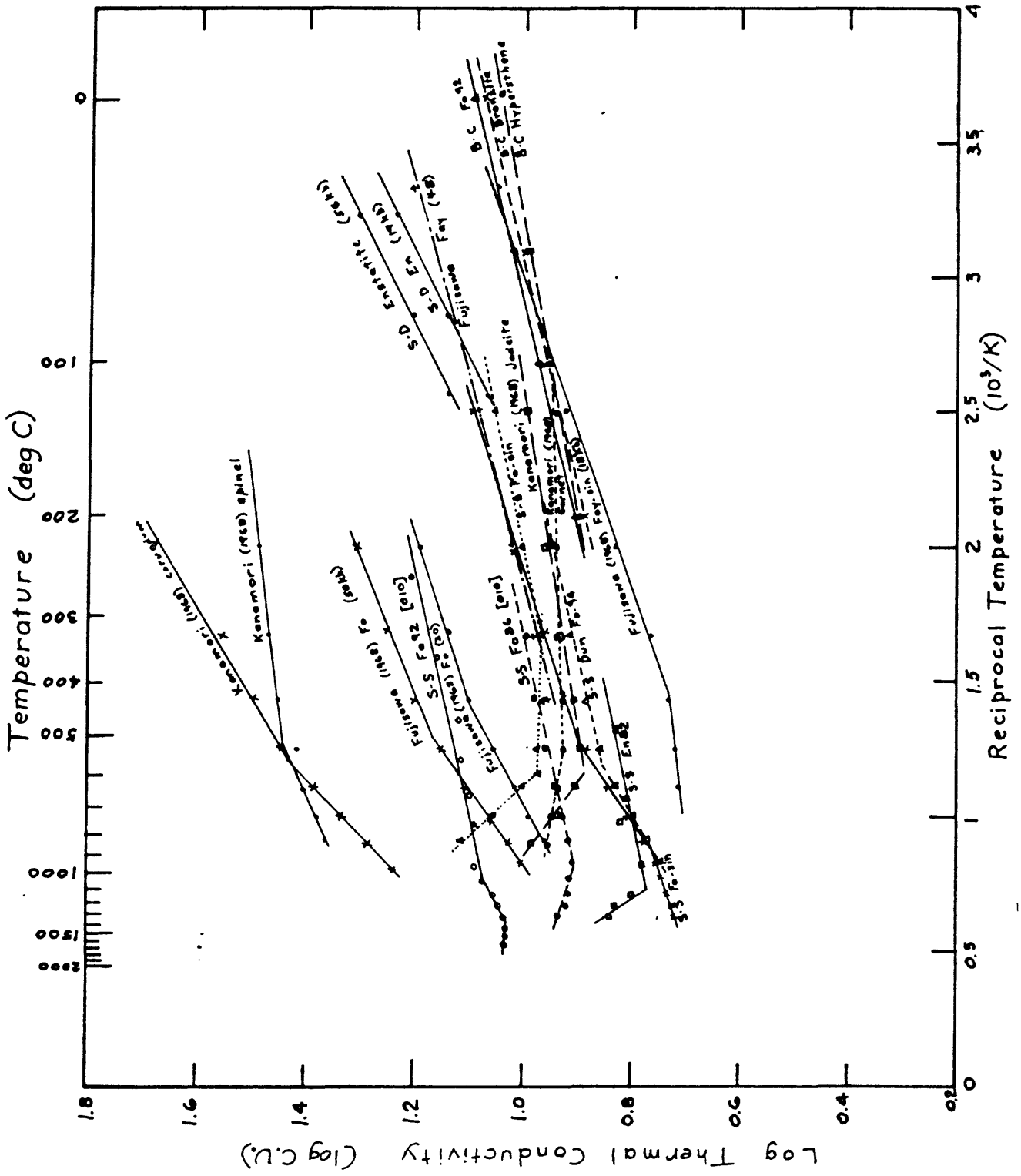

FIGURE 29. Semilogarithmic plot of thermal conductivity versus reciprocal temperature for mafic minerals.

TABLE 3.--Activation energies and intercept conductivity constants of Boltzmann equation for thermal conduction mechanisms in single crystal minerals (taken from figs. 28 and 29)

[Symbols and abbreviations indicate the following: ⊥, perpendicular; ||, parallel; C, C-axis; [010] and [001] crystallographic directions; av, average of three crystallographic directions or of polycrystalline aggregate of grains; kb, pressure in kilobars; Ls, limestone]

Mineral [1]	Orientation	Temperature ~Range	Constant (K_o)	Activation energy (E)	References
Quartz.....	⊥C	0-220	5.0	-30	Birch and Clark. 1940.
Do.....	⊥C	220-400	3.8	-40	Do.
Do.....	⊥C	120-220	5.0	-30	Kanamori and others, 1969.
Do.....	⊥C	220-550	3.7	-40	Do.
Do.....	⊥C	550-800	32.0	+120	Do
Do.....	⊥C	30-600	3.6	-40	Kanamori and others, 1968.
Do.....	⊥C	600-800	63.0	+180	Do.
Do.....	|| C	0-220	7.1	-30	Birch and Clark, 1940.
Do.....	|| C	220-400	3.7	-60	Do.
Do.....	|| C	30-220	4.4	-50	Kanamori and others, 1968.
Do.....	|| C	220-550	3.2	-70	Do.
Do.....	|| C	550-800	41.0	+120	Do.
Microcline (Or 61).....	av	30-200	4.5	+5	Do.
Do.....	av	200-500	7.5	+30	Do.
Do.....	av	500-850	20.0	+95	Do.
Microcline (Or 62).....	⊥(010)	80-200	4.5	+0.4	Magnitski and others, 1971.
Do.....	⊥(010)	200-450	3.2	-10	Do.
Do.....	⊥010)	450-900	4.5	+10	Do.
Do.....	|| (010)	80-220	6.1	+5	Do.
Do.....	|| (010)	220-650	2.8	-30	Do.
Do.....	|| (010)	650-900	4.1	-1	Do.
Plagioclase (An 12).....	av	0-200	4.6	-1	Birch and Clark, 1940.
Plagioclase (An 60).....	av	0-200	4.6	+5	Do.
Plagioclase (An 65).....	av	0-200	4.8	+5	Do.
Plagioclase (An 80).....	av	0-200	4.9	+5	Do.

TABLE 3.--Activation energies and intercept conductivity constants of Boltzmann equation for thermal conduction mechanisms in single crystal minerals (taken from figs. 28 and 29)--Continued

Mineral [1]	Orientation	Temperature Range	Activation Constant (K_o)	energy (E)	References
Plagioclase (An 15).....	av	80-300	5.6	+5	Magnitski and others, 1981.
Do.....	av	300-600	2.8	-30	Do.
Do.....	av	600-900	4.5	+5	Do.
Plagioclase (An 40).....	av	100-400	3.1	-10	Do.
Do.....	av	400-750	4.2	----	Do.
Do.....	av	750-900	14.0	+110	Do.
Hypersthene.....	av	0-200	5.1	-20	Birch and Clark 1940.
Bronzite.....	av	0-200	4.6	-20	Do.
Jadeite.....	av	100-550	6.2	-20	Kanamori and others, 1968.
Do.....	av	550-800	20.0	+70	Do.
Enstatite.....	av(19kb)	50-120	2.7	-50	Schloessin and Dvorak, 1972.
Do.....	av(56kb)	50-120	3.1	-50	Do.
Enstatite (En 82).....	av	400-1100	5.0	-20	Schatz and Simmons, 1972.
Do.....	av	1100-1300	21.0	+150	Do.
Olivine.....	av	0-200	4.6	-20	Birch and Clark, 1940.
Do.....	|| [001]	100-300	4.6	-0	Kanamori and others, 1968.
Do.....	|| [001]	300-600	9.8	±5	Do.
Do.....	|| [001]	600-800	41.0	+110	Do.
Forsterite (Fo 92).....	|| [010]	250-1000	9.7	-20	Schatz and Simmons, 1972.
Do.....	|| [010]	1000-1400	7.3	-50	Do.
Do.....	|| [010]	1400-1600	11.4	+10	Do.
Forsterite (Fo 86).....	|| [010]	300-900	6.5	-20	Do.
Do.....	|| [010]	900-1300	10.8	+30	Do.
Forsterite (Fo 94, dunite)	av	200-550	5.3	-20	Do.
Do.....	av	550-1000	3.1	-60	Do.
Forsterite (Fo 100 sintered).	av	150-500	4.9	-30	Do.
Do.....	av	500-900	2.8	-70	Do.
Do.....	av	900-1300	4.1	-30	Do.

TABLE 3.--Activation energies and intercept conductivity constants of Boltzmann equation for thermal conduction mechanisms in single crystal minerals (taken from figs. 28 and 29)--Continued

Mineral [1]	Orientation	Temperature Range	Constant (K_o)	Activation Energy (E)	References
Forserite.....	av(30kb)	200-450	7.5	-30	Fujisawa and others, 1968.
Do.....	av(30kb)	450-900	5.2	-50	Do.
Do.....	av(50kb)	200-500	8.1	-40	Do.
Do.....	av(50kb)	500-1000	5.0	-70	Do.
Fayalite olivine structure	av	20-400	3.0	-35	Do.
Do.....	av	400-650	4.4	-10	Do.
Fayalite spinel structure	av	20-400	5.5	-30	Do.
Garnet (py-al).....	av	100-500	8.1	-5	Kanamori and others, 1968.
Do.....	av	500-800	11.0	+20	Do.
Spinel.....	av	200-500	23.0	-10	Do.
Do.....	av	500-800	14.0	-40	Do.
Corundum.....	av	200-600	12.0	-60	Do.
Do.....	av	600-900	7.3	-90	Do.
Calcite.....	$\perp$C	0-400	3.4	-20	Birch and Clark, 1940.
Do.....	$\parallel$C	0-400	3.3	-30	Do.
Do.....	Ls	100-250	3.3	-20	Mirkovich, 1968.
Do.....	Ls	250-600	2.4	-35	Do.
Do.....	Ls	600-900	3.7	-5	Do.
Argonite.....	av	100-400	1.9	-30	Petrunin and Yurchak, 1973.
Halite.....	av	-35-200	2.7	-40	Birch and Clark, 1940; Alm and Backstrom, 1972.
Do.....	av	200-350	2.0	-50	Alm and Backstrom, 1972.
Do.....	av	350-600	1.6	-70	Do.
Do.....	av	600-800	0.8	-120	Schloessin and Dvorak, 1972.
Do.....	av(25kb)	-35-120	5.4	-40	Alm and Backstrom, 1972.
Do.....	av(29kb)	300-750	2.5	-90	Fujisawa and others, 1969.
Do.....	av(47kb)	300-750	2.0	-120	Do.
Do.....	av(47kb)	750-1200	4.4	-50	Do.
Quartz glass.....	av	30-450	5.5	+20	Kanamori and others, 1968.
Do.....	av	450-750	13.0	+70	Do.

[1] Percentage of pure phase is indicated in parentheses.

TABLE 4.--Rounded values of activation energies of mineral conduction mechanisms

Mineral	Activation energy, E, in 10^{-3}eV[1] (mechanism and temperature range)			
	Phonon (0-200 °C)	Imperfection (200-600 °C)	Radiation (600-1100 °C)	Ionic (>1100 °C)
Quartz.....	-40	-50	+120	- - -
Microline.....	+5	+30	+100	- - -
Plagioclase,				
sodic	-1	-30	+5	- - -
calcic.	+5	+10	+110	- - -
Pyroxene.....	-20	-20	+70	+150
Olivine.....	-20	-30	-50	+20
Garnet.....	- - -	-3	+20	- - -
Spinel.....	- - -	-10	-40	- - -
Corundum.....	- - -	-60	-90	- - -
Calcite.....	-20	-30	-5	- - -
Aragonite.....	-30	- - -	- - -	- - -
Halite.....	-40	-60	-120	- - -
Quartz glass...		+20	+70	- - -

[1]Activation energy, $\underline{E}$ in Boltzmann equation, $\underline{K} = \underline{K}_o \exp(-\underline{E}/\underline{k}\,\underline{T})$. Conversion is: 1eV = 1.6022 x10 $^{-19}$J.

TABLE 5.--Rounded values of intercept conductivity constant of minerals

Mineral	Intercept Conductivity (K_o)[1] in 10^{-3} cal/cm sec °C (mechanism and temperature range)		
	Phonon (0-200 °C)	Imperfection (200-600°C)	Radiation (600-1100 °C)
Quartz.....	5	3	40
Microline....	5	3	15
Plagioclase,			
sodic	5	3	5
calcic	5	5	15
Pyroxene.....	5	6	20
Olivine.....	5	5	10
Garnet.....		10	10
Spinel.....		20	15
Corundum.....		10	10
Calcite.....	3	2	4
Aragonite....	2		
Halite.....	3	2	1
Quartz glass		6	10

[1] Intercept conductivity, K_o, in Boltzmann equation, $K = K_o \exp(-E/kT)$.

MISCELLANEOUS THERMAL CONDUCTIVITIES

The thermal conductivities of a few substances found on the earth have had only peripheral attention but are of interest on occasion and are listed in table 6. Temperature effects are shown for some of the substances in the table as available. The data are from Clark (1966, Sec.21).

Table 6. Miscellaneous thermal conductivities and their temperature effects (after Clark, 1966, Sec. 21).

Material	Density (g/cm^3)	Temperature (deg C)		Thermal Conductivity (10^{-3} cal/cm s deg C)
Ice	0.9	0		5.0
		-130		6.1
Water	1.0	30	(1 bar)	1.46
		30	(4kb)	1.80
		70	(1 bar)	1.56
		70	(4kb)	1.94
		110	(l bar)	1.62
		110	(4kb)	2.05
Clay, red, deep-sea	1.5	4		2.2
Coal, anthracite	1.3	30		0.5
Graphite, c-axis	2.3	77		1000.
Sand, Hudson River	1.36	30		0.65
Loam, Barnes	1.16	30		0.39
Copper	8.9	0		960.
		200		910.
		500		840.
Iron	7.9	0		180.
		200		148.
		400		117.
		800		71.

PRESSURE EFFECT ON THERMAL CONDUCTIVITY

Most of the data available on the pressure effect on $\underline{K}$ are listed in table 6 for 19 common minerals and rocks, and the pressure effect is given by the coefficient $\underline{a}$ in the units 10^{-6} CU/CU/bar in the equation

$$\underline{K}_P = \underline{K}_o (1 + \underline{a}\,\underline{P}), \qquad (10)$$

and $\underline{a}$ can be calculated by

$$\underline{a} = (1/K_o)(\Delta\underline{K}/\Delta\underline{P}), \qquad (11)$$

where $\underline{K}_p$ is the conductivity, in CU, under pressure $\underline{P}$, in kb, and $\underline{K}_o$ is the conductivity at the initial pressure shown in the table. For $P < 1$ kb, the pressures were uniaxial, with a load applied in one direction in air, and for $P > 1$ kb, the pressure was hydrostatic in a confining fluid. Pressures marked zero, 0, are actually 1 atmosphere. Measurements were made on dry samples except as marked "wet", which were saturated with water.

In general, for rocks and minerals with $\gamma > 0.9$, the values of the coefficient $\underline{a}$ are linear with pressure in the range $0 < \underline{P} < 50$ kb. Values of $\underline{a}$ range from +0.5 to +5 percent/kb for these dense substances; an exception is quartz glass, $\underline{a} = 5$ percent/kb. In porous rocks, like sandstone, $\underline{a}$ is not linear with $\underline{P}$, but approximately linear segments of the data are given in the tables; for example, for the Berea sandstone, $\underline{a} = 300$ percent/kb, in the range, $1 < P < 70$ bars, and $\underline{a} = 18$ percent/kb, in the range, $70 < P < 250$ bars. The effect of adding water in pores of the rocks is large; there is a decrease in $\underline{a}$ by a factor of 6 for many rocks, both dense and porous, from a dry to a water-saturated condition.

The effect of temperature change on $\underline{a}$, that is, the second order effect, $\Delta\underline{K}/\Delta\underline{P}\,\Delta\underline{T}$, for the small ranges in $\underline{T}$ is quite small, so that $\underline{a}$ is essentially a constant for a temperature difference of 0 °C to 150 °C. The high-temperature data of Hughes and Sawin (1967) on a cemented aggregate of eclogite fragments are somewhat variable but are usable; the value of $\underline{a}$ progresses from 1.5 to 1.2 percent/kb for measurements at $\underline{T} = 80°$, 200°, 300°, and 400 °C; their data on a dunite aggregate are too scattered and irregular to approximate. The high-temperature results of Fujisawa and others (1968) were taken on sintered aggregates of halite and forsterite; $\underline{a}$ decreases (irregularly) about 50 percent for temperature rises of 400 °C and 600 °C respectively; however, mean values are given as an approximate measure of $\underline{P}$ effect.

Rodionov (1958) derived by statistical mechanics an equation for determining the effect of $\underline{P}$ on $\underline{K}$ of insulator compounds. The simplified expression he developed for the ratio of $\underline{K}_p$ at a given pressure to $\underline{K}_o$ at one atmosphere is

$$\underline{K}_p/\underline{K}_o = (\underline{V}_p/\underline{V}_o)^{1/3}\,(\alpha_p/\alpha_o)^2 \qquad (12)$$

in terms of the ratios of molar volumes $\underline{V}_p/\underline{V}_o$ and the thermal expansions α_p and α_o. His value for sodium chloride of $\underline{a} = 50$ Mb^{-1}, in the range $0 < P < 50$ kb, is comparable with the experimental result of Alm and Backstrom (1975) of 30 Mb^{-1} for $P < 30$ kb given in the table.

Table 7.--Effect of pressure on the thermal conductivity of certain minerals and rocks (continued)

Rock or mineral	Solidity[1] (γ)	Pressure coefficient[2] (a) (Mb^{-1})	Pressure range[3] (P) (kb)	Temperature range[4] (°C)	Reference
			Minerals		
Quartz, single crystal ∥ C.	>0.99	21.7	25-50	127-177	Darbha and Schloessin, 1975.
Quartz, single crystal ⊥ C.	>0.99	2.4	25-50	127-177	Do.
Do.....	>0.99	17.1	0-30	40	Kieffer and others, 1976.
Fused quartz.....	>0.99	-54	0-0.4	25	Goss and Combs, 1966.
Do.....	>0.99	-1	0-36	40	Kieffer and others, 1976.
Halite, single crystal.	>0.99	30.4	0-30	-28-113	Alm and Backstrom, 1975.
Do.....	>0.99	30.6	0-18	40	Kieffer and others, 1976.
Halite, sinter....	~0.98	36	0-12	30-75	Bridgman, 1924.
Do.....	~0.99	20	29-47	327-727	Fujisawa and others, 1968.
Enstatite, single crystal.	>0.99	5.6	19-34	33-113	Schloessin and Dvorak, 1972.
Do.....	>0.99	2.2	46-56	33-133	Do.
Do.....	>0.99	3	10-60	40	Schloessin and Beck, 1970.
Forsterite, sinter	~0.99	12	30-50	227-827	Fujisawa and others, 1968.
Talc, aggregate...	~0.99	15.7	0-12	30	Bridgman, 1924.
Mica, single crystal	>0.99	58	0-0.7	45	Clark, 1941.
Pyrophyllite, aggregate.	~0.99	2	10-60	40	Schloessin and Beck, 1970.
			Igneous rocks		
Basalt.....	0.96	4.7	0-12	30	Bridgman, 1924.
Do.....			2.2	0-12	75 Do.
Basalt (dry).....	0.983	182	0.03-0.97	31	Bucher and Decker, 1977.
Basalt (wet.....			34	0.03-0.97	31 Do.
Basalt (dry).....	0.976	212	0.03-0.10	31	Do.
Basalt (wet).....			226	0.03-87	31 Do.
Basalt (dry).....	0.966	56	0.03-97	31	Do.
Basalt (wet).....			38	0.03-97	31 Do.
Granite (wet).....	0.966	120	0-0.9	30	Walsh and Decker, 1966.

TABLE 7.--Effect of pressure on the thermal conductivity of certain minerals and rocks(continued)

Rock or mineral	Solidity[1] (γ)	Pressure coefficient[2] (a) (Mb^{-1})	Pressure range[3] (P) (kb)	Temperature range[4] (°C)	Reference
		Igneous rocks			
Granite (dry).....		19	0-0.9	30	Do.
Gabbro.....	~0.99	29	0-0.7	45	Clark, 1941.
Anorthosite.....	~0.99	15	0-0.7	45	Do.
Peridotite.....	~0.99	54	0-7.2	54	Kanamori and others, 1969.
Ecologite[5].....		13	0-17	80-400	Hughes and Sawin, 1967.
		Sedimentary rocks			
Siltstone.....	~0.9	30	0-12	30	Bridgman, 1924.
Shale.....	~0.9	145	0-0.7	45	Clark, 1941.
Slate.....	~0.95	58	0-0.7	45	Do.
Limestone.....	~0.95	1	0-12	30	Bridgman, 1924.
Do.....		6.7	0-12	75	Do.
Limestone (dry)...	0.97	189	0-0.7	45	Clark, 1941.
Do.....	0.87	102	0-0.7	45	Do.
Limestone (wet)...	0.87	15	0-0.7	45	Do.
Limestone (dry)...	0.57	319	0-0.7	45	Do.
Marble (dry).....	0.99	189	0-0.7	45	Do.
Marble (wet).....	0.99	29	0-0.7	45	Do.
Sandstone (dry)...	0.995	261	0-0.7	45	Do.
Sandstone (wet)...	0.995	58	0-0.7	45	Do.
Sandstone (dry)...	0.78	435	0-0.7	45	Do.
Sandstone (wet)...	0.78	87	0-0.7	45	Do.
Sandstone.....	0.838	3,000	0-0.2	30	Arnand and others, 1973.
Do.....	0.838	180	0.02-0.08	30	Do.
Do.....	0.838	3,000	0.0-0.07	30	Woodside and Messmer, 1961.
Do.....	0.838	550	0.07-0.25	30	Do.
Do.....	0.750	670	0.02-0.08	30	Anand and others, 1973.
Do.....	0.708	630	0.02-0.08	30	Do.

[1] The ratio of solid volume to bulk volume. Solidities which are marked with approximate (~) equality and greater than (>) were estimated from typical values. All other solidities were measured.

[2] Pressure coefficient $\underline{a} = (1 / \underline{K}_o)(\Delta \underline{K} / \Delta \underline{P})$, in the units 10^{-6}CU/bar, which equals 10 percent change in conductivity per kilobar. Conversion units are: 1bar=10^5 Pa, 1MPa = 10 bars, 1GPa = 10kb.

[3] Applicable range in pressure $\underline{P}$ in kilobars for $\underline{a}$; $\underline{K}_o$ is initial pressure.

[4] Applicable temperature or temperature range for $\underline{a}$.

[5] Cemented aggregate of crushed rock fragments.

THERMAL CONDUCTIVITY UNDER VACUUM

The effect on thermal conductivity $\underline{K}$ of removing air and water from the pores of a rock by drawing a vacuum is to lower the $\underline{K}$. Most measurements of $\underline{K}$ on rocks under a vacuum have been made on lunar basalt samples, and the following discussion and data are based on those results. No data are available for the effect of a vacuum on $\underline{K}$ of granite, limestone, sandstone or other common rocks, but in general, the observed reduction in $\underline{K}$ of basalt by removal of pore fluid was to be expected and occurs in the other rocks as well.

The basalt samples returned from the moon by astronauts of the Apollo program have been studied in great detail for their physical, chemical, and mineralogical properties. For the most part, the returned lunar rocks are basaltic in composition and much like terrestrial basalt; the texture varies from massive to highly vesicular; the structure varies from solid to breccia in outcrop, with fines in the regolith. Massive basalt contains about 75 percent crystalline pyroxene and plagioclase, which occur in volume ratios from 2:1 to 1:2; the remainder is glass and olivine or sometimes a large amount of ilmenite. The breccia and fines range from 20 to 75 percent glass.

In table 8 representative data are listed to show the effect of lowering the pore fluid pressure from atmospheric (10^5 Pa) to moderate vacuum (10^{-2} Pa) and even to the estimated fluid pressure on the moon (10^{-10} Pa). Solid basalt, breccia, and fines data are listed separately. (Note the change to 10^{-6}units for the fines conductivities.) As with basalt on the earth, $\underline{K}$ increases considerably with increasing solidity. Equivalents: 1atmos=10^5Pa=1bar=770 torr.

The effect of reducing pore fluid pressure on $\underline{K}$ of solid lunar rock and breccia is shown in table 8 by measurements made at 10^5 Pa and also under a vacuum of 10^{-2} Pa; the decrease in $\underline{K}$ was about 30 percent. In contrast, the $\underline{K}$ of fines from the lunar regolith under a pressure 10^5 Pa is 100 times larger than $\underline{K}$ under 10^{-3} Pa pressure (table 8, from Cremers, 1973). By comparing the two data sets, it was concluded that photon conduction by radiation in fines under vacuum is about equal to the phonon conduction through the solid grains and the pore gas (Cremers, 1973). A similar result was found for terrestrial basalt as described under "Mineral Conduction Mechanisms". A thermos bottle has much reduced heat loss by convective conduction into surrounding air by its vacuum barrier and has reduced radiative conduction by silvering the surfaces of the evacuated space.

In situ measurements by Langseth and others (1972) of $\underline{K}$ of the regolith on the moon at the Hadley Rille site (Apollo 15) were found to be 10 times higher than $\underline{K}$ of the fines measured in the laboratory (table 8). The difference was explained as due to the greater amount of rock fragments of in situ regolith at 0.5 - 1.4 m depth (γ = 0.5) and not to the much lower atmospheric pressure on the moon of 10^{-10} Pa.

The effect of temperature on solid rock lunar samples under 10^5 Pa and 10^{-2} Pa pore fluid pressures is indicated in table 8 for sample 10049, measured by Fujii and Osako (1973). Under both pressures, the $\underline{K}$ of solid basalt decreases sharply with decreasing temperature from a peak value (4×10^{-3}cal/cm s K) at about 300 K and approaches zero at absolute zero temperature. Under 10^5 Pa, $\underline{K}$ of lunar basalt decreases slightly (0.3×10^{-3} cal/cm s K) with increasing temperature from 300 K to above 600 K; under 10^{-2} Pa, the $\underline{K}$ increases slightly (0.5×10^{-3}cal/cm s K) from 300 K to 600 K. Similar results were obtained on some other samples (not listed in table 8) by Horai and Fujii (1972), Fujii and Osako (1973), and Mizutani and Osako (1974).

The temperature effect on diffusivity $\underline{k}$ of solid basalt is much larger than the effect on conductivity. Horai and Winkler (1976) found that $\underline{K}$ decreases from a much higher value at 100 K (10×10^{-3} cm^2/s) to a moderate value at and above 300 K (4×10^{-3}cm^2/s) under 10^5 Pa pressure. However, samples under 10^{-4} Pa pressure had essentially constant $\underline{k}$ (about equal to 3×10^{-3} cm^2/s) throughout the whole temperature range from 100 K to 500 K. (Lunar surface temperature at night is about 100 K and at noon about 350 K.)

The conductivity $\underline{K}$ of fines from the lunar regolith under vacuum increases exponentially with increasing temperature. The increase by a factor of two in $\underline{K}$ of sample 12001 (fines) at its natural density (1.97 g/cm^3) is shown in table 8 at temperatures of 100 K, 300 K, and 450K. Cremers (1973) states that the increase in $\underline{K}$ is by radiative (photon) conduction, and that his data fit the theoretical temperature-cubed relation of equation 8. Watson (1964) developed the following relation from experiments on silicate powders under vacuum: $\underline{K}_T = \underline{K}_C + \underline{K}_R T^3$, where subscripts are T for total, C for solid conduction, and R for radiative conduction.

TABLE 8. Effect of reducing pore fluid pressure by high vacuum on the thermal conductivity of lunar rocks.

Lunar sample (number)	Bulk density (g/cm^3)	Solidity (γ)	Temperature (K)	Pressure (Pa)	Thermal Conductivity (10^{-3}cal/cm sec K)	References, rock types
			SOLID ROCK			
10049	3.07	0.943	300	10^5	3.51	Horai and Fujii,
				10^{-2}	2.4	1972, basalt
10069	2.90	0.89	300	10^5	3.27	
				10^{-2}	1.6	
10049	3.07	0.945	100	10^5	2.34	Fujii and Osako,
			300		3.49	973, basalt
			500		3.38	
			100	10^{-2}	1.28	
			300		2.41	
			500		.75	
10069	2.90	0.89	300	10^5	3.26	
				10^{-2}	1.19	
terres-	2.76	0.952	300	10^5	4.47	Fujii and Osako,
trial				10^{-2}	3.64	1973, olivine basalt
12002,85	2.961	0.895	85	10^4	0.88	Horai and Winkler,
				10^{-1}-10^{-4}	0.47	1975, porphyritic
			315	10^4	1.86	basalt
				10^{-1}-10^{-4}	1.52	
			450	10^4	2.18	
				10^{-1}-10^{-4}	1.70	
70215,30	3.37	0.99	300	10^{-1}	3.19	Mizutani and Osako,
						1974, basalt
77017,24	2.48	0.75	300	10^{-1}	0.50	anorthosite
10057,20	2.9	0.88	300	10^5	3.6	Horai and Fujii,
			4		0.2	1972, basalt
			BRECCIA			
10046,65	2.3	0.70	300	10^5	1.65	Horai and Fujii,
			4		0.0025	1972
14311	2.71	0.951	300	10^5	3.15	Fujii and Osako,
				10^{-2}	2.37	1973

TABLE 8. Effect of reducing pore fluid pressure by high vacuum on the thermal conductivity of lunar rocks. (Continued)

Lunar sample (number)	Bulk density (g/cm^3)	Solidity (γ)	Temperature (K)	Pressure (Pa)	Thermal conductivity (10^{-6}cal/cm sec K)	References, rock types
			FINES[2]			
various	1.27	0.38	300	1	4.	Cremers, 1973
samples[1]	to 1.97	0.60		10	10.	
				10^2	23.	
				10^3	55.	
				10^4	122.	
				10^5	300.	
12001	1.30	0.39	300	10^{-3}	4.23	Cremers, 1973
	1.64	0.47			3.68	
	1.97	0.60	100	10^{-3}	2.9	
			300		3.8	
			450		6.0	
10084	1.64	0.50	300	10^{-3}	5.86	Cremers, 1973
10084	1.265	0.38	205	10^{-1}	4.09	Horai and Simmons,
			299		4.95	1972
			404		5.78	
10084	1.265	0.38	300	10^{-4}	4.6	Horai and Fujii,
12001	1.30	0.39			3.7	1972
14163,133	1.10	0.33	300	10^{-4}	3.13	Cremers, 1972
	1.30	0.39			3.27	
terres-	1.13	0.34	300	10^{-6}	3.53	Fountain and West,
trial	1.30	0.40			4.59	1973, basalt
	1.50	0.45			6.26	powder
in situ[3]						
0.5m	1.5	0.45	250	10^{-10}	34.	Langseth and others,
0.9m	1.6	0.49			41	1972, fragmental
1.4m	1.8	0.54			60.	regolith

[1]From log-log plot of data on lunar samples of Apollo 11 and 12, the Soviet Luna 16, and terrestrial basalt powder.
[2]Note the change in units for fines from 10^{-3} to 10^{-6} cal/cm sec deg K from the upper part of the table for solid rock and breccia.
[3]Conductivity measurements made in situ with a probe at the depths indicated below the lunar surface.

THERMAL EXPANSION AND DENSITY OF MINERALS

The densities d listed in table 9 are theoretical values from molar volumes of unit cells determined by X-ray methods (Robie and others, 1967). The data of the coefficient of mean volumetric thermal expansion α of mineral crystals in table 9 are calculated from Skinner's tables (1966), where

$$\alpha = (1 / V_o) (\Delta V / \Delta T) \qquad (13)$$

The temperature range to which the values of α apply here is between 20 °C and 400 °C, which will serve most practical purposes; the measurement pressure was 1 bar. At T > 400 °C even for single crystals, the thermal expansions are liable to irreversible changes as a consequence of the test, by formation of microfractures or by chemical effects, like oxidation, disordering, or phase transformations.

The thermal expansion of a rock cannot be measured reliably above about 100 °C without applying confining pressure to the rock sample because of irreversible changes in the rock. In explanation, Ide (1937) pointed out: "As the temperature of the sample rises, the crystals expand differently in different directions, depending on their composition and orientation. This unequal expansion may be expected to cause some internal cracking to take place along the lines of greatest stress. On cooling the specimen the fractures would remain". (See also the remarks, of E. B. Dane, Jr., in Skinner, 1966).

The thermal expansion α of a rock can be calculated as an average from values for the minerals of the mode of the rock (table 9) by use of Equation 1, similar to the conductivity calculation. To give a rough measure of values to be expected for rocks to 100 °C, data for several common rocks are given in table 10, taken from Skinner (1966). In addition, typical or "average" values of the bulk density of dense rocks ($\gamma > 0.98$) are listed in table 11. Density is needed in calculating diffusivity and thermal inertia from thermal conductivity, as explained in a section below. As with thermal expansion, the composite grain density of a dense rock can be calculated by use of Equation 1, substituting density for conductivity. Discontinuities at faults, joints and fractures, foliation and preferred grain orientations, and chemical oxidation and weathering zones are even more prevalent in rock in place, so calculated expansions and densities may be too high when applied to large rock masses.

TABLE 9.--Thermal expansion and density of minerals

Mineral	Formula	Density [1] (gm/cm^3)	Volumetric thermal expansion [2] (10^{-5}per °C)
	Quartz and feldspar		
Quartz.....	SiO_2	2.648	4.98
Orthoclase.....	$KAlSi_3O_8$	2.570	1.54
Microcline.....	$KAlSi_3O_8$	2.560	1.79
Albite.....	$NaAlSi_3O_8$	2.620	2.24
Anorthite.....	$CaAl_2Si_2O_8$	2.760	1.51
Celsian.....	$Ba(Al_2Si_2O_8)$	3.400	1.03
	Feldspathoid		
Nepheline.....	$Na_3K(Al_4Si_4O_{16})$	2.623	3.92
	Olivine		
Forsterite.....	Mg_2SiO_4	3.214	3.26
Fayalite.....	Fe_2SiO_4	4.393	2.84
Monticellite...	$CaMgSiO_4$	3.046	3.42
Zircon.....	$SrSiO_4$	4.669	1.11
	Pyroxene and amphibole		
Jadeite.....	$NaAlSi_2O_6$	3.347	2.45
Enstatite.....	$MgSiO_3$	3.194	2.77
Diopside.....	$CagMgSi_2O_6$	3.277	2.51
Augite.....	$Ca(Mg,Fe,Al)•(Al,Si)_2O_6$	3.41	2.19
Wollastonite...	$CaSiO_3$	2.909	2.95
Spodumene.....	$LiAlSi_2O_6$	3.188	1.31
Hornblende.....	$NaCa_2(Mg,Fe,Al)_5(Si,Al)_8O_{22}(OH)_2$	3.37	2.56

TABLE 9.--Thermal expansion and density of minerals (Continued)

Mineral	Formula	Density [1] (gm/cm^3)	Volumetric thermal expansion [2] (10^{-5} per °C)
	Aluminum silicate		
Kyanite.....	Al_2SiO_5	3.675	2.35
Andalusite.....	Al_2SiO_5	3.0915	2.82
Sillimanite....	Al_2SiO_5	3.247	1.40
	Garnet		
Almandite	$Fe_3Al_2(SiO_4)_3$	4.318	2.11
Grossularite	$Ca_3Al_2(SiO_4)_3$	3.595	2.10
Spessartite	$Mn_3Al_2(SiO_4)_3$	3.987	2.47
	Miscellaneous silicates		
Cordierite.....	$Mg_2AL_3AlSi_5O_{18}$	2.51	0.30
Topaz.....	$Al_2(SiO_4)(OH)_2$	3.531	1.72
Gehlenite.....	$Ca_2Al_2SiO_7$	3.021	2.45
	Oxides		
Magnetite.....	Fe_3O_4	5.200	3.50
Hematite.....	Fe_2O_3	5.275	3.10
Chromite.....	$(Fe,Mg)Cr_2O_4$	5.22	1.26
Corundum.....	Al_2O_3	3.987	0.74
Rutile.....	TiO_2	4.245	2.55
Spinel.....	$MgAl_2O_4$	3.583	2.37

TABLE 9.--Thermal expansion and density of minerals (Continued)

Mineral	Formula	Density [1] gm/cm^3)	Volumetric thermal expansion [2] (10^{-5} per ° C)
	Sulfides		
Pyrite.....	FeS_2	5.016	3.40
Sphalerite.....	ZnS	4.089	2.37
Galena.....	PbS	7.597	6.33
	Halides		
Halite	NaCl	2.163	13.83
Sylvite	KCl	1.987	12.77
	Carbonates		
Calcite.....	$CaCO_3$	2.710	2.01
Aragonite.....	$CaCO_3$	2.930	6.53
Strontianite...	$SrCO_3$	3.785	6.51

[1] Densities (d, in gm /cm ^{3}) were calculated from molar volumes of the crystal cells of minerals (from Robie and others, 1967).

[2] Volumetric thermal expansions were measured on single crystals and are given in units 10^{-5} per °C and apply to $20° < T < 400$ °C. (From Skinner, 1966.)

TABLE 10.--Thermal expansion of rocks for the temperature interval 20-100 °C

Rock type	Volumetric thermal expansion [1] (10^{-5} per ° C)
Granite, rhyolite	2.4
Diorite, andesite	2.1
Gabbro, basalt	1.6
Sandstone	3.0
Quartzite	3.3
Limestone	2.4
Marble	2.1
Slate	2.7

[1] Mean volumetric thermal expansion, $\alpha = (1/V_o)\ (\Delta V / \Delta T)$, in units of 10^{-5} per °C, from Skinner (1966).

TABLE 11.--Bulk density of common rocks

Rock type	Decimal porosity ϕ	Bulk density (g/cm^3)
	Igneous [1]	
Granite.....	----	2.67
Granodiorite.....	----	2.72
Syenite.....	----	2.76
Quartz diorite.....	----	2.81
Diorite.....	----	2.84
Gabbro.....	----	2.98
Diabase.....	----	2.97
Peridotite.....	----	3.23
Dunite.....	----	3.28
	Metamorphic [2]	
Granite gneiss.....	----	2.7
Quartz mica schist	----	2.8
Slate.....	----	2.8
Amphibolite.....	----	3.0
Eclogite.....	----	3.4
	Sedimentary [3]	
Sandstone.....	0.007	2.7
	0.10	2.5
	0.20	2.3
	0.30	2.2
Limestone.....	0.005	2.7
	0.05	2.6
Chalk.....	0.30	2.2
Dolomite.....	0.03	2.8
Shale.....	0.05	2.6
	0.20	2.4
Sand.....	0.50	1.9
Silt.....	0.75	1.5

[1] Averages from Daly, 1966; porosity not recorded.

[2] Averages from Clark, 1966; porosity not recorded.

[3] Averages from Manger, 1966. Bulk densities of sedimentary rocks are for samples saturated with water. Representative values of density and corresponding porosity are given; therefore, only two significant figures are shown.

SPECIFIC HEAT OF ROCK

Introduction

The uses of the specific heat of a rock at constant pressure $\underline{C}_p$ are many, from engineering purposes to theoretical analysis of the earth's interior. The following graphs (figs. 30-42) were prepared from the tables of Robie and Waldbaum (1967) and are given to provide reasonably accurate estimates of the $\underline{C}_p$'s of minerals from which to calculate $\underline{C}_p$ of rocks at the temperature of interest. A tabulation for common rocks of $\underline{C}_p$ values at various temperatures is also given for rough estimates in table 10. As is apparent from the graphs, the effect of the temperature on $\underline{C}_p$ is large and should be accounted for. An additional important consideration is the porosity of the rock, if it is more than a few percent.

The $\underline{C}_p$ of a rock can be measured, but the calorimetric apparatus required is rather elaborate (see Lindroth and Krawza, 1971), and the measurements are tedious. Alternatively, the $\underline{C}_p$ can be calculated either from the chemical or the mineral composition of the rock. The Neumann-Kopp rule utilizes the content of chemical elements, as described by Somerton (1958) and Lindroth and Krawza (1971). Whereas either the calorimetric determination or the chemical analysis of a rock require careful laboratory work, it is simpler to calculate $\underline{C}_p$ from the mode, the mineral composition of the rock. The mode can usually be determined adequately by hand-lens inspection or better by petrographic study of a thin section.

Graphs shown in figures 30-42 of the specific heat as a function of temperature of minerals provide adequate precision for estimating values for rock, with about 2 1/2 significant figures. Not all rock-forming minerals are shown in the figures, but representative values can be estimated from those minerals which are depicted. One set of the following graphs, figures 30-36, shows curves of specific heat per degree per unit weight (J/kg K), and the other set (figs. 37-42), shows specific heat per degree per unit volume (J/m^3K).

In heat conduction problems, the mass of the given rock per unit volume, its measured bulk density, is multiplied by the calculated average $\underline{C}_p$ per unit weight of the solid rock, to account for the porosity of the rock. The specific heat of the actual mass of mineral grains in unit volume of the rock is wanted. If the porosity is less than a few percent the average grain density can be used. However, the decimal fractions of the minerals in the rock must be in weight percent (in figs. 30-36).

It is much easier to use the curves in figures 37-42 for $\underline{C}_p$ per unit volume because the modes of rocks are invariably in volume percent. The porosity of the rock is accounted for by multiplying the combined $\underline{C}_p$ per unit volume by the rock solidity, γ.

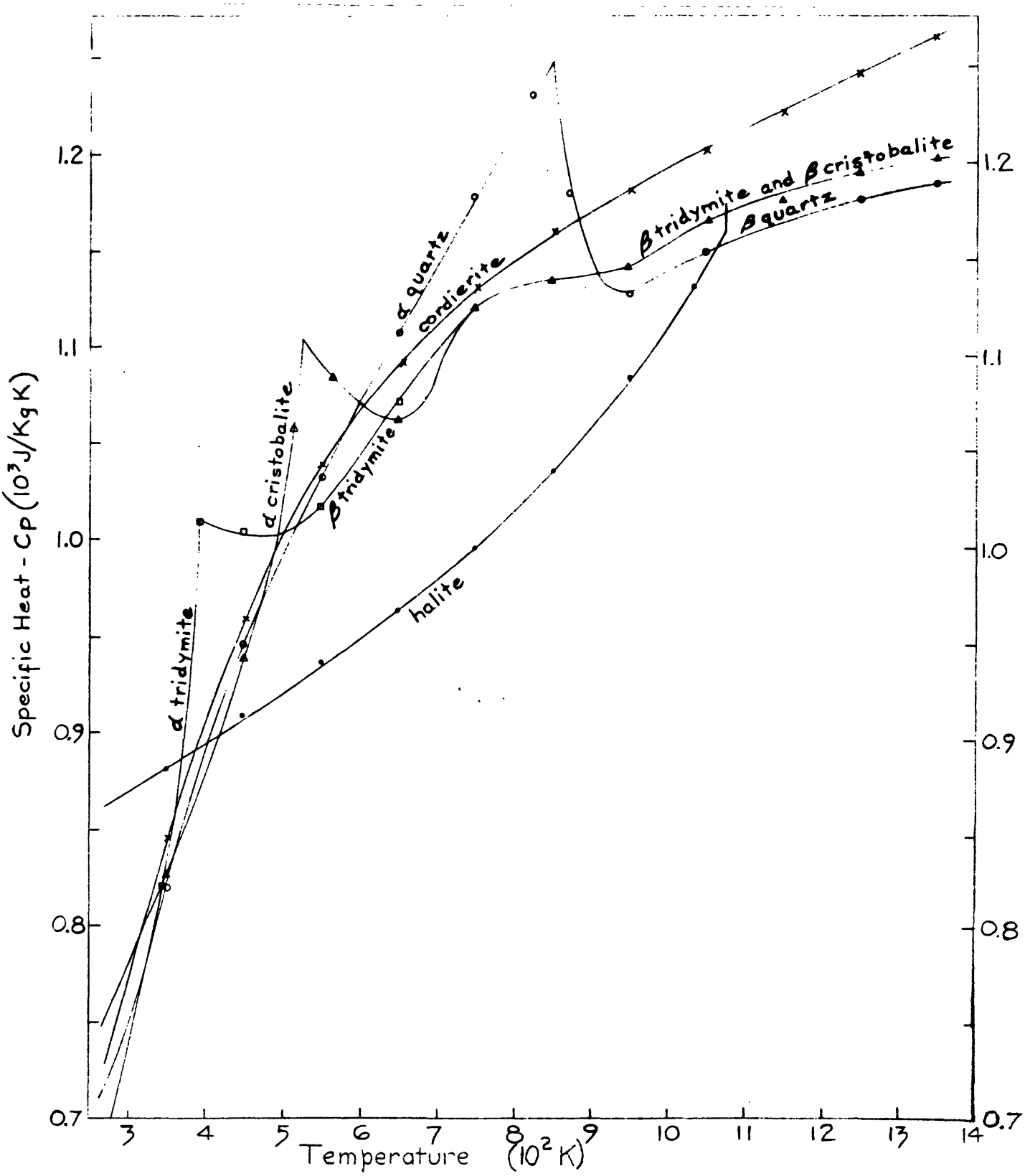

FIGURE 30. Specific heats per unit weight of silica minerals, halite, and cordierite in variation with temperature.

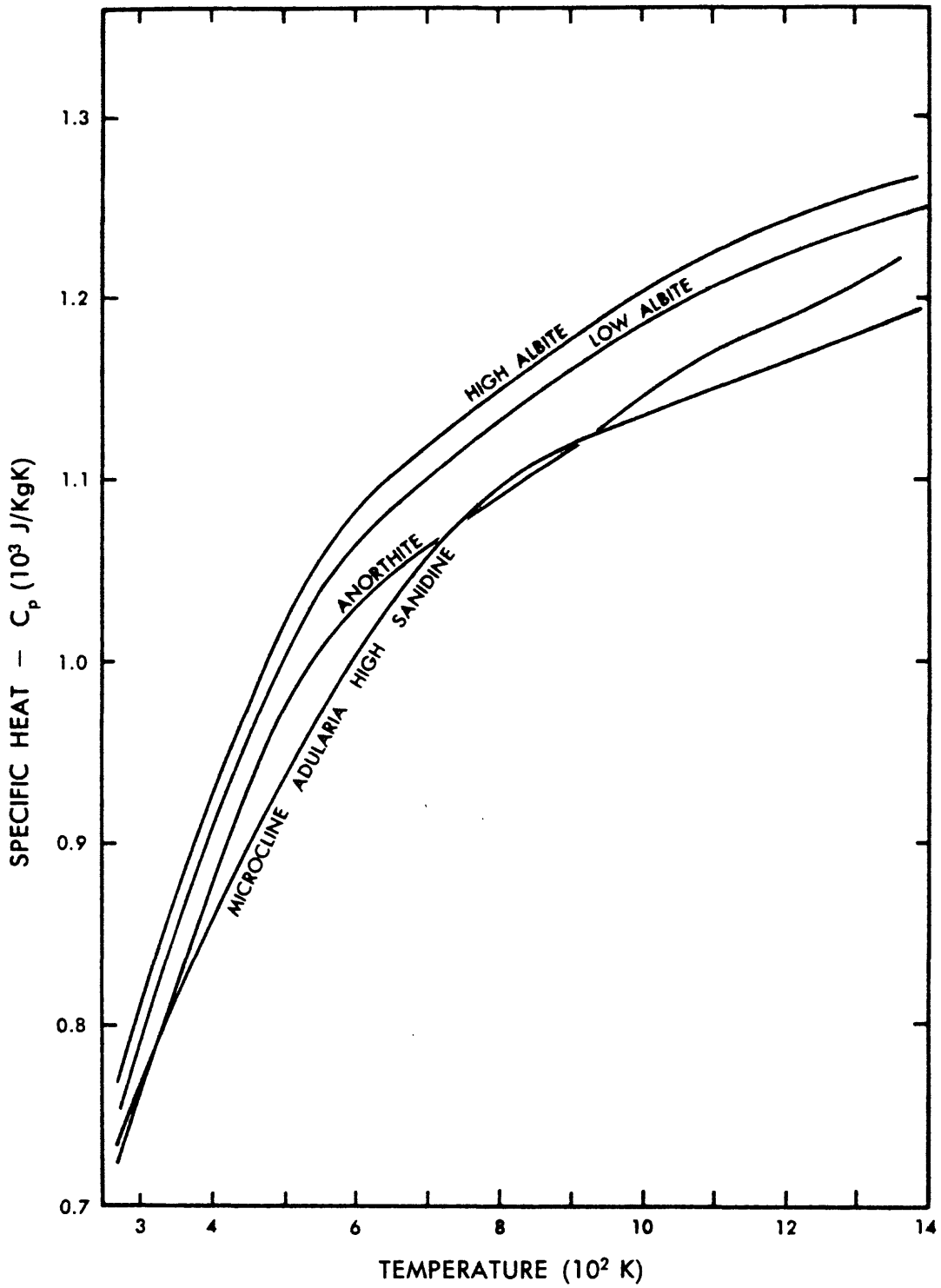

FIGURE 31. Specific heats per unit weight of feldspars in variation with temperature.

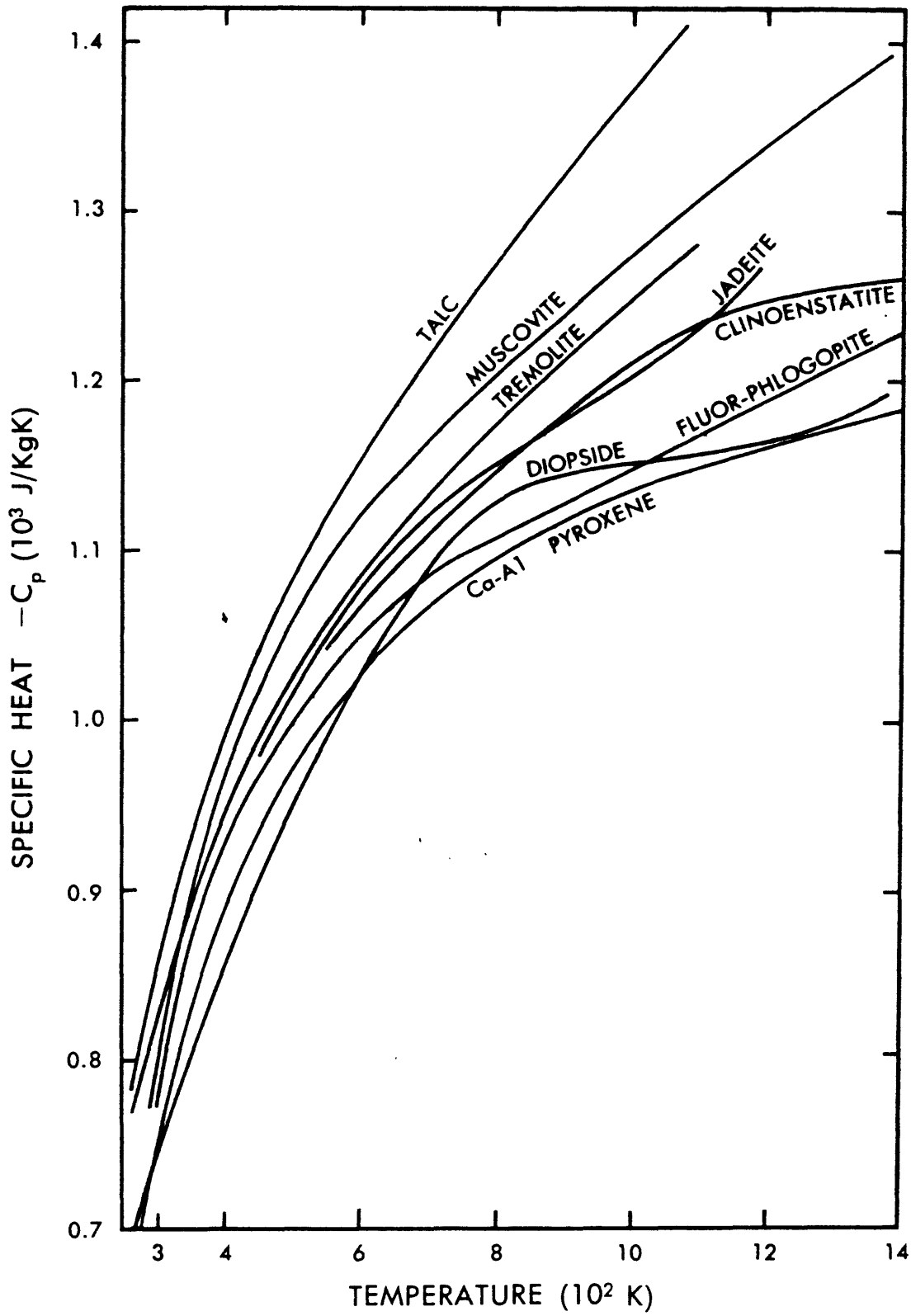

FIGURE 32. Specific heats per unit weight of certain pyroxenes, amphiboles, and micas in variation with temperature.

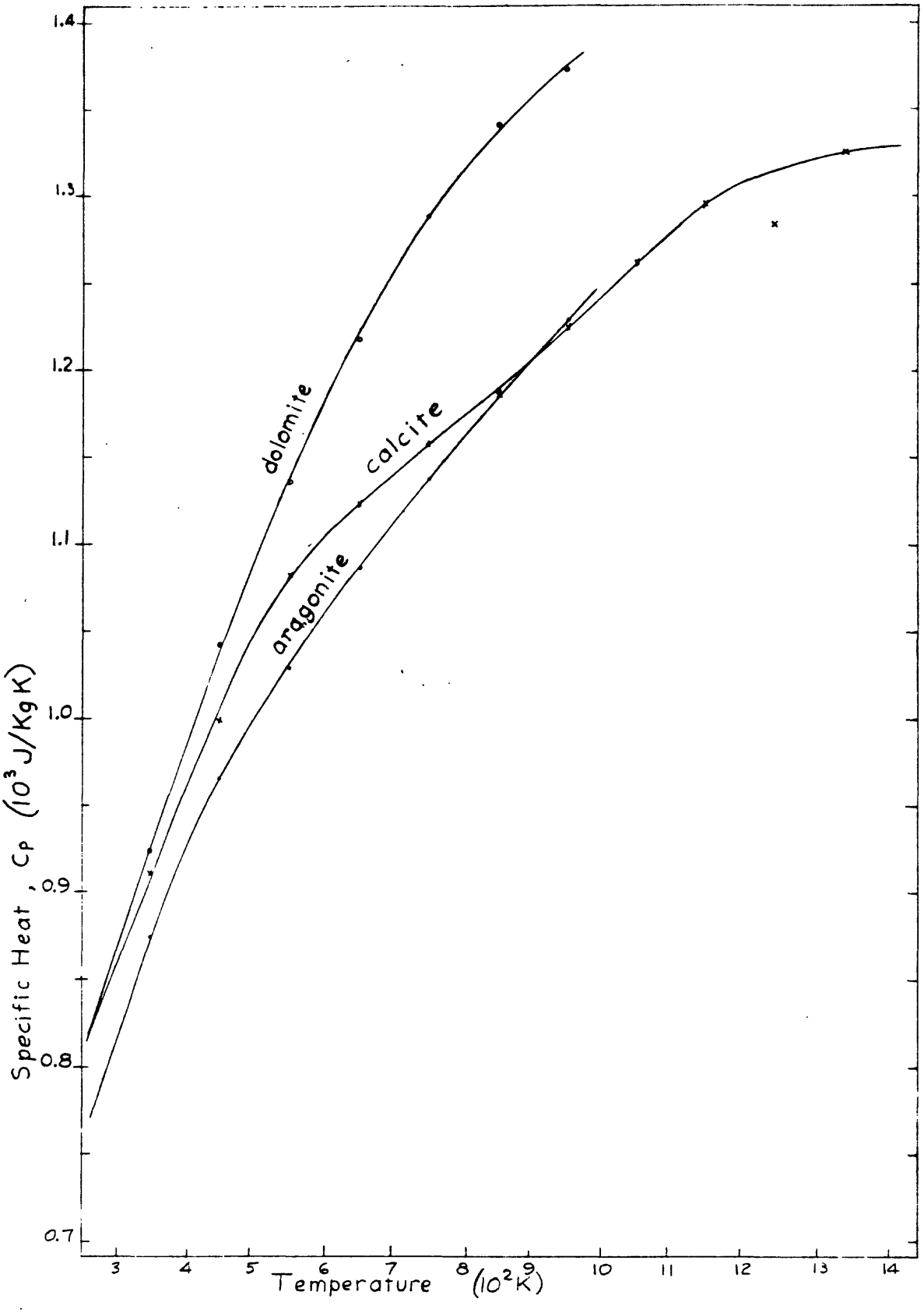

FIGURE 33. Specific heats per unit weight of calcite, dolomite, and aragonite in variation with temperature.

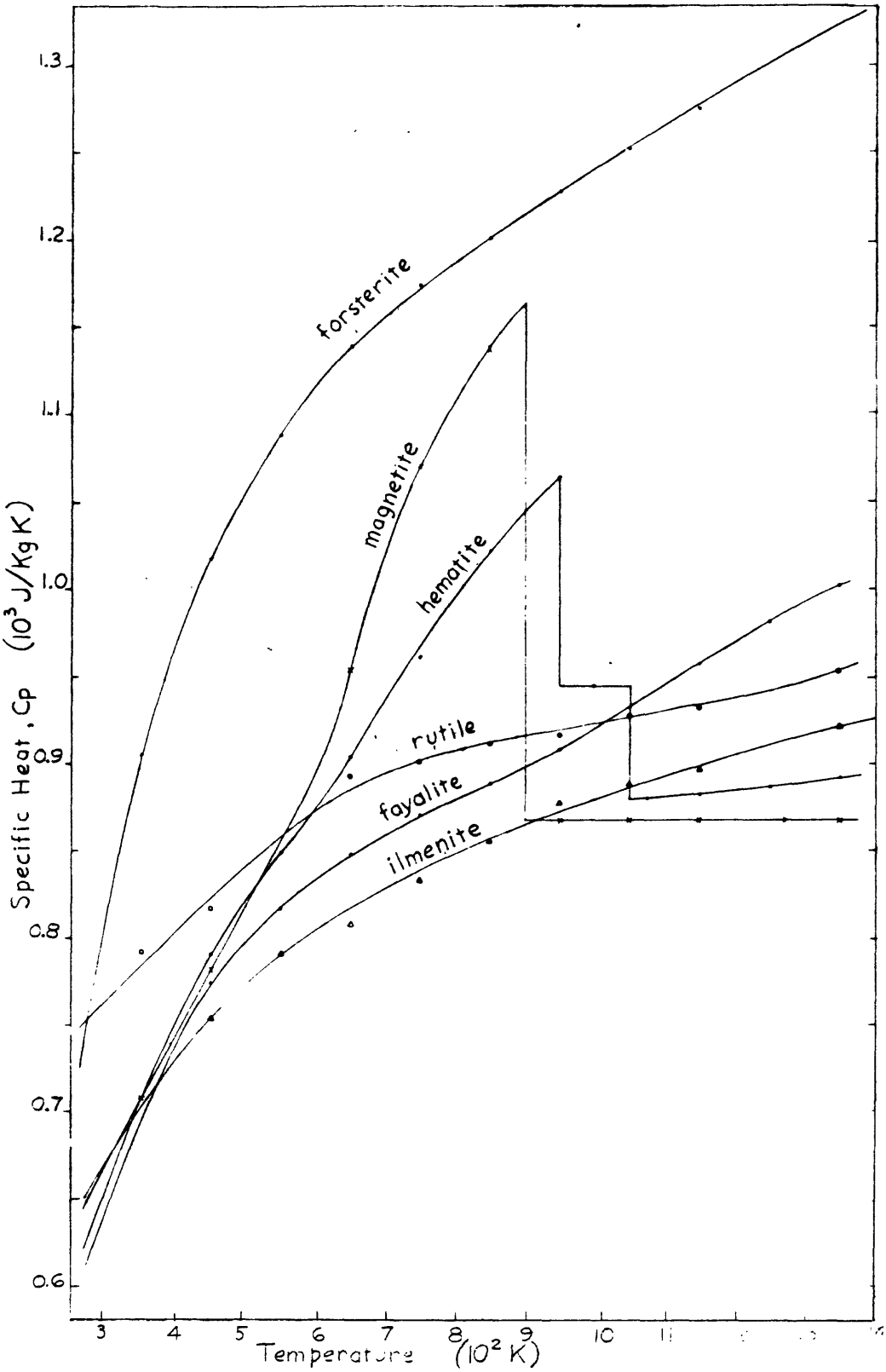

FIGURE 34. Specific heats per unit weight of olivines and iron oxides in variation with temperature.

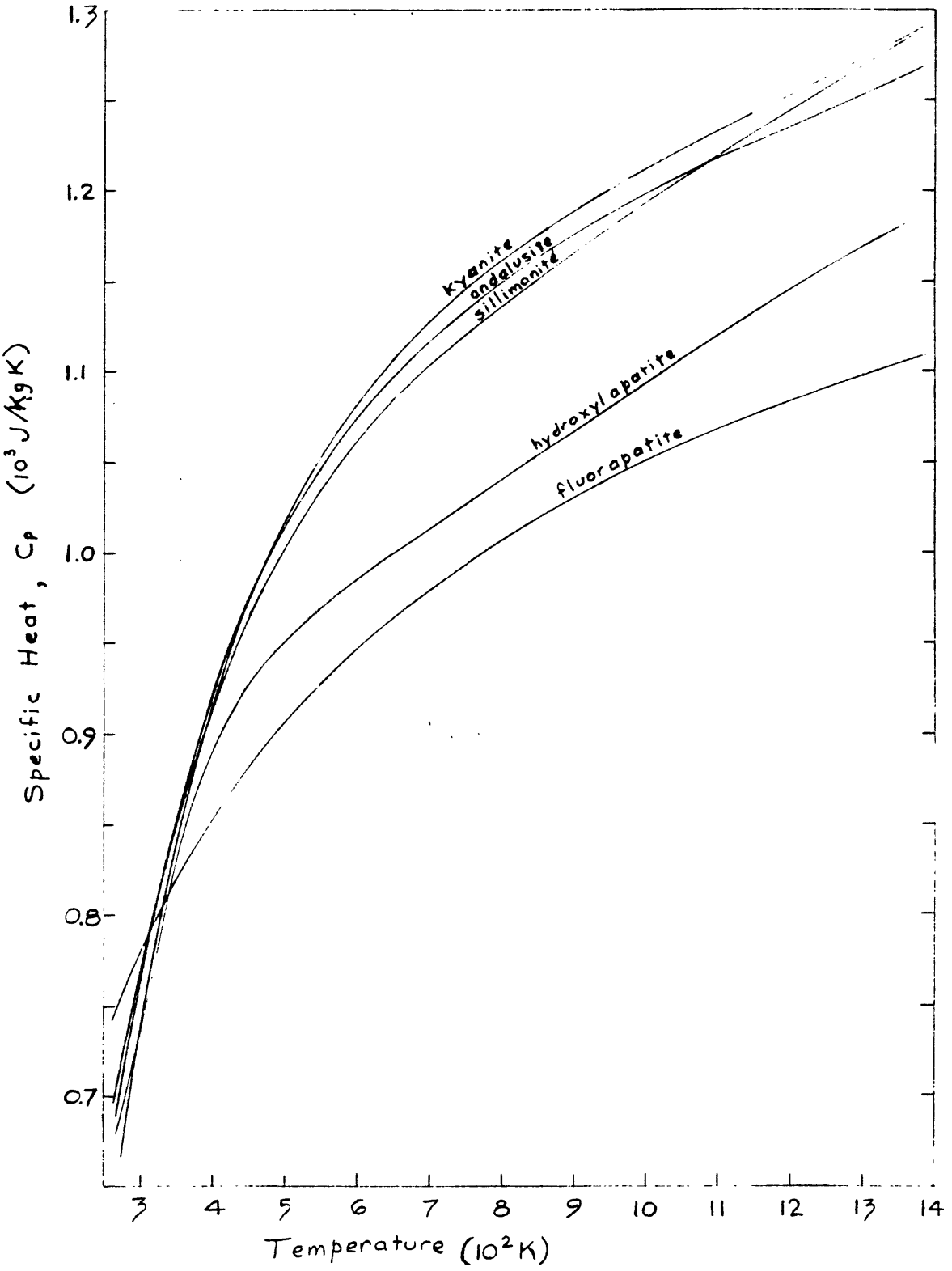

FIGURE 35. Specific heats per unit weight of aluminum silicate and apatite minerals in variation with temperature.

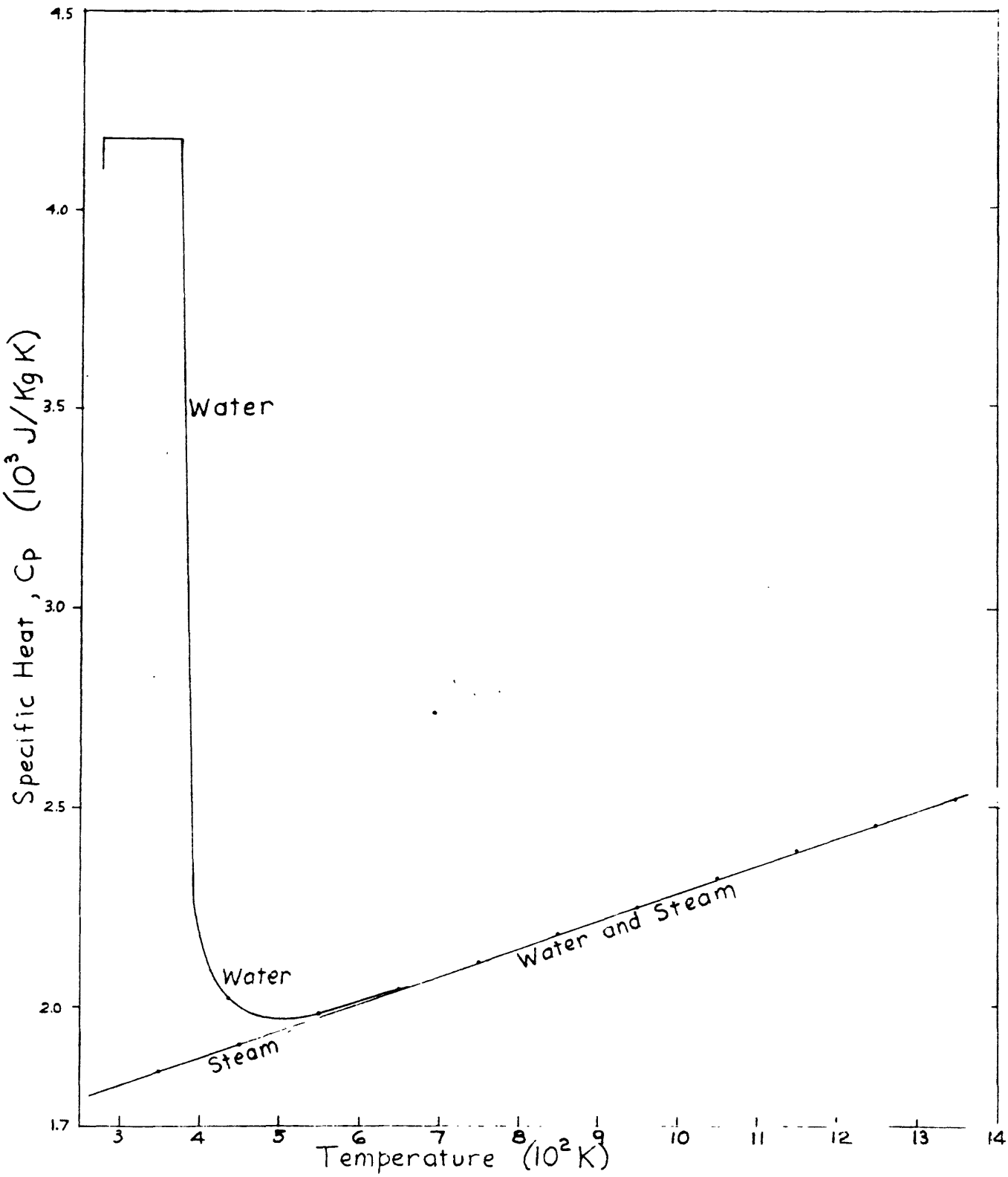

FIGURE 36. Specific heats per unit weight of water and steam in variation with temperature.

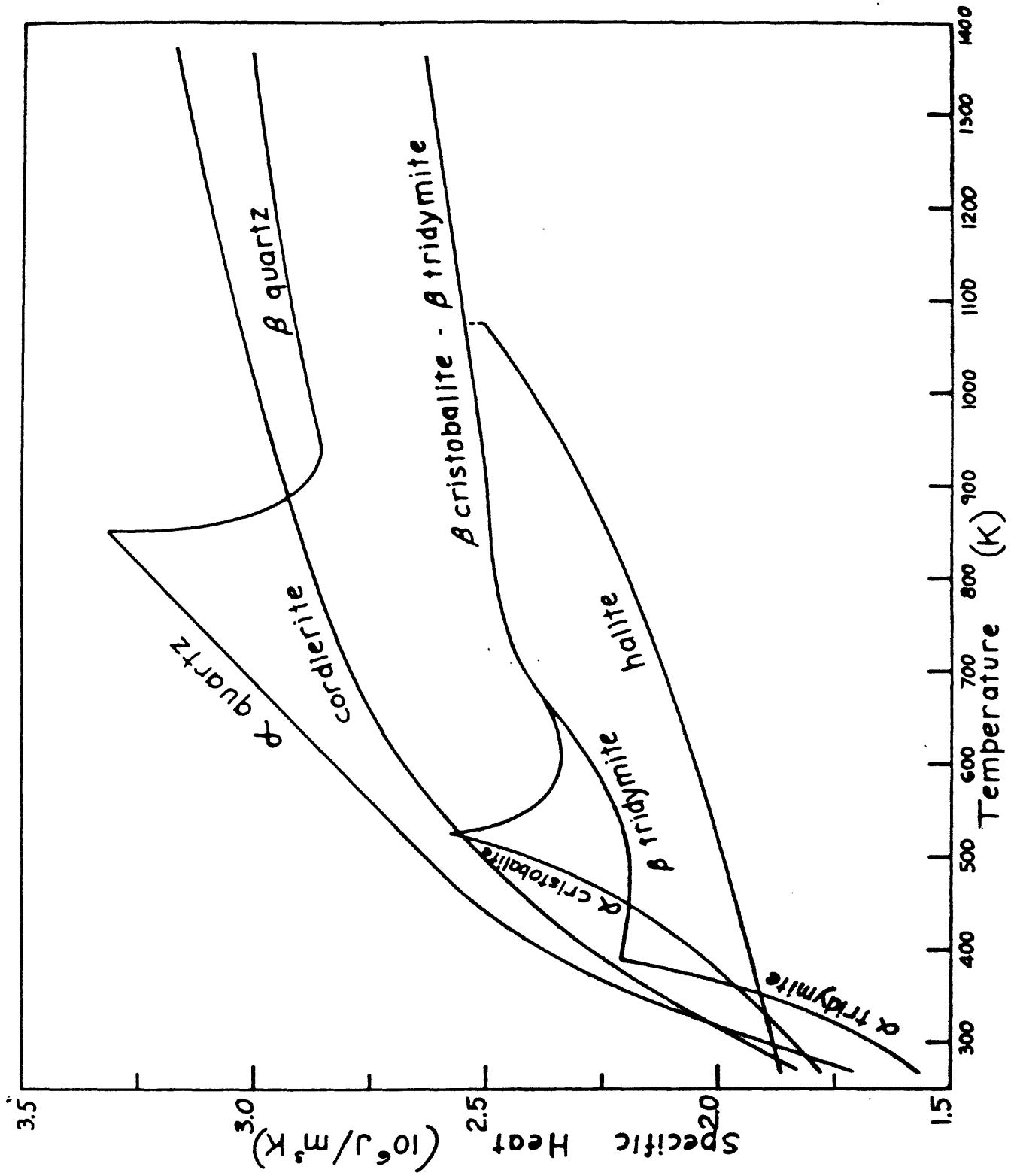

FIGURE 37. Specific heats per unit volume of silica minerals, halite, and cordierite in variation with temperature.

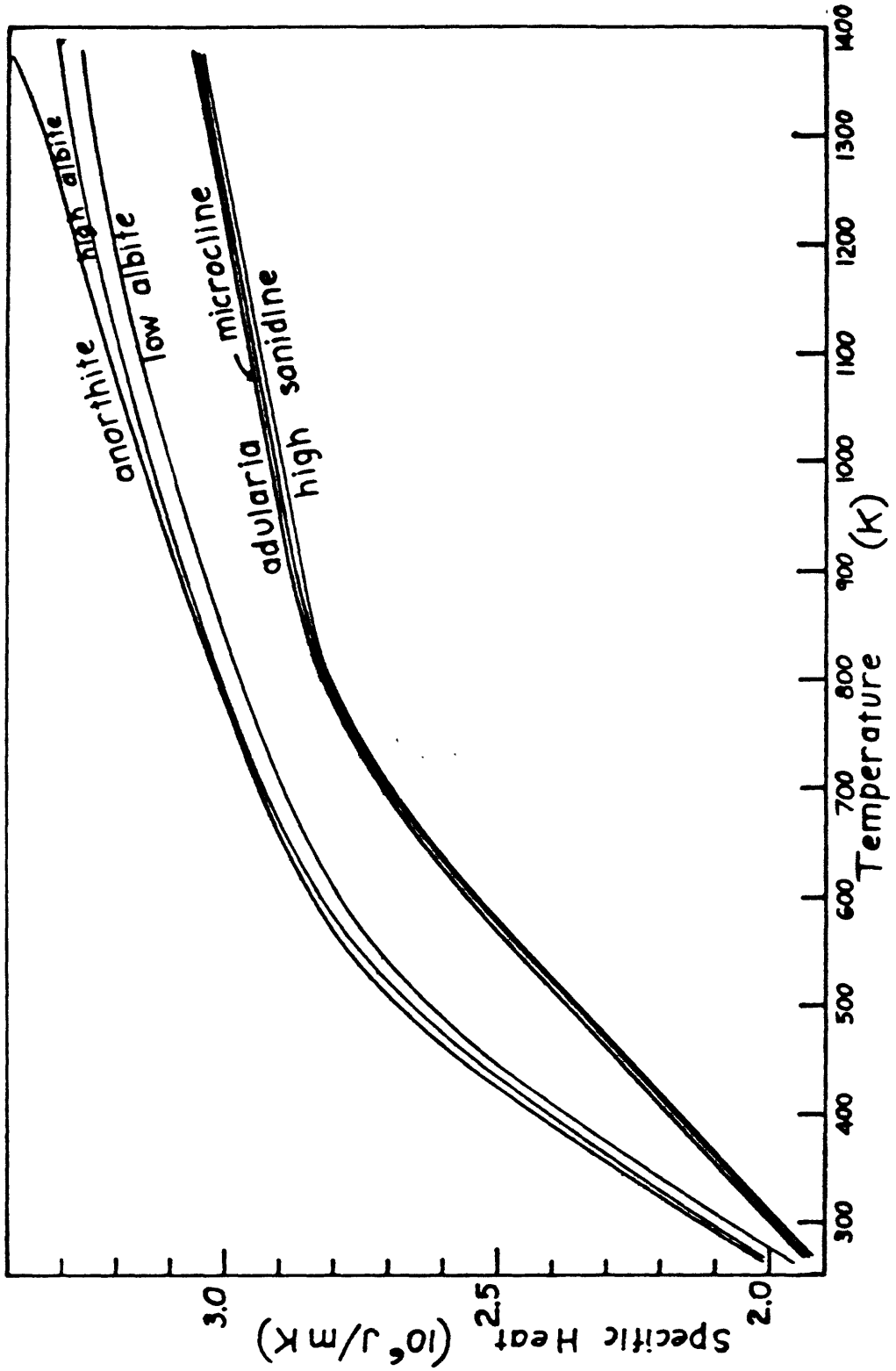

FIGURE 38. Specific heats per unit volume of feldspars in variation with temperature.

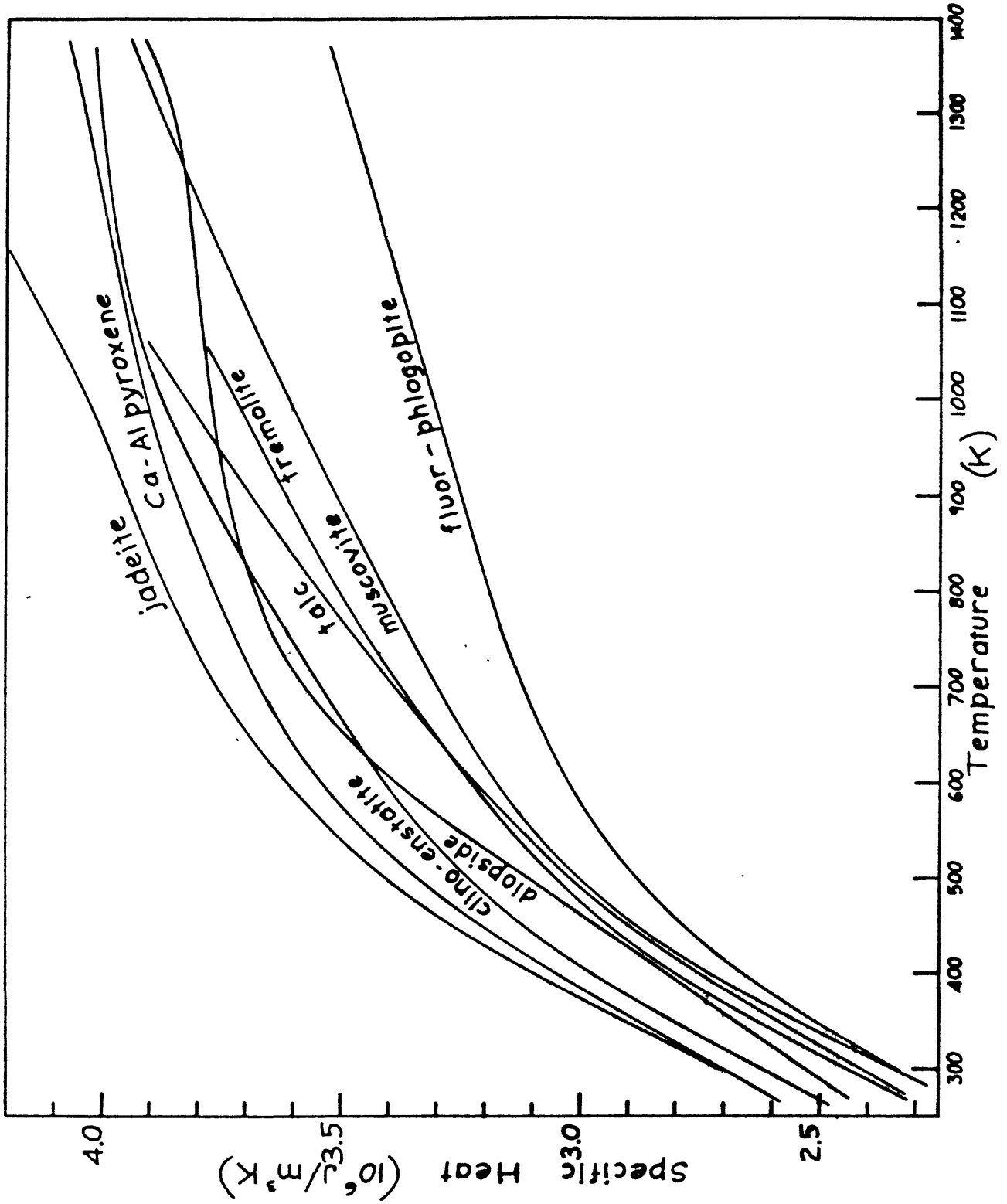

FIGURE 39. Specific heats per unit volume of pyroxenes, amphiboles, and micas in variation with temperature.

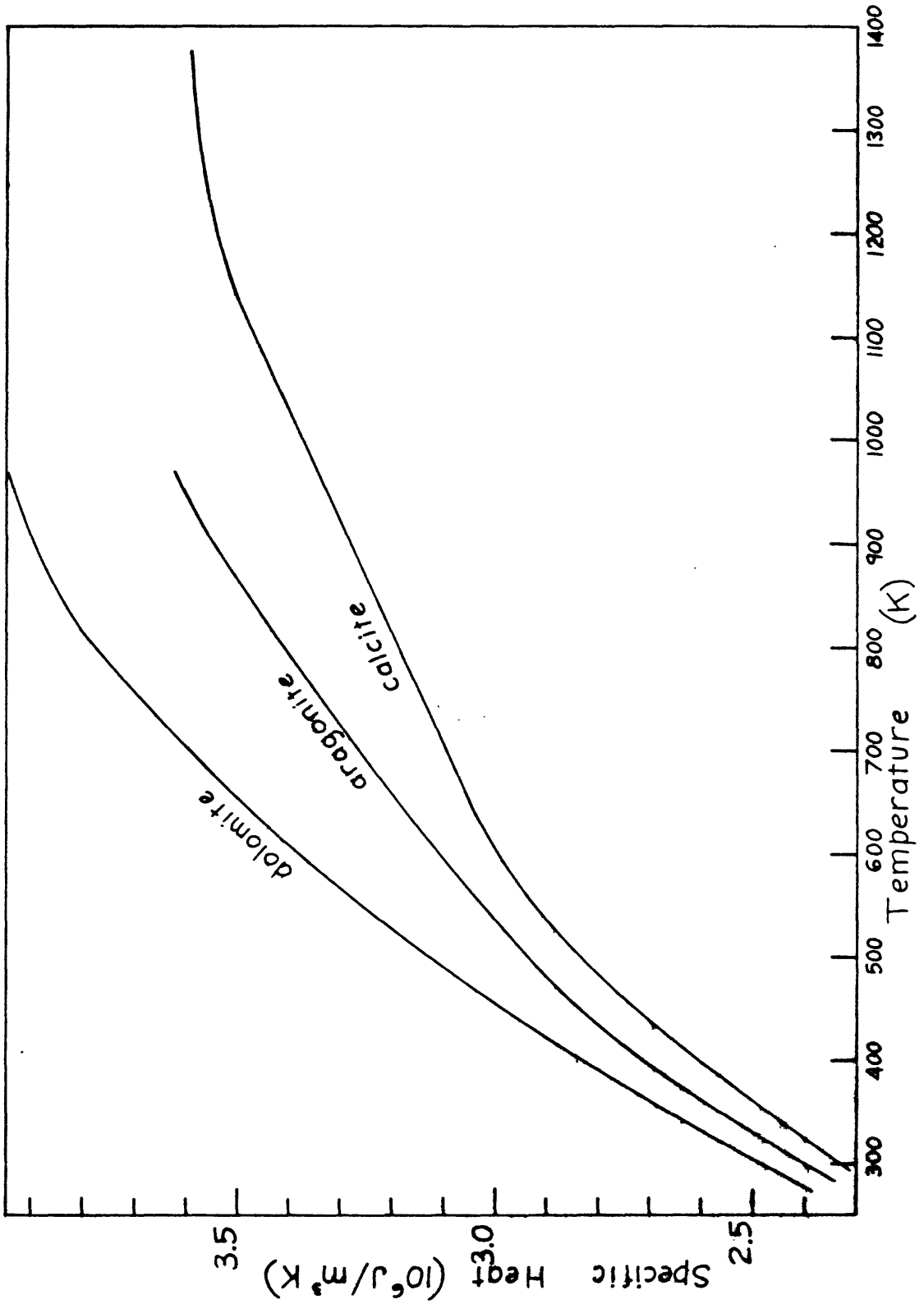

FIGURE 40. Specific heats per unit volume of calcite, dolomite, and aragonite in variation with temperature.

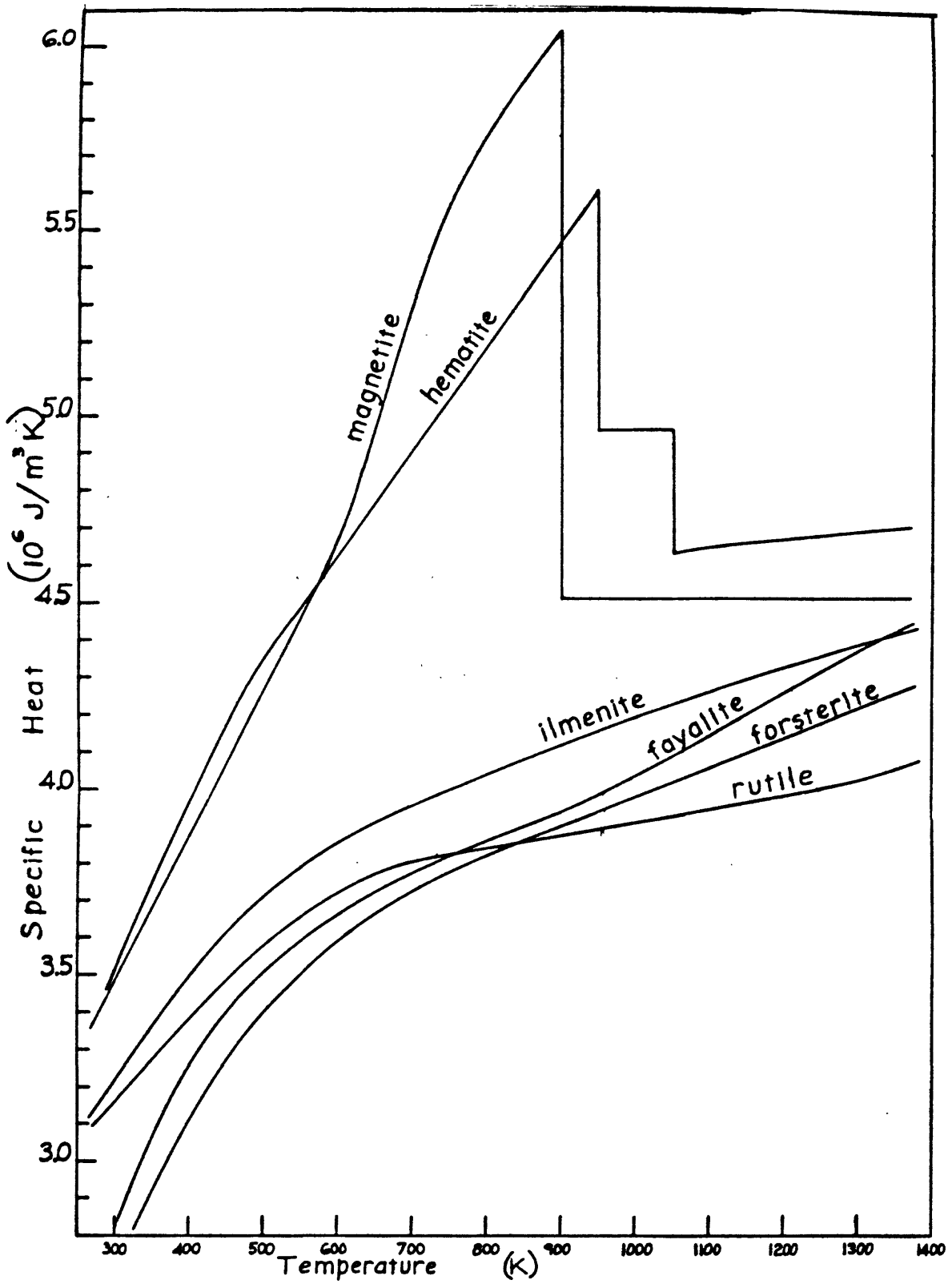

FIGURE 41. Specific heats per unit volume of olivines and iron oxides in variation with temperature.

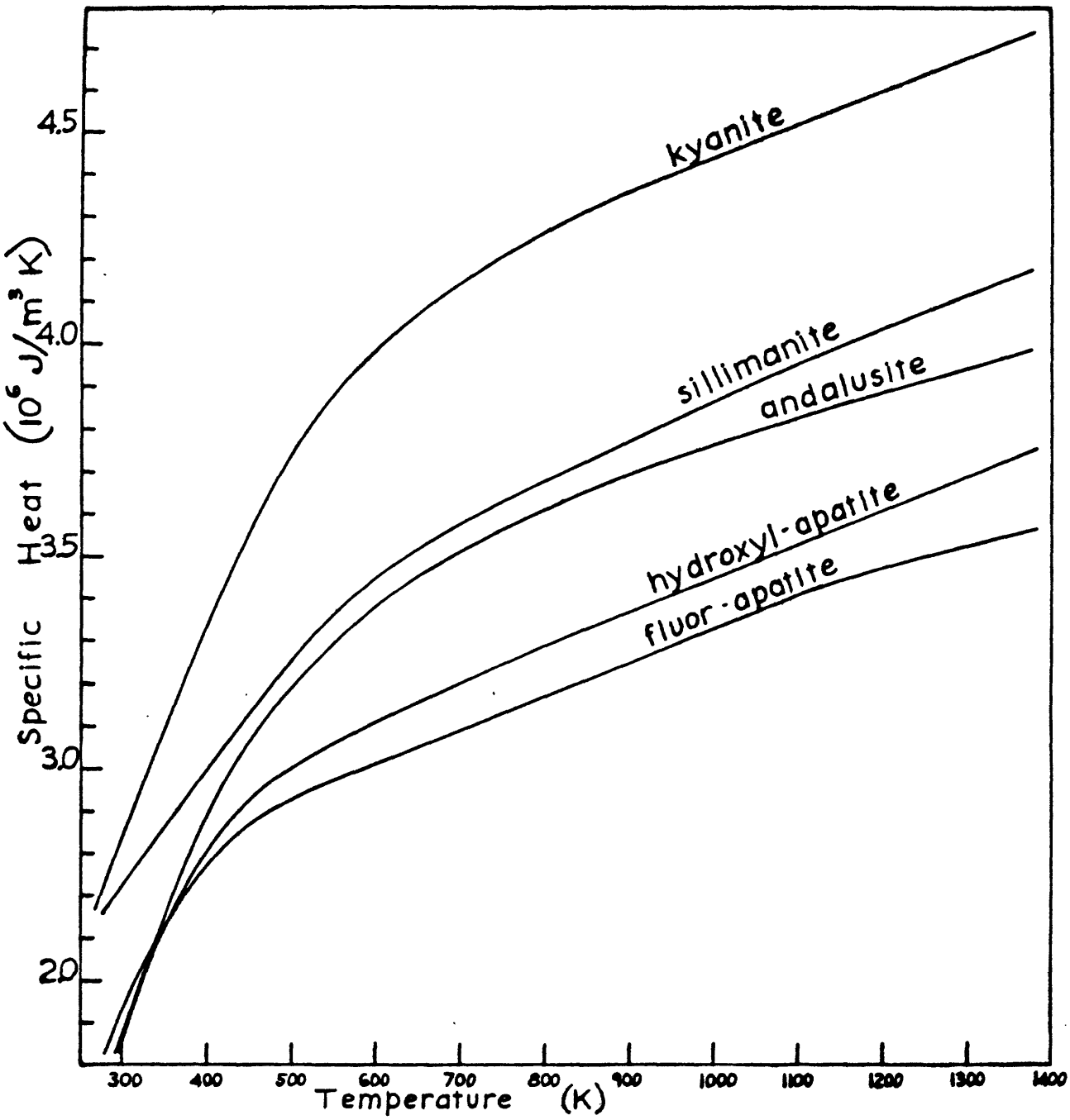

FIGURE 42. Specific heats per unit volume of aluminum silicate and apatite minerals in variation with temperature.

Calculation of Specific Heat

The calculation of the specific heat $\underline{C}_p$ of a rock at selected temperature from its mode in volume percent can be made using the parallel composite model of Equation 1 as follows.

$$\underline{C}_p = (\underline{x}_n \underline{C}_n) = \underline{x}_1 \underline{C}_1 + \underline{x}_2 \underline{C}_2 + \ldots \qquad (14)$$

where $\underline{x}_n$, (n = 1, 2, ...) is the volumetric decimal fraction of the content of minerals 1, 2, ..., and $\underline{C}_n$ is the specific heat per unit volume of the corresponding mineral constituent at constant pressure at a selected temperature, as determined from figures 37-42. The composite $\underline{C}_p$ is multiplied by solidity γ to account for the pore volume. To obtain $\underline{C}_p$ in heat units per unit weight from figures 30 to 36, $\underline{x}_n$ must be converted to decimal fractions by weight, dividing $\underline{x}_n$ by the constituent mineral densities and calculating the relative amounts of each mineral. It is easier to use Equation 14 with the mode in volume percent.

If one constituent of a rock is glass, the $\underline{C}_p$ of the glass can be assumed to be very nearly equal to the composite $\underline{C}_p$ for the rock. The mode of the rock can be recalculated by dividing each decimal fraction by fraction by one minus the decimal fraction of glass; the increased mineral decimal fraction values can then be used in equation 14.

Calculated values of $\underline{C}_p$ of rocks can be more accurate than observed values unless considerable care is taken experimentally. As an example, the results of Lindroth and Krawza (1971) on the $\underline{C}_p$ of six rocks measured with a calorimeter are compared in figure 43 with values of $\underline{C}_p$ calculated from the rock modes and figures 37-42.

The same minerals of the modes given by Lindroth and Krawza are not all illustrated in figures 37-42, but nearly equivalent minerals were selected to obtain values of $\underline{C}_p$. As seen in figure 43, in the range 100 °C to 600 °C, the calculated and observed values of $\underline{C}_p$ are within 5 percent of each other; however at $\underline{T} > 600$ °C, the divergence of the curves is clear. One reason for discrepancy is that separate fits of the equation were made by the authors above and below 575 °C, which created rather artificial curves in the higher $\underline{T}$ range. (Note especially the unlikely quartz transition in Dresser basalt in figure 43). Also, fits to their heat content data with second-degree equations (producing straight lines of $\underline{C}_p$) removes the more realistic downward curvature obtainable with the more commonly-used heat capacity equations (B.S. Hemingway, oral commun., 1979). In addition, there appear to be experimental errors in the measurements at the higher temperatures.

Table 12 (compiled by Goranson, 1942) lists specific heats of common rocks at temperatures to 1,800 °C.

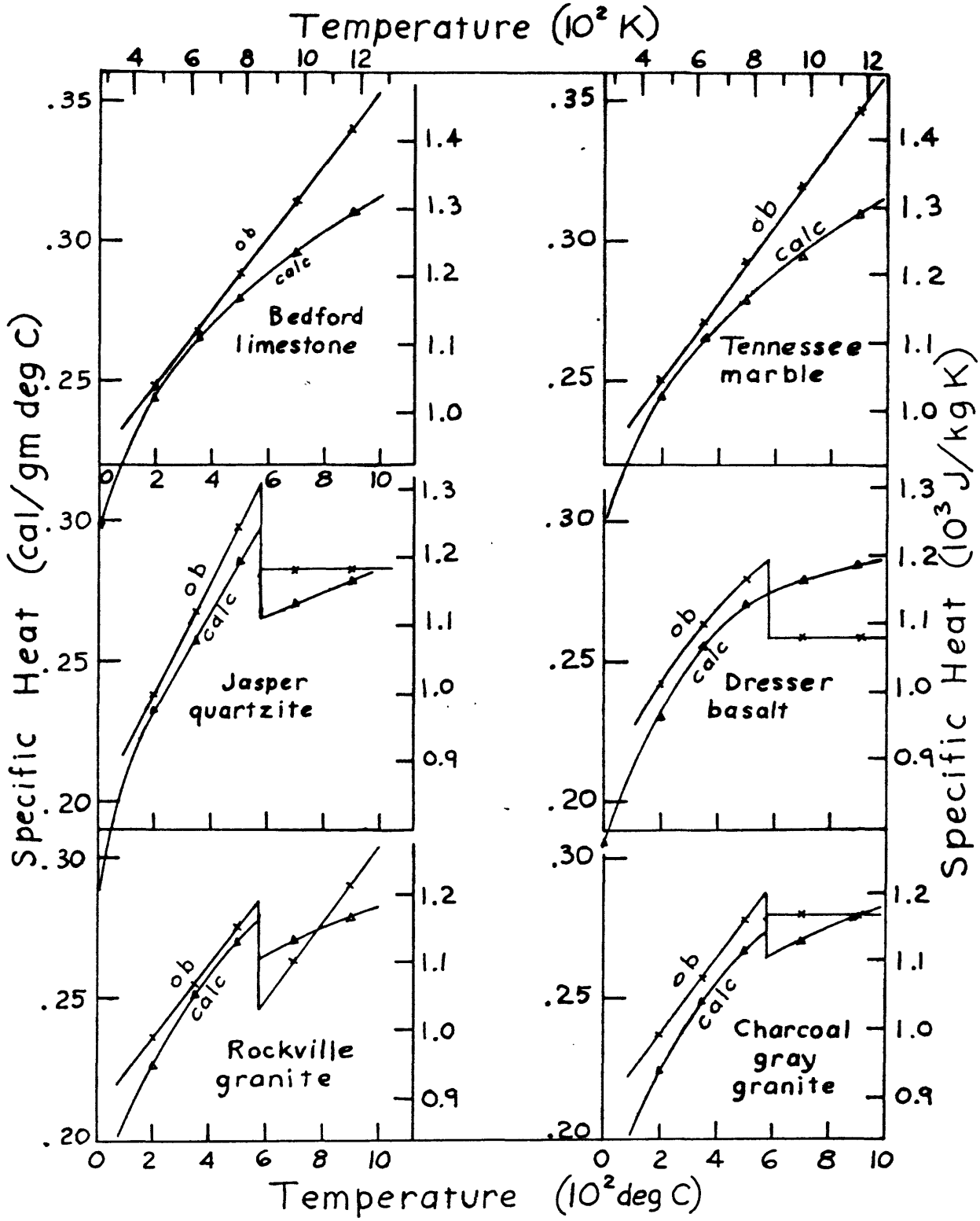

FIGURE 43. Comparison of calculated specific heats (from Figs. 37-42) with observed specific heats (Lindroth and Krawza, 1971) of six rocks.

TABLE 12.--Specific heats of common rocks at various temperatures (from Goranson, 1942)

Rock type	Specific heat (10^3 J/kg K)					
Temp. (°C)	0	50-65	200	400	800	1200
Granite..... 0.65		0.95	1.07	1.13		
0.80	0.77	0.95	1.09	1.39		
Granodiorite..... 0.70		0.97	1.09	1.18		
Diorite..... 0.71	0.81	0.99	1.09	1.18		
Basalt..... 0.85		1.04	1.15	1.32	1.49	
Diabase..... 0.70		0.87	0.98	1.19	1.36	
Gabbro..... 0.72		0.99	1.10	1.18		
Gneiss, granitic... 0.74	0.79	1.01				
Slate..... 0.71		1.00	1.10	1.20	1.27	
Quartzite..... 0.70	0.77	0.97	1.13	1.17	1.33	
Marble..... 0.79	0.85	1.00	1.13			
Sandstone.....	0.93					
Micaceous sandstone		0.73				
Clay, amorphous.... 0.75		0.94	1.13	1.51		
Clay, kaolin..... 0.80		0.94	1.08	1.78	1.78	
Shale.....	0.77					
Limestone.....	1.00					
	0.83					

DIFFUSIVITY AND THERMAL INERTIA

The diffusivity $\underline{k}$ is often used in the theoretical analysis of many heat conduction problems. It is related to thermal conductivity $\underline{K}$, bulk density $\underline{d}$, and specific heat $\underline{C}_p$ as follows:

$$\underline{k} = \underline{K}/\underline{d}\,\underline{C}_p \qquad (15)$$

Values of $\underline{k}$ have been obtained experimentally for many rocks, but not enough measurements of $\underline{k}$ have been made for graphs to be prepared showing variation with porosity and temperature. By the relation in Equation 12, it is simpler, therefore, to calculate the $\underline{k}$ of rocks.

Another similar parameter, of interest in periodic heat conduction problems, is called the thermal inertia $\underline{I}$. A current and important use of $\underline{I}$ is in infrared remote sensing studies to distinguish rock types by their values of $\underline{I}$ and diurnal observations of their emissivity and temperature. This parameter is occasionally used in heat flow between two rock layers of differing $\underline{I}$. It comprises the same factors as $\underline{k}$, and it is given by

$$\underline{I} = (\underline{K}\,\underline{d}\,\underline{C}_p)^{1/2} = \underline{K}/(\underline{k})^{1/2} \qquad (16)$$

Calculation of Parameters

Knowing the mineral composition of a rock in weight percent, values of $\underline{k}$ and $\underline{I}$ at a temperature of interest can be obtained by determining $\underline{K}$ from figures 21 to 27 (or Diment and others, USGS Open-file Report, 1988), $\underline{d}$ from table 7, and $\underline{C}_p$ from figures 30 to 36. If the mode of the rock is known, the volumetric $\underline{C}_p$, can be found directly from figures 37 to 42; however, in addition, the volumetric $\underline{C}_p$ must be multiplied by γ to account for the porosity. Interpolations for the plagioclase solid solution series is not difficult in figures 31 and 38; interpolations for the olivines is easy in figure 41, but because of the spread between curves for forsterite and fayalite in figure 34, interpolation is not so easy. Values of $\underline{K}$, $\underline{d}$, and $\underline{C}_p$ for minerals not appearing in the tables and figures may generally be taken with about the same accuracy as equivalent to values for minerals of the same group or of similar crystal structure that do appear.

By way of comparing calculated values of diffusivity $\underline{k}$ with experimental measurements of $\underline{k}$, the results of Lindroth (1974) on 4 rocks at 25° and 110 °C and at 1 atm are plotted in figure 44. The calculated $\underline{k}$ curves, shown from T from 0° to 200 °C, were derived by taking the mode of the rocks to find $\underline{C}_p$ values from figure 37-42; $\underline{K}$ values were taken from figures 1-19; calculation of $\underline{K}$ from the modes was deemed less certain (see earlier discussion). The calculated and observed values of $\underline{k}$ agree reasonably well for basalt and gabbro (marked "B, c" and "B, o"; "GB, c" and "GB, o" in fig. 43). The dunite ("D, c" and "D, o" in fig. 43) is highly fractured and serpentinized (not accounted for in the mode), so its $\underline{K}$ would be considerably reduced; as $\underline{k}$ varies directly with $\underline{K}$, the insulating effect of serpentine in the fractures would account for the much lower observed $\underline{k}$ than calculated $\underline{k}$ values. The lower observed $\underline{k}$ relative to calculated $\underline{k}$ for granodiorite ("GD, c" and "GD, o" in fig. 44) could be explained if the rock had a 10 percent porosity, but a more likely explanation is that the given modal quartz content is too high and should be 25 rather than 39 percent.

If only the rock type and not the mode of a rock is known, values for $\underline{k}$ and $\underline{I}$ can still be estimated. The conductivity can be estimated from figures 1-19 and tables 1-8; the density can be estimated from table 11; the specific heat can be estimated from table 12; and good values of $\underline{k}$ and $\underline{I}$ can be then be calculated. Low-precision values were obtained for $\underline{k}$ and $\underline{I}$ by Janza (1975) for remote sensing use and are given in Table 13; these data were calculated from measurements of $\underline{K}$, $\underline{d}$, and $\underline{C}_p$ at room temperature and pressure, and judging by the ranges of values, the sedimentary rocks had $\gamma = 0.8 - 0.9$, the massive rocks and other materials had $\gamma = 0.9 - 0.98$, and the water content was low to zero in all the rocks.

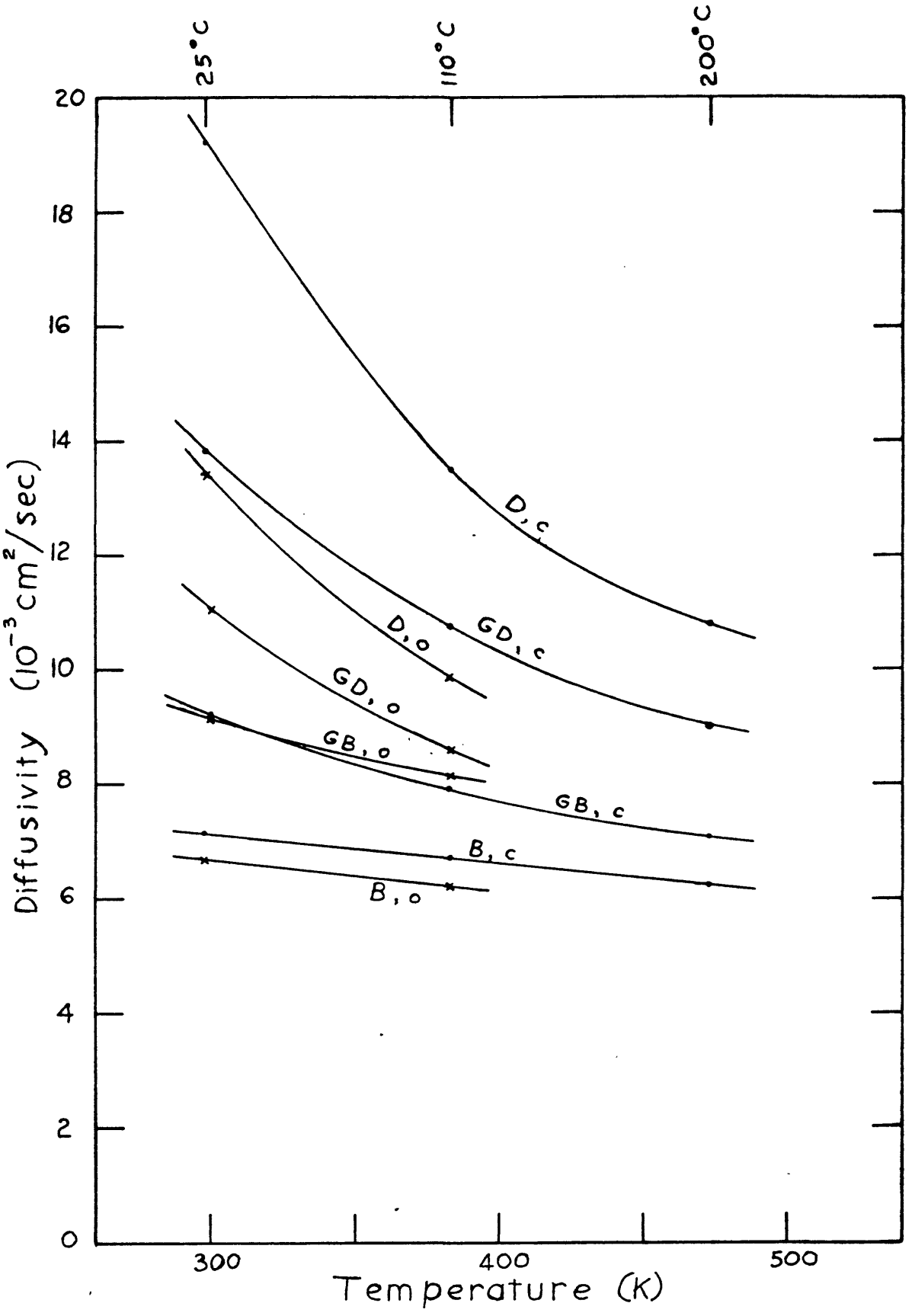

FIGURE 44. Comparison of calculated diffusivities (from Figs. 1-19 and Figs. 37-42) with observed diffusivities (Lindroth, 1974) of 4 rocks.

TABLE 13.--Diffusivity and thermal inertia of common rocks, calculated from thermal conductivity, density, and specific heat (Janza, 1975).

Material	Diffusivity, k (10^{-3} cm^2/sec)	Thermal inertia, I (10^{-3} cal/cm^2 deg C $sec^{1/2}$)
	Rocks	
Basalt	9	53
Gabbro	12	55
Granite	16	52
Rhyolite	14	47
Welded tuff	8	32
Obsidian	7	35
Pumice	4	9
Peridotite	17	84
Serpentine	13	63
Sandstone	13	54
Quartzite	26	74
Limestone	11	45
Dolomite	26	75
Marble	10	56
Shale	8	34
Slate	11	49
Clay soil	5	42
Gravel	8	33
Sandy gravel	14	50
Sandy soil	3	24
	Metals	
Aluminum	916	554
Copper	1,145	879
Lead	236	171
Nickel	239	450
Steel, carbon	173	360
	Thermal Standards	
Quartz, $\perp$ C	32	84
$\parallel$ C	53	109
Silica glass	9	35
	Air and Water	
Air, 20°C	211	1.3
Water, 20°C	1.5	38.5
100°C	1.7	39.3
	Miscellaneous	
Lucite	0.9	11
Nylon	1.4	15
Teflon	1.2	18
Wood	-	9
Glass	5.0	29

HEAT TRANSFER COEFFICIENTS

In Appendix I a short discussion is presented on the definition and use of the heat transfer coefficient $\underline{h}$ in convective heat transmission. The exchange of heat between rock and a gas or liquid flowing over it is important in tunnels, especially in deep mines with high rock temperatures and permeating hot water. Other applications of the basic equation A4 are in studies of radioactive waste disposal, geothermal resources, movement and eruption of magma, and ground water effects on heat generated by radiogenic elements and by magma in the crust and mantle of the earth.

In table 14 values of $\underline{h}$ are listed for a number of different engineering heat exchange devices and arrangements. It is necessary to give ranges of values of $\underline{h}$, of course, because $\underline{h}$ is not a true physical property; it is merely defined by equation A4 for given test conditions. The composition, velocity, and viscosity of fluid, the temperature difference between the fluid and the surface, and the surface roughness, temperature, and water content of the subsurface material (usually a solid but could be another fluid) affect the value of $\underline{h}$ though 4 orders of magnitude. Discussions of the entries in the table are provided to help in estimating $\underline{h}$ for various applications.

Item 1 in table 14, from Groeber and others (1961, table 8.1), provides data from free and forced convection measurements in heat exchangers, mostly utilizing metal tubes and containers. The metal surfaces are smooth and impervious, and so the kind of metal is unimportant in determining $\underline{h}$. The ranges of $\underline{h}$ reflect ranges of velocity, low to medium (1 to 10 m/s) in free convection, and medium to high (10 to 30 m/s) in forced convection; the ranges of $\underline{h}$ also reflect low, medium, and high temperature differences, (1°C, 10°C, and 30°C) between fluid and surface, $(\underline{T}_S - \underline{T}_F)$; (see table 16 and footnote.)

In item 2, table 14, $\underline{h}$ data (Weber and others, 1951) on various grades of purity of water are provided for low intensities of fluid velocity and heat flux. In item 3, the $\underline{h}$ values (Insinger and Bliss, 1940) are for boiling water flowing in chromium pipes at increasingly higher temperatures and heat flux through the pipes. Quenching of fused silica or ceramic in water at about 900°C was studied (item 4, Emery and others, 1981) to obtain its effect on stress intensity developed in cracks, and values of $\underline{h}$ were measured. For item 5, Hardee (1983) measured the heat transfer between molten (90 percent liquid) lava flowing on the surface of the Kilauea volcano, Hawaii, and a titanium probe inserted into the magma.

The remaining items, 6 to 10, provide data on air flowing in tunnels in mines. In item 6, the exchange of heat from the walls of phyllite rock to the ventilating air was studied by Barla and others (1983) with drill holes and temperature probes in a drift at 700 m depth. Item 7 also was provided from an air conditioning and ventilating study of Witwatersrand mines in South Africa at about 2000 m depth in quartzite (Van der Walt and Whillier, 1979); measurements were made with air in free convection in stoped-out regions and with air in forced convection in haulageways. Item 8 provides an average $\underline{h}$ used in a study modelling heat transfer in the Witwatersrand mines by Starsfield (1966). Item 9 provides the range of values of $\underline{h}$ from 1000 measurements of forced air ventilation made in a dry copper mine in Hungary (Danka and Cifka, 1984). Item 10 provides preliminary results from a forced air ventilation study by the author and Floyd C. Bossard, Ventilation Engineer, Anaconda Copper Company, on the 3200 level of the Kelley Mine in Butte, MT; some of the quartz monzonite walls in the workings were dry and others were quite wet with hot permeating water.

In fairly smooth-walled rock conduits, as well as in metal pipes, it has been observed that beneath the convecting fluid there is a thin fluid layer adjacent to the wall, that is at rest. It can be reasonably postulated that through this layer heat is transferred by conduction only, and consequently the conduction and convection equations, A1 and A4 in Appendix I, can be equated for the same rate of heat flow per unit area,

$$Q/A = \underline{h}(\underline{T}_S - \underline{T}_F) = \underline{K}/L\,(\underline{T}_S - \underline{T}_F) \qquad (17)$$

where Q is rate of heat transferred through the still layer of fluid of thickness L, A is area of surface, $\underline{h}$ is heat transfer coefficient, $\underline{K}$ is thermal conductivity of the fluid, $\underline{T}_F$ and $\underline{T}_S$ are temperatures of fluid above the layer and of the solid surface respectively. The temperature drop, $(\underline{T}_S - \underline{T}_F)$, is assumed to take place within the layer, and the following relation between $\underline{h}$ and $\underline{K}$ can be written.

$$L = \underline{K}/\underline{h} \qquad (18)$$

TABLE 14. Heat transfer coefficients (h) for various test conditions.

Item no.	Fluid	Heat transfer coefficient [1] (10^{-3} cal) / (cm^2 s degC)	Test conditions	References
1	Gases	0.05 - 0.5	free convection	Groeber and others,
	water	3 - 20	do.	1961, Ch. 8
	boiling water	30 - 500	do.	
	gases	0.3 - 3	forced convection	do.
	viscous liquids	1 - 15	do.	
	water	15 - 300	do.	
	condensing steam	30 -3000	do.	
2	Water: distilled	300	(temp. near 50°C,	Weber and others,
	boiler feed	150	veloc. 1-5 m/s,	
	brackish, river	70	temp.diff. 1°-5°C)	
	muddy, Del. R.	40		
	Chicago Sanitary	15		
3	Water,		chromium pipe,	Insinger and Bliss,
	boiling	3	flux: 0.05 HFU [2]	1940
		15	0.5	
		25	1.0	
4	Water	20 - 200	quench of fused SiO_2,	Emery and others,
			and ceramic, $\underline{T} = 900°C$	1981
5	Basalt lava,	1.12	$\underline{T} = 1088°C$	Hardee, 1983
	Kilauea	2.54	$\underline{T} = 1119°C$	
6	Air, ventilation	0.60 - 0.72	phyllite,	Barla and others, Campiano Mine, 1983
7	Air, ventilation	0.048- 0.096 0.072- 0.290	open stope haulageway	Van der Walt and Whillier, 1979
8	Air, ventilation	0.100	mine tunnels	Starfield, 1966
9	Air, ventilation	0.04 - 0.5	mine tunnel, dry	Danka and Cifka, 1984
10	Air, ventilation	0.1 - 10 10 - 50	mine tunnel, dry water evaporating	unpublished data, author

[1] Equivalents: $\frac{(10^{-3}\ \text{cal})}{(\text{cm}^2\ \text{s deg})} = \frac{41.86\ \text{W}}{\text{m}^2\ \text{K}} = \frac{7.373\ \text{Btu}}{\text{ft}^2\ \text{hr degF}}$

[2] HFU are heat flow units, 10^{-6} cal / cm^2 sec.

Values of L representing the thickness of a characteristic layer can be calculated from observations of $\underline{h}$ and $\underline{K}$ for various fluids under various conditions. Then transfer coefficients $\underline{h}$ can be estimated from applicable values of L and known values of $\underline{K}$ of a given fluid, as described below.

As most applications in mines, tunnels, and undergound permeable passageways involve only the fluids, air or water, the $\underline{K}$ values of air and water as a function of temperature are provided in table 15. Using appropriate values of $\underline{K}$ from table 15 and applicable values of $\underline{h}$ from table 14 in equation 18, layer thicknesses L were calculated to be used as characteristic values for estimating $\underline{h}$. The characteristic values of L are listed in table 16 in qualitative terms, low, medium, and high, according to the principal factors affecting $\underline{h}$, that is, temperature difference between fluid and surface and fluid velocity; estimated values are shown in the footnote to the table. Estimates of $\underline{h}$ can be made from values of L in table 16 and $\underline{K}$ in table 15 for substances and conditions not covered in table 14; such estimates of $\underline{h}$ are obviously only approximate but could provide limits to be expected in some applications.

To demonstrate that the characteristic thicknesses listed in table 16 are reasonable, a study by Jakob (1936) can be cited. In this paper on heat transfer by condensing steam, Jakob used data from his experiments to calculate the thickness of the static layer at the condensation surface to be 0.00003 cm, for a layer of steam, and to be 0.0009 cm, for a layer of water (compare table 16, last and third from last entries.)

Many investigations have been made of the heat transferred in secondary recovery of oil by flushing with hot water or steam. Observations have been made on the heat transferred from the fluid to volumes of broken rock, sand, glass beads, and other disaggregated solids. A review of some of these results are given by Ramey and others (1974).

TABLE 15. Thermal Conductivities (K) of air and water (After Weast and Astle, 1981.)

Fluid	Temperature (°C)	Thermal Conductivity (10^{-3} cal) (cm s deg C)
Air	30	0.063
	130	0.078
	230	0.092
	530	0.135
Water	30	1.45
	100	1.62[1]
	200	1.58[1]
	300	1.29[1]
Steam	30	0.043
	100	0.057
	200	0.078
	500	0.155

[1] Under saturation vapor pressure.

TABLE 16. Characteristic thickness of stationary fluid layer (L) for estimating heat transfer coefficient (h).

Convection type	Condition intensity [1]	Fluid type	Characteristic length, L (cm)
Free	Low - Medium	air	20 - 1
do.	Low - Medium	water, untreated	0.5 - 0.05
do.	Medium	water, distilled	0.005
Forced	Low - Medium	air	10 - 0.1
do.	Medium - High	water	0.1 - 0.005
do.	Medium	air, water sat'd.	0.1 - 0.01
Boiling water	Medium - High	water	0.05 - 0.001
Condensing steam	Medium	steam	0.01 - 0.0005
	High	do.	0.001 - 0.00005

[1] Condition intensity parameters have the following approximate values:

Condition Intensity	Temperature difference, $(\underline{T}_S - \underline{T}_F)$	Fluid velocity
	(°C)	(m / s)
Low	1	1
Medium	10	10
High	30	30

RADIOACTIVE HEAT GENERATION IN ROCKS

The energy produced by the decay of radioactive chemical elements in rocks is removed ultimately as heat. It is commonly accepted that the observed heat flowing by solid conduction from inside the earth is produced mostly by decay of the radioactive elements uranium **U**, thorium **Th** and potassium **K**. Current hypotheses about the origin of the earth conclude that the earth rather than being originally molten was formed by gravitational accretion of cold particles. Heat inside the earth was produced by the decay of radioactive particles, primarily **U, Th,** and **K** distributed in varying amounts in the rocks.

In table 16 are given the **U, Th,** and **K** contents of a variety of rocks, including common terrestrial rocks, rocks thought to make up the earth's upper mantle, lunar highlands and maria rocks, sedimentary rocks, and estimated averages for the upper and whole crust of the earth.

The decay energies of **U, Th,** and **K,** in combined isotope terrestrial abundances are converted to units of heat generation as follows (from Wetherill, 1966).

U : 0.231×10^{-7} cal/gs

Th : 0.634×10^{-8} cal/gs

K : 0.856×10^{-12} cal/gm sec

These heat generation rates were used to calculate the rates shown for the rocks listed in table 16.

Table 17. Median radioactive element contents and heat generation rates of "average" rocks. (adapted from Clark and others, 1966, Sec. 24.)

Rock type	Uranium content (ppm)	Thorium content (ppm)	Potassium content (percent)	Heat generation rate (10^{-13}cal) (gm sec)
Silicic igneous rocks	3.9	16	4.5	2.39
Granodiorite	2.3	9	2.6	1.33
Diorite	1.7	7	1.1	0.93
Mafic igneous rocks	0.5	2	0.3	0.27
Eclogite	0.3	0.5	0.3	0.11
Peridotite	0.02	0.06	0.001	0.008
Dunite	0.001	0.004	0.001	0.0003
Upper continental crust [1/]	2.8	11	3.4	1.6
Whole continental crust [1/]	1.2	5	2.0	0.77
Lunar highlands [2/]	3.7	14	0.4	1.76
Lunar maria [2/]	0.8	3	2.4	0.39
Shale and sandstone	3.7	12	2.7	1.85
Limestone	2.2	1	0.3	0.60
Quartzite	3.0	1	1.4	0.88
Oceanic red clay, Pacific	4.0	7	2.5	1.58

[1/] Adapted from Taylor and McLennan (1985)

[2/] Adapted from Horai and Fujii (1972)

APPENDIX I. MODES OF HEAT TRANSMISSION

The equations for the three types of heat transmission, conduction, convection, and radiation, and for the storage of heat can be used to show the the differences among the coefficients relating heat flow to temperature difference, length and area, mass, and time. The following discussion is mostly from Jakob (1949).

The equation for heat conduction within a body of a given substance (in solid , liquid, or gaseous state) includes the thermal conductivity constant, which is a property of the substance under given temperature, pressure, chemical, and physical conditions and is the principal subject of this handbook.

$$Q_C = \underline{K}(\Delta \underline{T})\, A/L \qquad A1)$$

where Q_c is conductive heat flow rate, $\underline{K}$ is thermal conductivity, $\Delta \underline{T}$ is temperature difference over a distance L through an area A. This law of heat conduction is Fourier's equation and represents the equality of heat entering a body to the heat stored in and leaving the body.

The Stefan-Boltzmann law of heat radiating from the surface of a black body in the wavelength range, 0.8 to 400 μ , is given as follows.

$$Q_R = \sigma\, A \underline{T}^4 \qquad (A2)$$

where Q_R is the radiative conduction flow rate, σ is the Stefan-Boltzmann constant, A is area of the black body surface, and $\underline{T}$ temperature. Emissivity is the property of a substance relating its radiative flux density to that of a black body, and expressed as their ratio.

The equation for storage of heat requires measurement of the specific heat of a substance in order to determine the rate of heat stored to the mass and temperature rise of a body of the substance.

$$Q_S = \underline{d}\,\underline{C_P}\, V\, (\Delta \underline{T}/\Delta t) \qquad (A3)$$

where $\underline{Q}_S$ is the amount of heat energy stored in a substance per unit time, $\underline{V}$ is the volume , $\underline{d}$ is density, $\underline{C}_P$ is specific heat per unit weight of the substance, $\Delta \underline{T}$ is temperature change, and Δt is the time interval of heat input. The substance properties, diffusivity $\underline{k}$ and thermal inertia $\underline{I}$, require measurement of heat storage; in fact $\underline{k}$ is the ratio of a heat conduction quantity to a heat storage quantity; both $\underline{k}$ and $\underline{I}$ require knowledge of $\underline{C}_P$ because of their use in heat transfer with either secular or periodic changes of heat stored in unit time.

Finally, the equation for heat transfer between a surface, usually of a solid, at a temperature $\underline{T}_S$, and a fluid at a temperature $\underline{T}_F$, in contact with the surface is a complicated one and serves only to define the factor $\underline{h}$, which is the ratio of the heat exchanged per unit area to the temperature difference.

$$Q_T = \underline{h}\, A\, (\underline{T}_S - \underline{T}_F) \qquad (A4)$$

where $\underline{Q}_T$ is the rate of heat transferred between surface and fluid, $\underline{h}$ is the heat transfer coefficient, A is area, and $(\underline{T}_S - \underline{T}_F)$ is temperature difference The equation is sometimes called Newton's law of cooling.

The heat transfer coefficient is not a constant or a property of the fluid because of the complications caused by the fluid dynamics and convection, and the mass transport and conduction of heat in the fluid. These complications lead to practical problems in measuring $\underline{T}_F$, because of its variation with distance from the surface to a constant value and because the distance is usually extremely small. Heat flowing across an imperfect contact between two solids may produce a considerable temperature drop due to the low conductivity of air in the gap. Rapidly moving air over a solid surface will have uniform temperature due to turbulence, but near the surface the velocity and temperature of the air decrease steeply through a very thin layer, to zero and $\underline{T}_S$ respectively. The value of $\underline{h}$ varies with the velocity and viscosity of the fluid, the roughness of the surface, the compositions of the fluid and the solid below the surface, and porosity and permeability of the solid.

It is common in the engineering practice of heat transfer between smooth metal tubes and water or other fluids to use dimensionless numbers to solve heat transfer problems. Thus, the dimensionless Nusselt number, $\underline{N}_U$, is the ratio of a heat transfer transfer coefficient $\underline{h}$ times length L to thermal conductivity $\underline{K}$.

$$\underline{N}_U = \underline{h}L/\underline{K} \qquad \text{(A5)}$$

The $\underline{N}_U$ number is used to calculate $\underline{h}$ for particular configurations and conditions of pipes and fluids; often the distance L used is merely the diameter of a pipe.

For free convection of the fluid, a dimensionless combination that is often used is

$$\underline{N}_U = f(\underline{G}_R, \underline{P}_R) \qquad \text{(A6)}$$

where $\underline{G}_R$ is the dimensionless Grashof number, which involves the thermal expansion coefficient, a temperature, a volume, and the kinematic viscosity squared; and $\underline{P}_R$ is the dimensionless Prandtl number, which involves the ratio of kinematic viscosity to diffusivity.

For forced convection in pipes, another dimensionless combination is used

$$\underline{N}_U = f(\underline{R}_E, \underline{P}_R) \qquad \text{(A7)}$$

where $\underline{R}_E$ is the dimensionless Reynolds number, which is the ratio of velocity and length to the kinematic viscosity.

In analysis of heat transfer between rock and a fluid, the simplest applications to evaluate are ventilation and air conditioning of tunnels for mines, highways, and railroads, although complications may arise when hot water permeates the wall rock to the tunnel surface and evaporates there. Mass transport of heat by deeper underground waterflow through permeable rock and in faults is especially difficult to evaluate because of irregularities in porosity and permeability of the rock, as well as irregularities in the hydrodynamics, convection, mass transport of heat, and thermal conduction of the water.

REFERENCES

Adler, David, Flora, L.P., and Senturia, S.D., 1973, Electrical conductivity in disordered systems: Solid State Communication, v. 12, p 9-12.

Alm, O., and Backstrom, G.,1975, Thermal conductivity of NaCl up to 40 k bar and 240-400 K: High Temperatures-High Pressures, v. 7, p. 235-239.

Anand, J., Somerton, W.H., and Gomaa, E., 1973, Predicting thermal conductivities of formations from other known properties: Society of Petroleum Engineers Journal, v. 13, p. 267-273.

Aronson, J.R., Bellotti, L.H., Eckroad, S.W., Emslie, A.G., McConnell, R. K., and von Thuna, P.C., 1970, Infrared spectra and radiative thermal conductivity of minerals at high temperatures: Journal of Geophysical Research, v. 75, p. 3443-3456.

Asaad, Yoursi, 1955, A study of the thermal conductivity of fluid-bearing porous rocks: University of California, Berkeley, Ph.D. Thesis, 71 p.

Barla, G., Innaurato, N., and Pantaleoni, G., 1983, Heat transfer in the rock mass around mine openings: International Society of Rock Mechanics Proceedings, 5th Symposium, v. 2, p. E141-E146.

Beck, A.E., and Beck, J.M., 1958, On the measurement of the thermal conductivities of rocks by observations on a divided bar apparatus: American Geophysical Union Transactions, v. 39, p. 1111-1123.

Beck, A.E., 1965, Techniques of measuring heat flow on land, in Terrestrial Heat Flow, Lee, W.H.K., ed., American Geophysical Union Monograph No. 8, p. 24-57.

Beck, J.M., and Beck, A.E., 1965, Computing thermal conductivities of rocks from chips and conventional specimens: Journal of Geophysical Research, v. 70, p. 5227-5239.

Beck, A.E., Anglin, F.M., and Sass, J.H., 1971, Analysis of heat flow data-in situ thermal conductivity measurements: Canadian Journal of Earth Sciences, v. 8, p. 1-19.

Benfield, A.E., 1947, A heat flow value for a well in California, American Journal of Science, v. 245, p. 1-18.

Birch, Francis, and Clark, Harry, 1940, The thermal conductivity of rocks and its dependence upon temperature and composition: American Journal of Science, v. 238, nos. 8 and 9, p. 529-558 and 613-635.

Birch, Francis, 1950, Flow of heat in the Front Range, Colorado, Geological Society of America Bulletin, v. 61, p. 567-630.

Bridgman, P.W. 1924, The thermal conductivity and compressibility of several rocks under high pressure: American Journal of Science, v. 7, p. 81-102.

Bullard, E.C., 1939, Heat flow in South Africa, Proceedings of the Royal Society, Series A, v. 173, p. 474-502.

Bullard, E.C., and Niblett, E. R., 1951, Terrestrial heat flow in England: Monthly Notices Royal Astronomical Society, Geophysical Supplement, v. 6, p. 222-238.

Butler, D.W., 1966, unpublished, in, Handbook of physical constants, Clark, S.P. Jr., ed.: Geological Society of America Memoir 97, Table 21-11, p. 479.

Carslaw, H.S. and Jeager, J.C., 1959, Conduction of heat in solids: Oxford University Press, London, 510 p.

Clark, Harry, 1941, The effects of simple compression and wetting on the thermal conductivity of rocks, American Geophysical Union Transactions, v. 22, Part II, p. 543-544.

Clark, S.P.Jr., and Niblett, E.R., 1956, Terrestrial heat flow in the Swiss Alps: Monthly Notices, Royal Astromical Society, Geophysical Supplement, v. 7, p. 176-195.

Clark, S.P.Jr., 1956, Effect of radiative transfer on temperatures in the Earth: Geological Society of America Bulletin, v. 67, p. 1123-1124.

___1957a, Radiative transfer in the Earth's mantle: American Geophysical Union Transactions, v. 38, p. 931-938.

___1957b, Absorption spectra of some silicates in the visible and near-infrared: American Mineralogist, v. 42, p. 732-742.

___1961, Heat flow in the Austrian Alps: Geophysical Journal, v. 6, p. 54-63.

Clark, S. P., Jr.,ed., 1966, Handbook of physical constants: Geological Society of America Memoir 97, 587 p.

Clark, S.P.Jr., Peterman, Z.E., and Heier, K.S., 1966, Abundances of uranium, thorium, and potassium, in Handbook of physical constants: Clark, S.P.,Jr., ed., Geological Society America Memoir 97, Section 24, p. 522-541.

Coster, H.P., 1947, Terrestrial heat flow in Persia: Monthly Notices Royal Astronomical Society, Geophysical Supplement, v. 5, no.5, p. 131-145.

Cremers, C.J., 1972, Thermal conductivity of Apollo 14 fines: Geochimica et Cosmochimica Acto, Supp. 5 v. 3, p. 2611-2617.

___1973, Thermophysical properties of Apollo 12 fines: Icarus, v. 18, p. 294-303.

Daly, R.A., 1966, Average densities of holocrystalline igneous rocks, in Handbook of physical constants, Clark, S.P. Jr., ed.: Geological Society of America Memoir 97, table 4-1, p. 20.

Danko, G., and Cifka, I., 1984, Measurement of the convective heat-transfer coefficient on naturally rough tunnel surfaces: in Homes, M. J. and Jones, M. J., eds., Third International Mine Ventilation Congress, Institute of Mining and Metallurgy, p. 375-380.

Darbha, D.M., and Schloessin, H.H., 1975: Anisotropic lattice thermal conductivity of α -quartz as a function of pressure and temperature, in Thermal Conductivity, Klemens, P.G. and Chu, T.K., eds.: Plenum Press, N. Y., p. 183-190.

Diment, W.H. 1964: Thermal conductivity of serpentinite from Mayaguez, Puerto Rico, and other localities, in A study of serpentinite-The AMSOC core hole near Mayaguez, Puerto Rico, Burk, C.A., ed, NAS-NRC Pub. 1188, p. 92-106.

Diment, W.H., and Werre, R.W., 1964, Terrestrial heat flow near Washington D.C.: Journal of Geoophysical Research, v. 69, p. 2143-2149.

Diment, W.H., Marine, I.W., Neiheisal, J., and Siple, G.E., 1965, Subsurface temperature thermal conductivity, and heat flow near Aiken, S.C.: Journal of Geophysical Research, v.70, p. 5635-5644.

Emery, A. F., Kobayashi, A. S., and Bieler, T. R., 1981, Consequences of varying surface heat transfer coefficients, material properties, and cyclical ambient temperatures upon stress intensity factors for edge cracks: in Freiman, S. W. and Fuller, E. R. Jr., eds., Fracture mechanics methods for ceramics, rocks, and concrete, American Society Testing Materials, STP 745, p. 257-272.

Eucken, A., 1911, Uber die Temperaturabhangigkeit der Warmeleitfahigkeit fester Nichtmetalle: Ann. Physik, v. 34, p. 185-221.

Fountain, J.A., Scott, R.W., and West, E.A., 1973, Thermal conductivity of particulate materials: Space Science Laboratory Technical Memorandum 64759, 64 p.

Fujii, Naoyuki, and Osako, Masahiro, 1973, Thermal diffusivity of lunar rocks under atmospheric and vacuum conditions: Earth Planetary Science Letters, v. 18, p. 65-71.

Fujisawa, Hideyuki, Fujii, Naoyuki, Mizutani, Hitoshi, Kanamori, Hiroo, and Akimoto, Syun-iti, 1968, Thermal diffusivity of Mg2 SiO_4, Fe_2 SiO_4, and NaCl at high pressures and temperatures: Journal of Geophysical Research, v. 73, p. 4727-4733.

Fukao, Yoshio, Mitzutani, Hitoshi, and Uyeda, Seiya, 1968, Optical absorption spectra at high temperatures and radiative thermal conductivity of olivines: Physics of Earth and Planetary Interiors, v. 1, p. 57-62.

Fukao, Yoshio, 1969, On the radiative heat transfer and thermal conductivity in the upper mantle: Bulletin of Earthquake Research Institute, v. 47, p. 549-569.

Goldsmid, H.J., and Bailey, A.E., 1960, Thermal conduction in mica along the planes of cleavage: Nature, v. 187, p. 864-865.

Goldsmid, H.J., 1965, The thermal properties of solids: Dover Publications, New York, 72 p.

Goranson, R.W., 1942, Heat capacity of rocks, in Handbook of physical constants, Birch, F., ed.: Geological Society of America Special Paper 36, Table 16-2, p. 235-236.

Goss, Ronald, and Combs, Jim, 1976, Thermal conductivity measurement and prediction from geophysical well log parameters with borehole application, in Proceedings of the Second United Nations Symposium on the Development and Use of Geothermal Resources: San Francisco, CA, 20-29 May 1975, v. 2 ,p. 1019-1027.

Greenberg, R.J., and Brace, W.F., 1969, Archie's law for rocks modeled by simple networks: Journal of Geophysical Research, v. 74, p. 2099-2102.

Groeber, H., Erk, S., and Grigull, Ulrich, 1961, Fundamentals of heat transfer: McGraw Hill, New York, 527 p.

Hardee, H. C., 1983, Heat transfer measurements of the 1983 Kilauea lava flow: Science, v. 222, p. 47-48.

Herrin, Eugene, and Clark, S.P.,Jr., 1956: Heat flow in West Texas and Eastern New Mexico: Geophysics, v. 21, p. 1087-1099.

Higashi, Akira, 1952, Thermal conductivity of frozen soil: Hokkaido University Faculty Science Journal, Series 2, v. 4, p. 95-106.

Horai, Ki-iti, 1971, Thermal conductivity of rock-forming minerals: Journal of Geophysical Research, v. 76, p. 1278-1308.

Horai, Ki-iti and Baldridge, Scott, 1972, Thermal conductivity of nineteen igneous rocks, I, II: Physics Earth Planetary Interiors, v. 5, p. 151-166.

Horai, Ki-iti, and Fujii, Naoyuki, 1972, Thermo-physical properties of lunar material returned by Apollo missions: The Moon, v. 4, p. 379-407.

Horai, Ki-iti, and Winkler, J.L.Jr., 1975, Thermal diffusivity of lunar rock sample 12002, 85: Lunar Science Conference Proc. v. 6, p. 3207-3215.

___1976, Thermal diffusivity of four Apollo 17 rock samples: Geochimica et Cosmochimica Acta, Supp. 7, v. 3, p. 3183-3204.

Hughes, D.S., and Sawin, Fred, 1967, Thermal conductivity of dielectric solids at high pressure: Physical Review, v 161, p 861-863.

Hurtig, E., 1965, Untersuchungen der Warmeleitfahigkeits anisotropie von Sandsteinem, Grauwacken und Quartziten: Pure Applied Geophysics, v. 60, p. 85-100.

Hurtig, E., 1968, Zum problem der Anisotropie petrophysikalischer Parameter im geologischen Korpern: Geophysik and Geologie, no. 12, p. 3-36.

Hutt, J.R., and Berg, Joseph, Jr, 1968, Thermal and electrical conductivities of sandstone rocks and ocean sediment: Geophysics, v. 33, p. 489-500.

Ide, J.M., 1937, The velocity of sound in rocks and glasses as a function of temperature: Journal of Geology, v. 45, p. 689-716.

Ingersoll, L.R., Zobel, O.J., and Ingersoll, A.C., 1954, Heat conduction; with engineering, geological and other applications: University of Wisconsin Press, Madison, 325 p.

Insinger, T. H., and Bliss, Harding, 1940, Transmission of heat to boiling liquids: American Institute of Chemical Engineers, Transactions, v. 36, p. 491-513.

Jakob, Max, 1936, Heat transfer in evaporation and condensation, II: American Society of Mechanical Engineers, Mechanical Engineering, v. 58, p. 729-739.

___1949, Heat transfer, Volume I: J. Wiley, New York, 758 p.

Janza, F.J., 1975, Interaction mechanisms, in Reeves, R.G.,Anson, Abraham, and Landen, David, editors, Manual of remote sensing, American Society of Photogrammetry, Falls Church, VA, p.75-179.

Kanamori, Hiroo, Fujii, Naoyuki, and Mizutani, Hitoshi 1968, Thermal diffusivity measurement of rock-forming minerals from 300 to 1100 K: Journal of Geophysical Research, v. 73, p. 595-605.

Kanamori, Hiroo, Mizutani, Hitoshi, and Fujii, Naoyuki, 1969, Method of thermal diffusivity measurement: Journal of Physics of the Earth, v. 17, p. 43-53.

Kawada, Kaoru, 1964, Studies of the thermal state of the earth. The 15th paper: Variation of thermal conductivity of rocks. Part 1: Bulletin of the Earthquake Research Institute, v. 42, p. 631-647.

___1966, Studies of the thermal state of the earth. The 17th paper: Variation of thermal conductivity of rocks. Part 2: Bulletin of the Earthquake Research Institute, v. 44, p. 1071-1091.

Kersten, M.S., 1949, Thermal properties of soils: Minnesota University Bulletin No. 28, Engineering Experimental Station, v. 52, 94 p.

Kieffer, S.W., Getting, I.C., and Kennedy, G.C., 1976, Experimental determination of the pressure dependence of the thermal diffusivity of teflon, sodium chloride, quartz, and silica: Journal of Geophysical Research, v. 81, p. 3108-3024.

King, Warren, and Simmons, Gene, 1972, Heat flow near Orlando, Florida and Uvalde, Texas determined from well cuttings: Geothermics, International Journal of Geothermal Research, v. 1, p. 133-139.

Klemens, P.G., 1958, Thermal conductivity and lattice vibration modes, in Solid State Physics, v. 7, Sietz, F. and Turnbull, D., eds.: Academic Press, New York, p. 1-98.

Kunii, D. and Smith, J.M., 1961, Thermal conductivities of porous rocks filled with stagnant fluid: Society of Petroleum Engineers Journal, v. 1, no. 1, p. 37-42.

Langseth, M.G.Jr., Clark, S.P.Jr., Chute, J.L.Jr., Keihm, S.J., and Wechsler, A.E., 1972, The Apollo 15 lunar heat-flow measurment: The Moon, v. 4, p. 390-410.

Lindroth, D.P., and Krawza, W.G., 1971, Heat content and specific heat of six rocks at temperatures to 1000°C: U. S. Bureau of Mines Report of Investigations 7503, 24 p.

Lindroth, D.P., 1974, Thermal diffusivity of six igneous rocks at elevated temperatures and reduced pressures: U. S. Bureau of Mines Report Investigations 7594, 33 p.

MacPherson, W.R., and Schloessin, H.H., 1982, Lattice and radiative thermal conductivity variations through high P, T polymorphic transitions and melting points: Physics Earth Planetary Interiors, v. 29, p. 58-68.

Magnitskii, V.A., Petrunin, G.E., and Yurchak, R.P., 1971, Povedenie tempera turoprovodnosti nektorik polevik shpaton i plagioklazon pri temperaturak 300-1200°K, Doklady Akademiya nauk SSSR, v. 199, p. 1058-1060.

Manger, G.E., 1966, Porosity and bulk density, dry and saturated, of sedimentary rocks, in Handbook of physical constants, Clark, S.P., Jr., ed., Geological Society of America Memoir 97, Table 4-4, p. 23-25.

McCarthy, K.A., and Ballard, S.S., 1960, Thermal conductivity of eight halide crystals in the temperature range 220K to 390K: Journal of Applied Physics, v. 31, p. 1410-1412.

Meincke, W., Hurtig, E., and Weiner, J., 1967, Temperaturnerteilung, Warmeleitfahigkeit und Warmefluss in Thuringer Becken: Geophysik und Geologie, no. 11, p. 40-71.

Mirkovich, V.V., 1968, Experimental study relating thermal conductivity to thermal piercing of rocks: International Journal of Rock Mechanics and Mining Sciences, v. 5, p. 205-218.

Misener, A.D., Thompson, L.G.D., and Uffen, R.J., 1951, Terrestrial heat flow in Ontario and Quebec: American Geophysical Union Transactions, v. 32, p. 729-738.

Mizutani, Hitoshi, and Osako, Masahiro, 1974, Elastic-wave velocities and thermal diffusivities of Apollo 17 rocks and their geophysical implications: Geochimica et Cosmochimica Acta, Supp. 5, v. 3, p. 2891-2901.

Moiseenko, von U.I., 1968, Warmeleitfahigkeit der Gesteine bei hohen Temperaturen, Freiberger Forschungshefte: Geophysik, no. C238, p. 89-94.

Mossip, S.C., and Gafner, G., 1951, The thermal constants of some rocks from the Orange Free State: Journal of Chemistry, Metallurgical & Mining Society, South Africa, v. 52, p. 61-67.

Parrott, J.E., and Stuckes, A.D., 1975, Thermal conductivity of solids: Pion Ltd., London, 157 p.

Peck, D.L., Hamilton, M.S., and Shaw, H.R., 1977, Numerical analysis of lava lake cooling models: pt. 2, Application to Alae Lava Lake, Hawaii: American Journal of Science, v. 277, p. 415-437.

Penner, E., 1963, Anisotropic thermal conduction in clay sediments, in International Clay Conference 1963, v. 1, International Series Monographs, Earth Science, v. 14, Rosenqvist, T., and Graffe-Petersen, P., eds., Pergamon Press, N.Y., p. 365-371.

Petrunin, G.I., Yurchak, R.P., and Tkach, G.F., 1971, Temperature conductivity of basalts at temperatures from 300 to 1200K: Fizika Zemli, no. 2, p. 65-68.

Petrunin, G.I., and Yurchak, R.P., 1973, Ob izmerenii temperaturprovodnosti gornik porod: Fizika Zemli, no. 11, p. 92-95.

Poole, H.H., 1914, On the thermal conductivity of some rocks at high temperatures: Philosophical Magazine, Series 6, v. 24, p. 45-62.

___1914, On the thermal conductivity and specific heat of granite and basalt at high temperatures: Philosophical Magazine, Series 6, v. 27, p. 58-83.

Ramey, H.J.,Jr., Brigham, W.E., Chen, H.K., Atkinson, P.G., and Arihara, N., 1974, Thermodynamic and hydrodynamic properties of hydrothermal systems: Stanford Geothermal Program, Report SGP TR -6.

Ratcliffe, E.H., 1959, Thermal conductivities of fused and crystalline quartz: British Journal of Applied Physics, v. 10, p. 22-25.

___1960, The thermal conductivities of ocean sediments: Journal of Geophysical Research, v. 65, p. 1535-1541.

Robertson, E.C., 1959, Physical properties of limestone and dolomite cores from the sandhill well, Wood County, West Virginia: West Virginia Geological Survey, Morgantown, West Virginia, Report of Investigations No. 18, 1959, p. 112-144.

___ 1979, Thermal conductivities of rocks: U.S. Geological Survey Open-File Report 79-356, 31 p.

Robertson, E.C., and Peck, D.L., 1974, Thermal conductivity of vesicular basalt from Hawaii: Journal of Geophysical Research, v. 79, p. 4875-4888.

Robie, R.A., Bethke, P.M., and Beardsley, J.M., 1967, Selected x-ray crystallographic data molar volumes, and densities of minerals and related substances: U. S. Geological Survey Bulletin 1248, 87 p.

Robie, R.A., and Waldbaum, D.R., 1968, Thermodynamic properties of minerals and related substances at 298.15°K (25.0°C) and one atmosphere (1.013 bars) pressure and at higher temperatures: U. S. Geological Survey Bulletin 1259, 256 p.

Robie, R.A., Hemingway, B.S., and Fisher, J.R., 1978, Thermodynamic properties of minerals and related substances at 298.15K and 1 bar (10^5 Pa) pressure and at higher temperatures: U. S. Geological Survey Bulletin 1452, 456 p.

Rodionov, X.P., 1958, Problem of the effect of hydrostatic pressure on the thermal conductivity of insulators: Physics of Metals and Metallography, v. 6, p. 160-164.

Sass, J.H., and Le Marne, A.E., 1963, Heat flow at Broken Hill, New South Wales: Geophysical Journal, v. 7, p. 477-489.

Sass, J.H., 1965, The thermal conductivity of fifteen feldspar specimens: Journal of Geophysical Research, v. 70, p. 4064-4065.

Sass, J.H., Lachenbrunch, A.H., and Munroe, R.J., 1971, Thermal conductivity of rocks from measurements on fragments and its appplication to heat-flow determinations: Journal of Geophysical Research, v. 76, p. 3391-3401.

Scharmeli, G.H., 1977, Identification of radiative thermal conductivity of olivine up to 25 kbar and 1500 K, in High-pressure science and technology, vol. 2, Timmerhaus, K. D., and Barber, M. S., eds.: Plenum Press, N. Y. p. 60-74.

Schatz, J.F., and Simmons, Gene, 1972, Thermal conductivity of earth materials at high temperatures: Journal of Geophysical Research, v. 77, p. 6966-6983.

Schloessin, H.H., and Dvorak, Z., 1972, Anisotropic lattice thermal conductivity in enstatite as a function of pressure and temperature: Royal Astronomical Society, Geophysical Journal v. 27, p. 499-516.

Schneider, W.A., 1961, Investigation of the radiative contribution to the thermal conductivity in sodium chloride, dunite and fused quartz: Ph.D. Thesis, Massachusetts Institute of Technology, June, 1961, 160 p.

Shankland, T.J., 1970, Pressure shift of infrared absorption bands in minerals and the effect on radiative heat transport: Journal of Geophysical Research, v. 75, p. 409-413.

Shankland, T.J., and Waff, H.S., 1974, Conductivity in fluid-bearing rocks: Journal of Geophysical Research, v. 79, p. 4863-4868.

Shankland, T.J., 1975, Electrical conduction in rocks and minerals: Parameters for interpretation: Physics Earth Planetary Interiors, v. 10, p. 209-219.

Shankland, T.J., Nitson, V.T., and Duba, A.G., 1979, Radiative heat transfer in olivine: Journal of Geophysical Research, v. 84, p. 1603-1610.

Skinner, B.J., 1966, Thermal expansion, in Handbook of physical constants, Clark, S.P. Jr., ed., Geological Society of America Memoir 97, Section 6, p. 75-96.

Smith, W.O., and Byers, H.G., 1938, The thermal conductivity of dry soils of certain of the great soil groups: Soil Science Society of America Proceedings, v. 3, p. 13-19.

Somerton, W.H., 1958, Some thermal characteristics of porous rocks: American Institute of Mining Engineering Transactions, v. 213, p. 375-378.

Stephens, D.R., 1963, High temperature thermal conductivity of six rocks: University of California Radiation Laboratory, Publication 7605, 15 p.

Starfield, A. M., 1966, Tables for the flow of heat into a rock tunnel with different surface heat transfer coefficients: South African Institute of Mining and Metallurgy, Journal, v. 66, kp. 692-694.

Sugawara, A., and Yoshizawa, Y., 1961, An investigation on the thermal conductivity of porous materials and its application to porous rock: Australian Journal of Physics, v. 14, no. 4, p. 469-480.

____1962, An experimental investigation on the thermal conductivity of consolidated porous materials: Journal of Applied Physics, v. 33, p. 3135-3138.

Sukharev, G.M., and Sterlenko, Z.V., 1970, Teplovie svotstva Peschankov, Nasishchennich Presnoi Vodoi and Neffi, (Thermal properties of sandstone saturated with distilled water and oil): Doklady Akademiya Nauk, SSSR, v. 194, p. 683-685.

Sukharev, G.M., Taranuka, U.K., Yaroshenko, A.A., Vlacova, C.P., and Blagonranov, N.S., 1972, Vliyanie na teplofizicheskie svoistva gornik porod ik kimicheskovo sostava: Doklady Akademiya Nauk, SSSR, v. 204, p. 196-199.

Taylor, S.R., and McLennan, S.M., 1985, The continental crust: its composition and evolution: Blackwell Scientific Publn., Boston, 312 p.

Van der Walt, J., and Whillier, A., 1979, Heat pick-up from the rock in gold mines: The water-rock thermal balance and the thermal efficiency of production: Mine Ventilation Society of South Africa, Journal, v. 32, p. 125-147.

Walsh, J.B., and Decker, E.R., 1966: Effect of pressure and saturating fluid on the thermal conductivity of compact rock: Journal of Geophysical Research, v. 71, p. 3053-3061.

Watson, K.E., 1964, Thermal conductivity of selected silicate powders in vacuum from 150 K - 350 K: Ph.D. thesis, California Institute of Technology.

Weast, R. C., and Astle, M .J., eds., 1981, CRC handbook of chemistry and physics: CRC Press, Boca Raton, FL, p. E-3, E-10, and F-12.

Weber, H. C., Berry, C. H.,McAdams,. W. H., and Hottel, H. C., 1955, Heat: Section 4, in Marks, L., S., ed., Mechanical Engineers Handbook, McGraw Hill, New York, 2,236 p.

Weber, M., 1895, Conductibilite calorifique des roches et des corps mauvais conducteurs: Sciences Physiques et Naturelles Archives, v. 23, p. 590-591.

Wetherill, G.W., 1966, Radioactive decay constants and energies, in Handbook of physical constants: Clark, S.P.Jr., ed., Geological Society America Memoir 97, Section 23, p. 514-519.

Woodside, William, and Messmer, J.H., 1961, Thermal conductivity of porous media, I. Unconsolidated sands, II. Consolidated rocks: Journal of Applied Physics, v. 32, p. 1688-1706.

Zierfuss, H., and Vliet, van der G., 1956, Measurement of heat conductivity of sedimentary rocks: American Association of Petroleum Geologists Bulletin, v. 40, p. 2475-2488.

Zierfuss, H., 1969, Heat conductivity of some carbonate rocks and clayey sandstones: American Association of Petroleum Geologists Bulletin, v. 53, p. 251-260.